

NEAR INFRARED REFLECTANCE SPECTROSCOPY OF BOVINE FECES FOR
DETECTION OF SOUTHERN CATTLE TICK *Rhipicephalus (Boophilus) microplus*
INFESTATIONS

A Thesis

by

BRIAN TAYLOR RICH

Submitted to the Office of Graduate and Professional Studies of
Texas A&M University
in partial fulfillment of the requirements for the degree of
MASTER OF SCIENCE

Chair of Committee,	Pete D. Teel
Committee Members,	Sonja L. Swiger
	Michael T. Longnecker
Head of Department,	Pete D. Teel

May 2019

Major Subject: Entomology

Copyright 2019 Brian Taylor Rich

ABSTRACT

The United States Cattle Fever Tick Eradication Program serves to prevent the re-establishment of cattle fever ticks (*Rhipicephalus (Boophilus) spp.*), and the risk of Texas cattle fever from Mexico. The primary detection method for fever ticks on cattle is through the manual palpation of restrained animals in an attempt to feel for attached ticks. This method involves using bare hands to feel through the hair coat of the host animal for attached ticks, but due to their small size only adults and engorged nymphs are usually discovered in this way. The threshold tick population for detection by human inspection affected by many variables from weather related influences to risks inherent with physical examination of restrained cattle. New methods for detecting animals infested with cattle fever ticks are needed to improve the reliability of human inspection.

Ticks mediate host immune responses for successful blood feeding. Interactions of host immune, endocrine and digestive systems impact digestion and resulting fecal chemistry. These studies were conducted to determine whether near-infrared reflectance spectroscopy could detect differences in fecal samples from infested and non-infested cattle, to determine the effects of fecal ageing and environmental exposure on NIR spectra, and to compare the abilities of a bench-top and portable spectrometer for NIR assessment of bovine feces from tick infested cattle. Fecal samples were taken daily from 6 *Bos taurus* cattle infested with *R. microplus* and 6 non-infested *Bos taurus* cattle fed on a standardized pelleted diet for 60 days. Fecals were ground, dried and subjected to NIRS scans by a FOSS 6500 spectrometer, and the resulting spectra were analyzed using GRAMS IQ. Analysis revealed fecal chemistry changes consistent with the on-host phase of the life cycle of *Rhipicephalus (Boophilus) microplus*. Cluster analysis indicates exposure of fecal pats for 12-days in open and shaded habitats during cool and warm

weather periods did not change NIR spectra. NIR spectra from fecal samples can be collected and analyzed by low-cost portable systems and these systems offer the ability to conduct analyses in the field and on demand.

ACKNOWLEDGEMENTS

I would like to thank the members of my committee, Dr. Pete D. Teel, Dr. Michael T. Longnecker, Dr. Sonja L. Swiger and Dr. Donald B. Thomas for their continued guidance and support throughout the entirety of this study. I would also like to recognize the support of my parents, William and Gloria Rich, whose unwavering support encouraged me to always put forth my best efforts. I would like to extend my thanks and gratitude to Dr. Adalberto A. Pérez de León, Dr. John A. Goolsby and all of the staff at the USDA Knipling-Bushland U.S. Livestock Insects Research Laboratory and the USDA Cattle Fever Tick Research Laboratory for their support and hard work supplying materials necessary for the study. I am grateful to Dr. Jay Angerer and all the support staff at the Grazing Animal Nutrition Laboratory for their patience and assistance in working through software and sample issues. I wish to thank my good friends and colleagues here at the Texas A&M Tick Research Laboratory, and in particular Samantha Hayes and Taylor Donaldson, for their immense support and shoulders to cry on. I would like to thank Dr. Kenneth R. Summy, who saw potential in me and will always be missed. Finally, I would like to single out and offer my eternal gratitude to Dr. Donald B. Thomas and Dr. David C. Robacker, who gave me my first opportunity in the field of entomology, and without whose time, patience, constant guidance and friendship I would not be here today.

CONTRIBUTORS AND FUNDING SOURCES

This work was supervised by a thesis advisory committee, consisting of Dr. Pete D. Teel, Major Advisor, and Dr. Sonja Swiger, Professors of Entomology in the Department of Entomology, Dr. Michael T. Longnecker, Professor of Statistics, Department of Statistics, and Dr. Donald B. Thomas, Special Appointment to the committee. Dr. Thomas is a Research Entomologist with the USDA, ARS, U.S. Cattle Fever Tick Laboratory, Edinburg, Texas. Dr. Jay Angerer, Associate Professor, Department of Ecosystem Science & Management and Director of the Texas A&M AgriLife Blackland Research and Extension Center's Grazing Animal Nutrition Laboratory, provided the use of portable spectroscopy equipment and guidance in the use of GRAMS spectral software. Dr. Douglas R. Tolleson, Associate Professor of Range Management, Texas A&M AgriLife Research Station, Sonora, Texas, consulted with the project team on spectral analysis. All of the work for the thesis was completed independently by the student, Mr. Brian Taylor Rich.

This work was financially supported in parts by USDA, ARS, Cooperative Agreement 58-6205-4-012 entitled Cattle Fever Tick Detection by Near Infra-Red Spectroscopy (NIRS) Analysis of Bovine Feces, and by the Texas A&M AgriLife Research Insect Vector Diseases Grant, Project 8911 entitled Technology for Non-invasive Detection of Tick-infested Cattle by Near Infra-Red Reflectance Spectroscopy of Bovine Feces.

NOMENCLATURE

NIRS	Near Infrared Reflectance Spectroscopy
fcNIRS	Fecal Near Infrared Reflectance Spectroscopy
CFT	Cattle Fever Tick(s)
USDA	United States Department of Agriculture
ARS	Agricultural Research Service
CFTEP	Cattle Fever Tick Eradication Program
FCP	Fecal FCP
TAHC	Texas Animal Health Commission
APHIS	Animal and Plant Health Inspection Service
CW	Cool Weather
WW	Warm Weather

TABLE OF CONTENTS

	Page
ABSTRACT.....	ii
ACKNOWLEDGEMENTS.....	iv
CONTRIBUTORS AND FUNDING SOURCES	v
NOMENCLATURE	vi
TABLE OF CONTENTS.....	vii
LIST OF FIGURES	viii
LIST OF TABLES	xiii
1. INTRODUCTION	1
2. STUDY OBJECTIVES.....	10
3. MATERIALS AND METHODS.....	11
3.1 Objective-1 Fecal chemistry change in tick infested animals.	11
3.2 Objective-2 Impact of Environmental Exposure and Age.....	13
3.3 Objective-3 Comparison of portable and benchtop NIR spectrometers	15
4. RESULTS	16
4.1 Objective-1 Fecal chemistry change in tick infested animals.	16
4.2 Objective-2 Impact of Environmental Exposure and Age.....	19
4.3 Objective-3 Comparison of portable and benchtop NIR spectrometers	20
5. CONCLUSIONS AND DISCUSSION	22
REFERENCES	28
APPENDIX A FIGURES	31
APPENDIX B TABLES.....	80

LIST OF FIGURES

	Page
Figure 1. Blueprint with measurements illustrating the blind stalls where stanchions are positioned so that animals are facing East and are able to turn their heads to look out of the stall when the stall door is open	34
Figure 2. Number of engorged female <i>Rhipicephalus (Boophilus) microplus</i> collected per day from cattle infested with six geographic/acaricide resistant tick strains (color coded) on day zero	35
Figure 3. NIRS FCP illustrated by spectrograph. Each peak and valley represents a point of absorption or reflection with the factor loading as the “y” axis and the spectral units (in nanometers) as the “x” axis.....	36
Figure 4. NIRS FCP illustrated by spectrograph	37
Figure 5. NIRS FCP illustrated by spectrograph	38
Figure 6. NIRS FCP illustrated by spectrograph	39
Figure 7. NIRS FCP illustrated by spectrograph	40
Figure 8. NIRS FCP illustrated by spectrograph	41
Figure 9. NIRS FCP illustrated by spectrograph	42
Figure 10. NIRS FCP illustrated by spectrograph	43
Figure 11. NIRS FCP illustrated by spectrograph	44
Figure 12. NIRS FCP illustrated by spectrograph	45

	Page
Figure 13. NIRS FCP illustrated by spectrograph	46
Figure 14. NIRS FCP illustrated by spectrograph	47
Figure 15. Three-dimensional Cluster analysis of daily fecal spectra (576nm – 1226nm) from 6 <i>Bos taurus</i> cattle infested with <i>R. microplus</i> and 6 non-infested <i>Bos taurus</i> cattle over the course of 59 days.....	48
Figure 16. Three-dimensional Cluster analysis of daily fecal spectra (576nm – 1226nm) from 6 <i>Bos taurus</i> cattle infested with <i>R. microplus</i> and 6 non-infested <i>Bos taurus</i> cattle over the course of 59 days.....	49
Figure 17. Three-dimensional Cluster analysis of daily fecal spectra (576nm – 1226nm) from 6 <i>Bos taurus</i> cattle infested with <i>R. microplus</i>	50
Figure 18. Three-dimensional Cluster analysis of daily fecal spectra (576nm – 1226nm) from 6 <i>Bos taurus</i> cattle infested with <i>R. microplus</i>	51
Figure 19. Three-dimensional Cluster analysis of daily fecal spectra (576nm – 1226nm) from 6 <i>Bos taurus</i> cattle infested with <i>R. microplus</i>	52
Figure 20. Three-dimensional Cluster analysis of daily fecal spectra (576nm – 1226nm) from 6 non-infested <i>Bos taurus</i> cattle	53
Figure 21. Three-dimensional Cluster analysis of daily fecal spectra (576nm – 1226nm) from 6 non-infested <i>Bos taurus</i> cattle	54
Figure 22. Three-dimensional Cluster analysis of daily fecal spectra (576nm – 1226nm) from 6 non-infested <i>Bos taurus</i> cattle	55
Figure 23. Three-dimensional Cluster analysis of daily fecal spectra (576nm – 1226nm) from 6 <i>Bos taurus</i> cattle infested with <i>R. microplus</i> from day-1 through day-59	56

	Page
Figure 24. Three-dimensional Cluster analysis of daily fecal spectra (576nm – 1226nm) from 6 <i>Bos taurus</i> cattle infested with <i>R. microplus</i> from day-1 through day-59	57
Figure 25. Three-dimensional Cluster analysis of daily fecal spectra (576nm – 1226nm) from 6 <i>Bos taurus</i> cattle infested with <i>R. microplus</i> collected on day-34 (exposed to elements for 12 days)	58
Figure 26. Three-dimensional Cluster analysis of daily fecal spectra (576nm – 1226nm) from 6 <i>Bos taurus</i> cattle infested with <i>R. microplus</i> collected on day-34 (exposed to elements for 12 days)	59
Figure 27. Three-dimensional Cluster analysis of daily fecal spectra (576nm – 1226nm) from 6 <i>Bos taurus</i> cattle infested with <i>R. microplus</i> collected on day-34 (exposed to elements for 12 days)	60
Figure 28. Three-dimensional Cluster analysis of daily fecal spectra (576nm – 1226nm) from 6 <i>Bos taurus</i> cattle infested with <i>R. microplus</i> collected on day-34 (exposed to elements for 12 days)	61
Figure 29. Three-dimensional Cluster analysis of daily fecal spectra (576nm – 1226nm) from 6 <i>Bos taurus</i> cattle infested with <i>R. microplus</i> collected on day-34 (exposed to elements for 12 days)	62
Figure 30. Twelve-day warm season comparison of temperature, relative humidity and dew point between non-shaded and shaded environments during exposure of fecal pies (days shown as “x” axis, percent/degrees Celsius shown as “y” axis) prepared from the feces of non-infested control cattle and cattle that were infested with <i>R. microplus</i>	63
Figure 31. Twelve-day cool season comparison of light intensity measured in lux between shaded and non-shaded environments during exposure of fecal pies (hours of time shown as “x” axis, lux amount shown as “y” axis) prepared from the feces of non-infested control cattle and cattle that were infested with <i>R. microplus</i>	64

	Page
Figure 32. Twelve-day warm season comparison of temperature, relative humidity and dew point between non-shaded and shaded environments during exposure of fecal pies (days shown as “x” axis, percent/degrees Celsius shown as “y” axis) prepared from the feces of non-infested control cattle and cattle that were infested with <i>R. microplus</i>	65
Figure 33. Twelve-day warm season comparison (July 13 th to July 25 th 2017) of light intensity measured in lux between shaded and non-shaded environments during exposure of fecal pies (hours of time shown as “x” axis, lux amount shown as “y” axis) prepared from the feces of non-infested control cattle and cattle that were infested with <i>R. microplus</i>	66
Figure 34. Three-dimensional Cluster analysis of daily fecal spectra (800nm – 1800nm) from 6 <i>Bos taurus</i> cattle infested with <i>R. microplus</i> from day-1 through day-59 demonstrating that this spectral range yields no separation of spectra.....	67
Figure 35. NIRS FCP illustrated by spectrograph produced by the Ocean Optics NIR-512 spectrometer	68
Figure 36. NIRS FCP illustrated by spectrograph produced by the Ocean Optics NIR-512 spectrometer	69
Figure 37. NIRS FCP illustrated by spectrograph produced by the Ocean Optics NIR-512 spectrometer	70
Figure 38. NIRS FCP illustrated by spectrograph produced by the FOSS 6500 spectrometer.....	71
Figure 39. NIRS FCP illustrated by spectrograph produced by the FOSS 6500 spectrometer	72
Figure 40. NIRS FCP illustrated by spectrograph produced by the FOSS 6500 spectrometer	73

	Page
Figure 41. NIRS raw spectrograph produced by the FOSS 6500 (top) and the Ocean Optics NIR-512 (bottom) spectrometers using the same fecal samples from the infested animals in objective-1	74
Figure 42. Three-dimensional Cluster analysis of daily fecal spectra generated by the Ocean Optics NIR-512 (800nm – 1800nm) from 6 <i>Bos taurus</i> cattle infested with <i>R. microplus</i> from day-1 through day-59 demonstrating that this spectral range yields no separation of spectra	75
Figure 43. Three-dimensional Cluster analysis of daily fecal spectra generated by the Ocean Optics NIR-512 (800nm – 1800nm) from 6 <i>Bos taurus</i> cattle infested with <i>R. microplus</i> from day-1 through day-59 demonstrating that this spectral range yields no separation of spectra	76
Figure 44. Three-dimensional Cluster analysis of daily fecal spectra generated by the Ocean Optics NIR-512 (800nm – 1800nm) from 6 <i>Bos taurus</i> cattle infested with <i>R. microplus</i> from day-1 through day-59 (Days 1-22 indicated in red, all other days in black) demonstrating that this spectral range yields no separation of spectra.....	77
Figure 45. Three-dimensional Cluster analysis of daily fecal spectra generated by the Ocean Optics NIR-512 (800nm – 1800nm) from 6 <i>Bos taurus</i> cattle infested with <i>R. microplus</i> from day-1 through day-59 (Days 24-40 indicated in red, all other days in black) demonstrating that this spectral range yields no separation of spectra.....	78
Figure 46. Three-dimensional Cluster analysis of daily fecal spectra generated by the Ocean Optics NIR-512 (800nm – 1800nm) from 6 <i>Bos taurus</i> cattle infested with <i>R. microplus</i> from day-1 through day-59 (Days 41-59 indicated in red, all other days in black) demonstrating that this spectral range yields no separation of spectra.....	79

LIST OF TABLES

	Page
Table 1. Basic components of pelleted feed from three samples of the pelleted feed from the same lot with components listed on the right and the sample date shown on the top	80
Table 2. Factors 1-25 for each analysis illustrating the cumulative contribution to spectral variance	81
Table 3. Tick Strain Characterization showing the geographic origins of each strain of <i>Rhipicephalus (Boophilus) microplus</i> with the strain, acaricide resistance, geographic origin, generation as of April 2016, number of engorged females produced from a single initialized cohort of approximately 5000 larvae and the survivorship percentage for that cohort	82
Table 4. Summary report of 25 factors derived from eigenvalues generated by GRAMS IQ software after analyzing NIR spectra (Objective-1 spectra, 400nm – 2498nm) from fecal samples of cattle infested with <i>Rhipicephalus (Boophilus) microplus</i> and non-infested cattle using the FOSS 6500 spectrometer	83
Table 5. Summary report of 25 factors derived from eigenvalues generated by GRAMS IQ software after analyzing NIR spectra (Objective-1 spectra, 576nm – 1126nm) from fecal samples of cattle infested with <i>Rhipicephalus (Boophilus) microplus</i> and non-infested cattle using the FOSS 6500 spectrometer	87
Table 6. Summary report of 25 factors derived from eigenvalues generated by GRAMS IQ software after analyzing NIR spectra (Objective-1 spectra, 576nm – 1126nm) from fecal samples of cattle infested with <i>Rhipicephalus (Boophilus) microplus</i> using the FOSS 6500 spectrometer	90
Table 7. Summary report of 25 factors derived from eigenvalues generated by GRAMS IQ software after analyzing NIR spectra (Objective-1 non-infested spectra, 576nm – 1126nm) from fecal samples of non-infested cattle using the FOSS 6500 spectrometer	94

Table 8. Summary report of 25 factors derived from eigenvalues generated by GRAMS IQ software after analyzing NIR spectra (800-1800nm) from fecal samples of cattle infested with <i>Rhipicephalus (Boophilus) microplus</i> using the FOSS 6500 spectrometer	98
Table 9. Summary report of 25 factors derived from eigenvalues generated by GRAMS IQ software after analyzing NIR spectra (800-1800nm) from fecal samples of cattle infested with <i>Rhipicephalus (Boophilus) microplus</i> using the Ocean Optics NIR-512 spectrometer	101

1. INTRODUCTION

Detection of cattle fever ticks (CFT) on cattle is a cornerstone of the U.S. Cattle Fever Tick Eradication Program (Graham and Hourrigan 1977). The most common method employed to detect Cattle Fever Ticks on animals is by using physical senses to look and feel for attached ticks. This process is often referred to as “scratching for ticks” as it involves a scratching action with fingers through the hair coat of animals to feel for the ticks where they attach to the skin. Human tactile sense can detect objects as small as 5mm based on mechanoreceptors and free nerve endings in our fingertips, allowing for detection of most small sized objects like ticks (Sutherst and Wharton, 1978). However, immature stages and unfed adult CFT are 3mm or less (Roberts, 1968). Partially fed nymphs and feeding adults reach the detectable size and still must be distinguished from other objects in the hair coat of cattle such as warts, scabs, dried mud, and dried manure.

Physical scratch inspection of animals to detect CFT isn't perfect and may be negatively impacted by a variety of uncontrollable factors. The process of inspection involves gathering cattle from rangeland or pastures, and herding them through narrow alleyways and chutes where open slats or bars permit inspectors to have access to animals for scratching. Scratching animals also comes with the risk of injury to inspectors. Frequent gathering of cattle for tick inspection and/or treatment can be problematic as ranchers often wish to minimize working cattle to reduce animal stress and production costs. The likelihood of detecting ticks by scratch inspection of cattle does not remain stable through time, but varies dynamically with tick population dynamics, the number of animals inspected, the condition of handling facilities and weather

conditions during inspection (Graham and Hourigan, 1977). The number of animals inspected in a herd depends on the quarantine status, and will range from 100% on infested premises to a small sample size on non-quarantined herds passing through an auction facility.

Stray cattle and other animals that cross the Rio Grande from Mexico may harbor unwanted CFT infestations. The U.S. Department of Agriculture's Animal and Plant Health Inspection Service, Veterinary Services Tick Force monitors the Rio Grande and permanent quarantine zone along the Texas/Mexico border while animal health inspectors of the Texas Animal Health Commission provide surveillance at livestock sale facilities and other venues within Texas. Horse mounted inspectors, known as the "Tick Riders", patrol the Tick Eradication Quarantine Area (TEQA) which runs along more than 200 miles of the Rio Grande from Del Rio, TX to the Gulf of Mexico covering approximately 1,400 square miles (Giles et. al, 2014). These inspectors are responsible for capture, containment, scratch inspection and treatment of stray animals.

The U.S. Cattle Fever Tick Eradication Program was established following historical discoveries linking CFT with pathogens causing a deadly malady among cattle and methods to eliminate ticks from infested premises (Graham and Hourigan 1977). New World explorers and colonists brought cattle along with CFT and pathogens during the 1600's. CFT established across the southern U.S. where there was supportive climate and made expansions northward during the late 1800's as ranchers in Texas drove herds of cattle up to railroad terminals for markets in northern cities.

Cattle in Missouri and Kansas that pastured where the cattle drives passed began to die of a mysterious illness that came to be known as "Splenic Fever", "Texas Fever" and "Texas Cattle Fever" because of its association with Longhorn cattle being driven north from Texas. To

protect their cattle, states along the cattle trails passed quarantine laws routing cattle away from settled areas or restricting the passage of herds to the winter months, when there was less danger from Texas fever (Haley, 1935).

Dr. Daniel Salmon, chief of the Bureau of Animal Industry (BAI), approved a plan in 1884 to investigate the common theory that ticks were responsible for Texas cattle fever. Dr. Theobald Smith and Dr. Frederick Kilbourne ultimately proved and announced in 1893 that *Rhipicephalus (Boophilus) annulatus* acquired a pathogen, *Babesia bigemina*, from cattle sick with Texas Cattle Fever and subsequently transmitted the pathogen to non-infected cattle resulting in clinical disease. It was later discovered that Texas Cattle Fever also involved *R. (B.) microplus* transmission of the pathogen *Babesia bovis* (Curtis and Francis et al., 1892). No other vectors were discovered in the U.S. Furthermore, researchers found that elimination of the tick by cultural farming practices combined with dipping vats to treat animals with acaricides prevented the disease and led to the idea that eradicating the ticks was essential to disease prevention, and the development of the cattle industry throughout the southern U.S. (Graham and Hourrigan 1977). State and federal tick eradication efforts initiated in 1906-1907 slowly removed Texas cattle fever from 14 southern states and California. CFT were declared eliminated north of an established quarantine line along the Rio Grande in 1943 (Malone, 1989). Today, both *Rhipicephalus (Boophilus) annulatus*, the cattle tick, and *Rhipicephalus (Boophilus) microplus*, the southern cattle tick, and the causal agents of Texas cattle fever remain endemic in the Mexican border states of Tamaulipas and Nuevo Leon posing constant threat of re-establishment to the U.S.

The focus of the present study is the detection of cattle infested with *R. microplus*. A review of the biology and ecology of this tick can be found in Núñez et al. (1985) and is briefly

described here. *Rhipicephalus microplus* originated in tropical and sub-tropical forests of India where they prefer to parasitize ungulates including cattle and wildlife species including Nilgai antelope (Angus B. M., 1996). The host range includes horses, goats, sheep and deer.

Rhipicephalus microplus benefit from warm weather, and the ticks ~~and~~ can produce up to six generations per year depending on precipitation, temperature and humidity. These ticks complete the entire parasitic phase of their life cycle on a single host, feeding as larvae, then nymphs and ultimately adults before dropping engorged and gravid females (Cooley, 1946).

Adult mated females lay up to 4,500 eggs in pasture habitats after dropping free from their hosts, with larvae emerging in 14-146 days depending on temperature. After emerging from their eggs, larvae climb vegetation to attach to the next host. Larvae attach to the dewlap, brisket, neck, axillae, groin, abdomen, escutcheon and the genitalia (Legg, 1930). Larvae feed, engorge and molt to the nymphal stage in 7-12 days. Nymphs will reattach, continue feeding and engorge before molting again to the adult stage in 5-17 more days. Adults reattach and feed to complete the final phase of development and mating. Males repeatedly alternate between feeding and mating, remaining on the host until they die. Mated females engorge to their maximum size before detaching from the host. Utech et al. (1978b) estimated the mortality of *R. microplus* during the feeding phase from larvae to successfully engorged females to range from 80-99% depending on cattle breed and other factors.

Through the parasitic phase of development tick increase in size. Núñez et al. (1985) describes that larvae are approximately 0.60mm to 0.66mm long and from 0.40mm to 0.43mm wide. The larvae engorge to around 1.15mm to 2mm long before molting into nymphs. Newly molted nymphs, which are a bit smaller than the fully engorged larvae, are approximately 1mm in length and can engorge to about 2.5mm to 5mm in length. After molting, adult males range in

size between 2mm and 2.5mm with a width of 1.15mm to 1.30mm. Molted females range in size from 2mm to 3.1mm and from 1.1mm to 1.6mm wide. When the females reach a size of 4mm to 6mm (semi-engorged) they await mating before increasing in size to 7mm to 13mm long and 4mm to 8mm wide (engorged). Semi-engorged females are visible on the host at 17 to 18 days post-larval infestation.

Completion of the parasitic phase of the *R. microplus* life cycle from a cohort of larvae infesting cattle produce engorged females over an approximate 3-week period. Hitchcock (1955) reported engorged female drop from 18.9 to 35 days post larval infestation. Núñez et al. (1985) reported females dropped from their host 20.5 to 41 days after infestation. This is consistent with the findings of Legg, who observed that females began to drop from their hosts between the 20th and 35th day (Legg, 1930).

Detection of CFT is essential to surveillance, quarantine, and regulatory treatments as well as clearance and release of quarantined animals and premises. U.S. cattle are naïve to *Babesia* infection and could suffer as much as 80-90% mortality should CFT become re-established (Bram et al. 2002). Infestations of Cattle Fever Ticks, both *R. (B.) microplus* and *R. (B.) annulatus*, in South Texas have significantly increased in recent years, from 19 recognized infested premises in fiscal year 2003 to 146 in fiscal year 2009 (Duhaime, 2009). While inspections have continued along the border for domesticated animals, wildlife continue to be an issue as they freely range across the border and are difficult to assess for tick burden (Perez de Leon et al. 2012).

The United States experienced losses in excess of one-hundred million dollars each year from the two CFT species prior to their eradication (\$2,591,700,000.00 in adjusted dollars today), and it is estimated that a reintroduction would produce losses in excess of one billion

dollars annually (APHIS, 2010). CFT eradication in the U.S. is estimated to have saved the cattle industry 3 billion dollars annually since the U.S. was declared free of bovine babesiosis and CFT (Graham and Hourrigan, 1977). In Mexico, the ticks are a limiting factor for national mobilization, export of live cattle to the United States and other countries; and for the introduction of highly specialized breeds. Costs from attempting to control *R. microplus* in Mexico total more than 573 million U.S. dollars annually (Rodríguez-Vivas et al. 2017).

Re-establishment of CFT in the Southern U.S. poses significant economic risks to the cattle industry. Cattle and calves rank among the top five agricultural commodities in nine of the 13 Southern Region states with cash receipts ranging from 5.3% (Florida) to 46% (Oklahoma) of all agricultural commodities. Texas ranks 6th in overall value of agricultural exports with cash receipts from cattle and calves totaling in excess of \$10 billion (TDA, 2012). The cost of a relatively small fever tick outbreak outside of the quarantine zone in Texas could be as high as \$123 million in the first year, including capital costs and ongoing variable, annual costs (Anderson, 2010). U.S. cattle are naïve to *Babesia* infection and could suffer as much as 80-90% mortality should CFT become re-established (Bram et al. 2002).

Infestations by ectoparasites like *R. microplus* cause physiological stress on the part of the host as it attempts to counter the parasite (Sonenshine and Roe, 2013). Reducing stress on livestock during handling is intended to reduce sickness and enable cattle to go back on feed more quickly (Grandin et al., 1998). During the blood feeding process, *R. microplus* secretes saliva into the feeding lesion to maintain blood flow and evade countermeasures by the immune system. Several authors have summarized the effects of tick saliva. “Tick saliva contains an array of pharmacological compounds that include immune-modulators, inhibitors of pain/itch

response, anticoagulants, inhibitors of platelet aggregation, and vasodilatory molecules, all of which contribute to both successful feeding and what is essentially an outright defeat of the host immune and hemostatic defenses” (Ribeiro, 1995). ”Various elements of host immune defenses modulated by bioactive compounds that have been characterized in tick saliva include the diminished killing activity of natural killer cells” (Kubes et al., 2002), “inhibition of T-lymphocyte *in vitro* proliferation” (Schoeler and Wikel, 2001), “suppression of the production of pro-inflammatory cytokines, and induction of a polarized Type 2 immune response” (Brossard and Wikel, 1997). *Rhipicephalus microplus* is capable of effectively neutralizing the host immune response so that it may remain attached and feed unabated, free from processes that might close the feeding lesion. Studies of tick saliva have demonstrated that it has the capability of preventing angiogenesis, preventing the host from shunting blood flow away from the feeding lesion, and include cytotoxic and cytolytic properties that act against various cell types (Sousa et al., 2015). This does not mean that the host's body stops trying to counter the parasite, only that it is effectively a zero sum game. Products to counter the parasite are still produced; steroids and hormones are still dumped into the system and energy is expended in an attempt to overwhelm the parasite. Depending on the size of the tick infestation, this can put a noticeable strain on the host as evidenced by weight loss and other physical symptoms (Little, 1963). The host is not only suffering a reduction to total available resources in the form of blood loss, but also in the resources needed to produce anti-tick products like clotting factors and immune proteins.

There are more than 36,000 known tick salivary proteins from ticks in the family Ixodidae (Tirloni et al., 2014) with many genus specific proteins that can effectively limit host response. For example, *Rhipicephalus (Boophilus) microplus* uses the “Boophilin” protein, an enzyme that can inhibit the activity of Thrombin, Trypsin, Factor Xa, Factor XIIa, Plasma

kallikrein, Factor VIIa, Plasmin, u-PA, sc-tPA and Tryptase (Sandra Macedo-Ribeiro et al., 2008). Due to the manner in which different tick taxa use their salivary products to counter immune responses (Mária Kazimírová et al., 2013), these products would likely differ depending on the variety of tick involved. While the pathways between immune-modulation on the part of *R. microplus* and the physiological stresses this tick can induce in their hosts is poorly understood, it may be possible to detect these stresses with the help of emerging technologies like NIRS.

The Near Infrared spectrum (NIR) refers to long wavelengths outside the visual range, from around 780nm to approximately 2500nm in length. NIR wavelengths from 850nm to 1250nm are of particular importance as absorbance in this region can be used to identify pure substances and is known as the “fingerprint region”, so-called because different compounds produce different and specific spectra when exposed to NIR (Klein, 2015). Near Infrared Reflectance Spectroscopy (NIRS) functions by focusing an infrared source, typically a laser, on a substance and then analyzing the light reflected back to a detector. NIR wavelengths are partially absorbed by organic molecules causing a vibration as they bend/stretch. By measuring the reflectance as an indirect measure of NIR absorbance, specific chemical properties of organic molecules can be determined.

Commercially available NIRS systems are relatively inexpensive, accurate and are capable of delivering rapid results (approximately 35-50 seconds on the Ocean Optics reflection probe) while operating in a wide range of environmental conditions (-20°C to 80°C). There is no need for invasive procedures that can potentially alter or destroy samples using NIRS as only the surface of samples will be scanned with some minor penetration depending on pack size and

shape of particles (Coates, 2000). In addition, unless the sample is sensitive to infrared light the sample can be scanned repeatedly with only a small increase in temperature.

NIRS benchtop spectrometers like the FOSS 6500, can perform rapid scans to a relatively high degree of NIR sensitivity. For example, the FOSS NIRSystems model 6500 (6500, FOSS Analytical, Slangerupgade, Denmark) can perform 1.8 scans every second of operation at wavelengths from 400nm to 2500nm. It can also be operated with minimal training as the software provided, Spectra Suite (Ver. 1.5.2., Ocean Optics Inc, Dunedin, Florida), is intuitive and easy to use. The benchtop method does require drying and milling of fecal material before analysis. This means that despite its speed, the benchtop spectrometer will require time to dry, grind and prepare samples before it can be employed, but is ideal for operations in which large numbers of samples need to be scanned.

The Ocean Optics spectrometer to be used for this study (NIR-512, Ocean Optics, Winter Park, Florida) offers the ease of portability with the ability to process both wet and dry (raw/processed) samples in a rapid fashion for wavelengths of 800nm to 1800nm. The NIR-512 requires the use of an external light source, and in this case a Mikropack HL-2000 halogen light source (Mikropack, Ocean Optics, Winter Park, Florida) was used. Depending on hardware limitations, the software can process reflectance data in approximately thirty-five to fifty seconds at wavelengths from 360nm to 2000nm. Because the device requires a light calibration before use, it can be employed in a wide range of light levels and even outdoors.

2. STUDY OBJECTIVES

1) Determine the threshold and magnitude of fecal chemistry change due to infestation by the Southern Cattle Tick, *Rhipicephalus (Boophilus) microplus*. 2) Determine whether fecal-chemistry profiles (FCP) of feces from cattle infested with *R. microplus* change in response to environmental exposure and age of fecal samples. 3) Compare fecal NIR spectra obtained from fecal NIRS between the Ocean Optics portable spectrometer and the benchtop FOSS 6500 NIR System spectrometer.

3. MATERIALS AND METHODS

3.1 Objective-1 Fecal chemistry change in tick infested animals.

Fecal samples were collected during a prior experiment involving 6 heifers each infested with *R. microplus* and 6 non-infested control animals (IACUC Approved Protocol# 2015-10A/2015-10B/2016-2025 10B Rev) at the USDA, ARS, Cattle Fever Tick Research Laboratory, Edinburg, TX. The 6 infested cattle were scheduled to be infested with a single strain of *R. microplus*, however it was later discovered that each animal was infested with a single and different strain of *R. microplus*. The six tick strains of *R. microplus* were defined by geographic origin and by type and degree of acaricide resistance. The strains were identified by name as Deutch, Las Palmas, Fipronil, Lajas, San Alfonso, and Santa Luiza. Summary characteristics of each tick strain, including duration in colony, are provided in Table 3. Twelve heifers weighing 134 kg to 188 kg of *Bos taurus* breeding, and having no prior experience with ticks were utilized in the study. The animals were pre-conditioned as a cohort. They received vaccinations that included Bovi-Shield Gold (IBR, BVD I and II, P13, and BRSV) per label instructions (2ml vaccine IM per animal)(Bovi-Shield Gold, Zoetis Animal Health, Parsippany, New Jersey), Vision 8 + Spur (blackleg, red water, and H. Somnus) per label instructions (2ml vaccine SQ per animal) (Vision 8 + Spur, Merk Group, Darmstadt, Germany) and were boosted 21-28 days later with a repeat dose per label instructions (2ml vaccine SQ per animal). They each received an oral treatment with 10 g Safe-guard Paste dewormer (fenbendazole 10%) (Safe-Guard, Merk Group, Darmstadt, Germany)per label instructions, and a subcutaneous treatment with LA200 (Liquamycin LA-200, Merk Group, Darmstadt, Germany) per label instructions (4.5ml per 45.4 kg). They also received Vitamin AD (Vitamin AD₃ Injectable, AgriLabs, St. Joseph, Missouri)

per label instructions (2ml IM injection per animal). Evaluations for *Babesia* infection were made using a nested PCR test with the first amplification with *Babesia* specific primers and the second with *B. bovis* and *B. bigemina* specific primers (Guerrero, F. D , et al., 2007). The animals were acclimated to the testing site first in a paddock on the dietary ration (see Table 1).

The animals were randomly assigned to either an infested or non-infested treatment group (6 animals per group), and randomly assigned to an individual stall in the testing barn (Figure 1). Fecal samples weighing approximately 450 grams were retrieved from each cow stall for twenty days before infestation and for the forty-three days during infestation. Samples were placed into large zip-lock bags, labeled as to cow number and date, frozen at -20C until being shipped to the Tick Research Laboratory, Texas A&M AgriLife Research, College Station, TX.

Fecal material was allowed to thaw for 24 hours before being placed into 15 X 9 centimeter paper boats and labeled with cow number and collection date. Labeled samples were then placed into a drying oven (Isotemp 737F, Thermo Fisher Scientific Inc, Waltham, Massachusetts) at 60°C for 72 hours before being milled into 1 mm particles in a laboratory mill (UDY Cyclone model 3010-039, Fort Collins, CO). The milled fecal material was placed into labeled coin envelopes (size and Company) and taken to the Texas A&M AgriLife Grazing Animal Nutrition Laboratory (GAN) in Temple, TX, where spectroscopic analysis was performed using a Foss® NIRS 6500 series scanning spectrometer with spinning cup attachment (FOSS Analytical, Slangerupgade, Denmark). Spectral data were sent to the Tick Research Laboratory for analyses using GRAMS (Graphical Relational Array Management System) spectroscopy software suite (Ver. 9.3, Thermo Fisher Scientific Inc, Waltham, MA). Stepwise cluster analyses were completed using the raw spectra from all 12 animals, spectra from control animals compared

with those from infested animals, and spectra from infested animals compared to spectra from their respective pre-infestation periods.

The discriminate analysis was run using a cross-validation calibration type and with a standard normal variate de-trending process. Baseline effects were removed from the model by use of the 1st derivative of the spectra and using the Savitzky-Golay method.

3.2 Objective-2 Impact of Environmental Exposure and Age.

Bulk fecal samples (approximately 1kg) were collected from the stalls of infested and non-infested control animals during a 24-hour period 24 days post-infestation to provide adequate quantities of feces for the age-exposure investigation. The fecal collection date corresponded to the peak period of engorgement of adult *R. microplus*. Samples were frozen at -20C and shipped to the Tick Research Laboratory for use in the fecal age-exposure study. Thawed samples were placed into aluminum pie tins with a capacity equal to that needed for multiple spectral analysis (14.6 cm x 3.8 cm deep pot pie tin). Three sets of nine “pies”, six from animals infested with *R. microplus*, as well as three controls from the non-infested animals were used in testing for shifts in fecal chemistry when examined by NIRS. Pies were made by depositing fecal material into the aluminum pie tins to ensure even size and consistency so that six even aliquots could be obtained. Pie tins were labeled with the cow number, and either “S” or “O” for “Shaded” and “Open” exposure.

Two trials were conducted to assess the impact of age and exposure on NIR spectra. The first study was initiated on 1 March 2017 and designated the “cool season study” and the second study was initiated on 15 July 2017 and designated the “warm season study”. Two treatment levels of environmental exposure were created for these trials in a Bermuda grass paddock

located behind the Tick Research Laboratory. One exposure level was unshaded open exposure and the other a shaded exposure, created by suspending a canopy of polypropylene landscape fabric (RSI Premium Landscape Fabric, Riverstone Industries Corporation, 40 Richboynton Road Dover, NJ 07801) over the top and sides of the samples to prevent sunlight from reaching them.

Pies were randomized for placement in a 1-meter by 1-meter test area for each treatment to eliminate variability based on spatial location. In addition to the pies, a hygrometer, thermometer and light sensor, HOBO model UA-002-08 and HOBO Pro v2 model U23-00x (Hobo logger, Onset Computer Corporation 470 MacArthur Blvd. Bourne, MA 02532) was employed for each sample area to record environmental conditions throughout the study.

The pies were sampled by removing wedges measuring taken on exposure day 2 and every other day (days 4, 6, 8, 10 and 12). Wedge samples were first harvested from an arbitrary point at the end of the tin, with subsequent samples taken from the opposite side of the pie from each new wedge to minimize a sample edge effect from exposed pie wedges. To further reduce edge effect, only the inner portion of the wedge was retained for analysis.

Wedge samples were placed into paper boats and labeled with the cow number, sample date, “S” or “O” for shade or open treatment, and a designator for either “warm season” or “cool season” study before being dried for seventy-two hours in a drying oven at 60°C. Dried samples were ground into particulates measuring no more than one mm using a laboratory mill (UDY Cyclone model 3010-039 , Fort Collins, CO). Ground samples were scanned with the portable Ocean Optics NIR 512 spectrometer (Ocean Optics NIR 512, Ocean Optics, Inc. 830 Douglas Ave. Dunedin, FL 34698 USA) equipped with QR400-7-VIS-BX probe. Three scans per sample were performed with the probe set just above the sample surface (approximately 1mm-2mm).

Spectral data were captured using Spectrasuite software (Spectrasuite ver. 2.0.162, Ocean Optics inc, Largo FL) and saved as a common .spc file that could also be used with our analysis software. The ground sample was then taken to the GAN Laboratory to be analyzed using the FOSS 6500 NIRS spectrometer (FOSS 6500, FOSS Analytical, Slangerupgade, Denmark).

3.3 Objective-3 Comparison of portable and benchtop NIR spectrometers

Spectra generated by the Ocean Optics were first captured using Spectra Suite and saved as common spc files before being collated into a training set for use with GRAMS IQ. Spectral data collected with the portable and benchtop spectrometers were analyzed using GRAMSIQ (GRAMS Ver. 9.3, Thermo Fisher Scientific Inc, Waltham, MA). Spectra were analyzed for variation among spectra, and then subjected to cluster analysis to compare the results by instrument type. Due to the limited spectrum from the portable probe a spectral range of only 800nm-1800nm), an accurate comparison will include the same spectral range on the benchtop spectrometer.

4. RESULTS

4.1 Objective-1 Fecal chemistry change in tick infested animals.

The complete tick drop data for engorged females from each animal identified by infesting strain is summarized in Figure 2. Raw spectral data from daily fecal samples of all 12 animals were analyzed using GRAMS IQ by discriminate analysis using a cross validation calibration type, with a standard normal variate de-trending process. Baseline effects were removed from the model by use of the 1st derivative of the spectra and using the Savitzky-Golay method. This method sorts the spectra by variation, looking at the entirety of the spectra, finding the most common variations, and assigning each variation as a primary “factor”. Each of the factors represents a unique FCP with successive factors representing FCPs with different chemistries (Figure 3 - 14). Once the first factor was assigned the software examines the remaining spectra to find the next most common variation and assigns that as the next factor. The software repeats this process for the remaining spectra until all the possible variations are identified (Figure 4 Figure 14). Factors are listed from 1 to 25 with the most common variations listed first and less common variations listed last. Cluster analyses can be performed with the three most common variations plotted as “x”, “y” and “z” provide a basis for comparative assessments. Statistics for the process can be found in tables 4 - 7. In the calculations performed by the GRAMS IQ software, eigenvalues are generated for each factor. These eigenvalues, a measure of the relative weight of a given factor, are a measure of the importance of the factors statistically. Using the total percent variance for each factor allows for a determination of the maximum number of factors that fit a model by calculating when the total reaches 100%, signifying that all variation has been accounted for by the listed factors.

Initial analyses of the bovine fecal samples examined the entirety of the NIR spectra as well as part of the visible spectrum (400nm to 2498nm). This resulted in a model that was not reliable, as the first three factors were only representative of 54.2% of the total spectral variation (Figure 3 – 5).

The spectral range was then progressively limited through a series of analyses in order to maximize the contributing spectral range while mitigating the effects of non-contributing spectral range (noise). Repeated analyses were conducted using limited portions of the spectral range starting by examining the peaks and valleys, regions that exhibited high and low levels of reflectance, and whose first three factors explained the greatest amount of variation. The spectral region that yielded the most contribution to the first three factors was within the 576nm to 1126nm range. Within this narrowed spectral range, the first three factors explained 94.7% of the total variation among sample spectra (see Figure 6 - 8). With the majority of the variation represented by those first three factors, the sample spectra were analyzed by cluster analyses.

Sample spectra were identified by the same unique identifier in GRAMS IQ as they had for the physical samples, allowing for the changes in fecal chemistry over time to be observed. Sample spectra from the six control animals were expected to exhibit minimal fecal chemistry change over time, as they were all on a uniform diet and not subject to infestation by *R. microplus*. If the hypothesis was to be proved correct, the six tick infested animals would demonstrate a change in fecal chemistry and cluster separations reflecting the life cycle of the ticks; while the control spectra were not expected to change.

Sample spectra in the narrowed wavelength 576-1126nm showed distinct separations within the cluster analysis. However, sample spectra for control animals followed the same separations indicating similar shifts in fecal chemistry as those from the infested animals.

Sample spectra clusters from the non-infested animals were almost indistinguishable from those of the infested animals (see Figures 18 through 21).

An alternative analysis was conducted using daily fecal spectra from the pre-infestation period with each tick-infested animal using its own pre-infestation samples as its respective control. The days observed that make up the majority of variation within the spectra occur from day 1 to day 21 and we identify it as the Low Stress period. This period of time includes the pre-infestation period and ten days post infestation accounting for the larval and early to mid nymphal feeding periods (Núñez et al., 1985). Since all the animals had been kept on a uniform diet (see Table 1), the option to use each animal's pre-infestation period as a control was viable (Tolleson et al., 2007).

Analysis of sample spectra (576-1126nm) from the 6 tick-infested animals, including the pre-infestation and infestation periods, produced 11 factors with the first three representative of 87.9% of total variance among spectra (Figure 9 – 11). The cluster analysis of the sample spectra from the infested animals resulted in three distinct clusters. The first cluster was comprised from samples originating from day-1 to (12 days prior to infestation) through day-22 (12 days post infestation), corresponding with the period of time in which larval and nymphal feeding would be taking place on the host (Figure 17). The second cluster was comprised of samples within the period of time from day-24 (14 days post infestation) to day-35, corresponding to the time when it is expected to find meta-nymph and early adult feeding (Figure 18). The third cluster is comprised of samples from day-41 through the end date of day-59 (the period of time when we would expect about half of the engorged females to have completed feeding, and drop from the host, to drop completion for all surviving females) (Figure 19). We have denoted these clusters as “low stress”, “stress” and “decreasing stress” as they

occur chronologically in the time periods for which there would be no/low feeding, heavy feeding and a period of reduced feeding to a cessation of feeding. The results of cluster analysis of the non-infested animals yielded similar results to those of the infested animals (Figure 20 – 22). The first three factors under the narrowed spectrum resulted in 87.4% representation of all variation among non-infested spectra (Table 2).

4.2 Objective-2 Impact of Environmental Exposure and Age.

Analyses for objective-2 spectra followed the same processes as the spectra for objective-1, with analysis using GRAMS IQ by discriminate analysis using a cross validation calibration type, with a standard normal variate de-trending process. Baseline effects were removed from the model by use of the 1st derivative of the spectra and using the Savitzky-Golay method. Objective-2 spectra (warm and cool season, exposed and shaded) from the first 24 hours of exposure were included in a new cluster analysis with the objective-1 spectra. Since the objective-2 spectra came from the samples used on day-34 of the objective-1 study (mother samples), then any degradation or change in fecal chemistry as a result of environmental exposure would result in a shift away from the day-34 spectra. The spectra did not exhibit this behavior, and clustered with the original spectra from day-34 in the objective-1 study (Figure 23 and Figure 24).

Spectra from the cool-season study was analyzed for differences between exposed and shaded treatments (Figure 25), but no separation of spectra occurred and samples clustered together. The same process was performed for the warm-season study with similar results (Figure 26). Spectra from the cool-season and warm-season studies were analyzed together with the total variation among spectra for the first three factors representing 91.1%, and demonstrated

no separation of spectra. Spectra from the cool and warm-season studies were also analyzed to determine if there was a separation based on age. Cool-season spectra (exposed and shaded treatments) from the first six days of exposure were compared to the spectra from the remaining days of exposure, but there was no separation of spectra with spectra from all 12 days of exposure clustering together (Figure 28). Spectra from the warm-season study (exposed and shaded treatments) was analyzed in the same way with spectra from the first six days of exposure clustering with the spectra from the remaining days of exposure. These analyses indicate that there is no discernable difference, by fcNIRS, between exposed samples from either the cool-season or warm-season out to 12 days of exposure and the original samples from the threshold study (mother samples).

4.3 Objective-3 Comparison of portable and benchtop NIR spectrometers.

The Ocean Optics NIR-512 spectrometer was discovered to be pre-set at purchase to read NIR spectra between 800nm-1800nm. The spectral range of the NIR-512 spectrometer did not match the optimal spectral range for fecal analysis determined using the FOSS 6500 spectrometer (576nm-1126nm) in objective-1. Thus the raw spectra were analyzed using both instruments within the spectral range 800nm-1800nm to compare corresponding discriminate cluster analyses from each instrument.

The first three factors for 800nm-1800nm spectra generated by the FOSS 6500 (Figure 38 – 40) represented 87.9% of the total variation among spectra. Factors 1-3 represented 58.4%, 21.4% and 12.6%, respectively. Using these 3 factors, there was no visible cluster separation evidenced by two slightly different 3-dimensional view rotations illustrated by Figures 33 and 34. The first three factors for 800nm-1800nm spectra generated by the Ocean Optics NIR-512

(Figure 35 – 37) were representative of 89.5% of the total variation among spectra. For this instrument, factors 1-3 represented 69.8%, 13.5% and 3.8% of variation, respectively. The second and third factors were representative of a much smaller amount of total variation (13.5% 3.8%) compared to the much higher percent of variation for the same factors generated by the FOSS spectra (21.4% and 12.6%). Using these three factors, there was no visible cluster separation evidenced as illustrated in Figure 42 - 43. A comparison of spectral resolution of the raw spectra produced by each spectrometer is illustrated in Figure 41. The spectral resolution produced by the NIR512 produced jagged, rough FCPs from the NIR exposure different from the smooth resolution produced by the FOSS 6500 spectrometer.

5. CONCLUSIONS AND DISCUSSION

The cluster analysis used primary factors that had the highest representation of spectral variation for the first three FCPs so that those FCPs could be appropriately mapped to the “x”, “y”, and “z” axes, and demonstrate any shifts in fecal chemistry from one axes to the next as they occurred chronologically. Each peak and valley (areas of reflection and absorption) in the raw spectra was analyzed in order to determine how much they contributed to the spectral variation for the first three factors. By narrowing the spectral range, the maximum contributing range was found to be (576nm – 1126nm), and it was possible to eliminate non-contributing wavelengths (noise). All these processes allow for visualization of chemistry changes in the daily collected fecals chronologically.

Spectra from the infested animals appear to follow chronologically the parasitic phase of the life cycle of *R. microplus*, with the first cluster shift occurring during the late nymphal and early adult feeding (day-20 or day-21 with adjustment for the 72-hour rumen passage time). This shift occurs when three animals that dropped first (64, 68, 72) had dropped half, or more than half, of the total females they produced. The remaining animals at that time were about to reach the halfway point for the total females that dropped. This suggests that the shift may be related to a slowing or cessation of blood feeding.

Host attempts to combat tick burden may be considered a “cost of fitness” (Tolleson et. al, 2011) and as tick burden decreases, so should the drain on available host resources. This would not only have the effect of lessening the blood imbibed by the ticks, but also the saliva that they secrete into the host. It then makes sense as to why there is a cluster shift at approximately 22 days post-infestation when half of the replete females have dropped (or are

about to drop). There are metabolic, endocrine and immune consequences as a result of tick mediated protein-energy loss (Tolleson et al., 2011). Under real world conditions hosts acquire ticks throughout the season of activity depending upon grazing behavior through infested habitats and may also acquire multiple tick species. A natural infestation would likely produce a cumulative, and perhaps sustained effect on fecal chemistry. Using a single infestation of approximately 5000 larvae to infest each animal made it far more likely that the surviving ticks were in numbers sufficient to cause a fecal chemistry change. Before studies into staggered, cumulative infestations consisting of all parasitic phases of *R. microplus* can occur, it is necessary to estimate the impact of a single cohort. The design used here also provided insight into the generalized fecal chemistry changes occurring from infestation by a single species, as well as when those changes occurred. Improvements to the experimental design should include a barn layout that permits the animals to see each-other to minimize the possible impacts of empathy stress, while maintaining biosecurity that ensures that non-infested animals do not become infested.

Detection of *R. microplus* is critical to surveillance and operations of the CFTEP in securing the US from Texas cattle fever. It is unknown at this point whether it is possible to identify cattle co-infested with multiple tick species that include *R. microplus*. Cattle in this region are subject to multiple-species infestations including *Amblyomma americanum*, *A. maculatum*, *A. tenellum*, *A. mixtum*, *Otobius megnini*, *Dermacentor variabilis*, and *D. albipictus*. There are more than 3,600 unique salivary proteins identified from Ixodid ticks (Tirloni et al., 2014) Some of these proteins, such as Boophilin, are unique to *R. (Boophilus)* ticks. Boophilin is thought to act as an inhibitor the activity of Thrombin, Trypsin, Factor Xa, Factor XIIa, Plasma kallikrein, Factor VIIa, Plasmin, u-PA, sc-tPA and Trypsase (Sandra Macedo-Ribeiro et al.,

2008). How these proteins are used and whether they would create resulting fecal chemistry changes detectable by NIRS remains to be determined.

The discovery that the 6 infested animals were each infested with a separate strain of *R. microplus* provided an opportunity to observe variation within the species and measure the responses accordingly, although without replication within strain. This does not invalidate the study as each strain is still *R. microplus*, and merely provides a range of variation within that species. Taking into account, the range of survivorship, 8% - 77%, this gives us a range of infestation severity that is potentially useful when considering how many ticks are needed to trigger a change in fecal chemistry.

The similarity of cluster analyses between infested and non-infested control animals in this study were of particular concern and not expected. The fecal spectra over time demonstrate chemistry shifts consistent with progressive phases of blood feeding by immature ticks to adult feeding on infested animals. . Under the optimized spectral range, the spectra from non-infested animals appeared to mimic the cluster shifts of the spectra from the infested animals. There was no evidence indicating that non-infested animals were indeed infested. The reason as to why the non-infested animals were experiencing the same stress response as the infested animals may be due to isolation of individuals in blind stalls following their social acclimation of the 12 animals together during pre-conditioning.

USDA personnel noted regular nocturnal vocalizations among the 12 project animals during their isolation in the barn. Similar shifts of NIR fecal spectra among the non-infested animals to those of infested animals suggest that non-infested animals were somehow stressed in a similar way to the infested group. Ongoing, complimentary analyses of the fecal samples of infested and non-infested animals to compare changes in amino acids and other organic

compounds by gas chromatography and mass spectroscopy, as well as fecal microbiome analyses may provide further comparisons. The 12 animals had been raised together as a single cohort, and then separated and isolated for the study. The layout of the barn they were housed, (Figure 1) had each animal isolated in a blind stall, where they were unable to see each-other. This means that the only social interaction they had with other animals was from what the animals could hear. Given that half their number were experiencing a CFT infestation, it is possible that the non-infested animals were simply empathizing the stress response of their infested counterparts. By not being able to see the other animals, but hearing their distress due to infestation, it seems likely that the non-infested group may have experienced a “placebo” non-infestation, given that they could only hear the distress of infested animals. Cattle often interpret strange sights or sounds as a sign of danger (Grandin, 1993a), and sequestered away from the other calves was likely conducive to this kind of stress. Barn and stall design may be an important variable, and animals should be able to see each other to mitigate social stress in future experimental designs as much as possible with consideration given to bio-security (preventing non-infested animals from becoming infested).

NIR spectra of feces from *R. microplus*-infested animals exposed to cool and warm season variables of heat, light and moisture did not affect spectral clustering for the experimental period of 12 days exposure. This finding suggests there is stability in fecal chemistry detectable by NIRS. Differences between ageing studies and “exposed vs shaded” may be present, but do not appear to represent significant differences between ageing samples and the original samples. Using the original fecal source (objective-1) cluster analysis as a control shows that regardless of age, the environmentally aged fecal spectra (objective-2) still cluster with the original samples (Figure 23). It is only when examined with a much smaller sample size, each ageing study alone,

that some outliers appear. This would seem to indicate that while differences may be perceived between study samples on the basis of age, these differences are not enough to separate them when combined with the original fecal source. New variables, UV light exposure as well as exposure to insect activity (dung beetles, fly larvae) should be tested in the future, so as to determine if spectra separation found in the warm weather spectra on day-5 and day-6 are anomalous or caused by variables not tested.

The spectral range of the Ocean Optics NIR-512 spectrometer that was available for this study was limited to 800nm-1800nm. This precluded this instrument from evaluating fecal spectra within what was determined to be the optimal spectral range of 576nm-1126nm using the FOSS 6500 spectrometer. The 800-1800 spectral range reduced the optimal 576-1126 range, that included wavelengths that did not contribute to spectral separation on one end, and eliminated wavelengths that did contribute on the other. This has the effect of adding non-contributing spectral wavelengths (noise) to the analysis. Resolution, as shown in Figure 41, appears to be the primary point of difference between spectrometers. The NIR-512s accuracy is mitigated by things like ambient light, failure to properly calibrate for current light levels, distance from sample material and quality of the reflectance light source. In the FCPs shown in Figure 35 – 37, there is a jaggedness illustrated that appears the result of variables in the NIR-512 that are not present in the FOSS-6500 in Figure 38 – 40. In the case of the FOSS 6500, only NIR wavelengths are emitted onto the sample using a specialized bulb that does not vary in intensity and is monitored by self-calibration. The FOSS 6500 also uses specialized cups that limit reflection to the sample alone and do not permit ambient light to contaminate scans. This allows for more precise measurements, that were difficult to obtain with the NIR-512 model available for this experiment.

In summary, the use of NIRS indicates that fecal chemistry changes as a result of infestation by *R. microplus* and that detection is consistent with blood-feeding phase of the on-host portion of the life cycle. Under exposure to the open environment, those changes are still detectable at the conclusion of the twelve-day experimental period. The FOSS 6500 was superior to the Ocean Optics NIR-512 spectrometer for fecal NIR spectral analysis within the limited spectral range, but modification to spectral range and improved sensitivity of newer portable NIR spectrometers could have the potential to put them on par with benchtop devices for applications in field-based fecal spectroscopy.

REFERENCES

- Angus, B.M. (1996).** *The history of the cattle tick Boophilus microplus in Australia and achievements in its control.* International Journal for Parasitology, 26(12), 1341-1355. doi: 10.1016/s0020-7519(96)00112-9
- Bram, R. A., George, J. E., Reichar, R. E., and Tabachnick, W. J. (2002).** *Threat of foreign arthropod-borne pathogens to livestock in the United States.* Journal of Medical Entomology. 39.405-416
- Brossard, M., Wikel, S.K., (1997).** *Immunology of interactions between ticks and hosts.* Med. Vet. Entomol. 11, 270–276.
- Cooley, R. A. (1946).** *The Genera Boophilus Rhipicephalus, and Haemaphysalis (Ixodidae) of the New World.* Washington: National Institutes of Health Bulletin No. 187, 1–54.
- Controlling Cattle Fever Ticks. (2010, August).** Retrieved September 12, 2017, from https://www.aphis.usda.gov/publications/animal_health/content/printable_version/cattle_fever_ticks.pdf
- Curtis, C., and Francis, M. (1892).** *The Cattle Tick: Biology, Preventive Measures.* Bulletin No. 24. College Station, TX: Texas Agricultural Experiment Station.

Coates, D. B. 2000. *Faecal NIRS – What does it offer today’s grazier?*

Trop. Grassl. 34:230–239.

Graham, O. H., and Hourrigan, J. L. (1977). *Eradication programs for the arthropod parasites of livestock.* J. Med. Entomol. 13, 629–658.

Grandin, T. (1993). *Handling facilities and restraint of range cattle.* *Livestock Handling and Transport.*, 103-125

Grandin, T., Oldfield, J., & Boyd, L. (1998). *Review: Reducing Handling Stress Improves Both Productivity and Welfare.* The Professional Animal Scientist, 14(1), 1-10. doi:10.15232/s1080-7446(15)31783-6

Guerrero, F. D., Bendele, K. G., Davey, R. B. and George, J. E. (2007). *‘Detection of Babesia bigemina infection in strains of Rhipicephalus (Boophilus) microplus collected from outbreaks in south Texas.’, Veterinary parasitology, 145(1–2), pp. 156–63. doi: 10.1016/j.vetpar.2006.11.014.*

Haley, J. E. (1935). *Texas fever and the Winchester quarantine.* Canyon, TX: Panhandle-Plains Historical Society.

Hitchcock, L. (1955). Studies on the parasitic stages of the cattle tick. *Boophilus Microplus* (Canestrini) (Acarina: Ixodidae). *Australian Journal of Zoology*, 3(2), 145.

doi:10.1071/zo9550145

Hoogstraal, H., and Aeschlimann, A. (1982). Tick-host specificity. *Bull. Soc. Entomol. Suisse* 55, 5–32.

Kazimírová, M., & Štibrániová, I. (2013). Tick salivary compounds: Their role in modulation of host defences and pathogen transmission. *Frontiers in Cellular and Infection Microbiology*, 3.

doi:10.3389/fcimb.2013.00043

Kubes, M., Kocakova, P., Slovak, M., Slavikova, M., Fuchsberger, N., & Nuttall, P. A. (2002). *Heterogeneity in the effect of different ixodid tick species on human natural killer cell activity.* *Parasite Immunology*, 24(1), 23-28. doi:10.1046/j.0141-9838.2001.00434.x

Little, D.A., (1963). *The effect of cattle tick infestation on the growthrate of cattle.* *Aust. Vet. J.* 39, 6.

Legg J. (1930). Some observations of the life history of the cattle tick (*Boophilus australis*). *Proc. Roy. Soc. Queensland* 41: 121-132.

Logue, J. N. (1995). *Beyond the Germ Theory – The Story of Dr. Cooper Curtice.* College Station: Texas A&M University Press.

Malone, J. B. (1989). Texas fever, two-headed calves and the Hatch Act – 100 years and counting for veterinary parasitology in the United States. *Vet. Parasitol.* 33, 3–29.

Núñez, J. L., Muñoz-Cobeñas, M. E., & Moltedo, H. L. (1985). *Boophilus microplus: The common cattle tick*. Berlin: Springer.

Olafson, P. U., Thomas, D. B., May, M. A., Buckmeier, B. G., & Duhaime, R. A. (2018). *Tick Vector and Disease Pathogen Surveillance of Nilgai Antelope, Boselaphus tragocamelus, in Southeastern Texas, USA*. *Journal of Wildlife Diseases*. doi:10.7589/2017-09-239

León, A. A., Teel, P. D., Auclair, A. N., Messenger, M. T., Guerrero, F. D., Schuster, G., & Miller, R. J. (2012). Integrated Strategy for Sustainable Cattle Fever Tick Eradication in USA is Required to Mitigate the Impact of Global Change. *Frontiers in Physiology*, 3.
doi:10.3389/fphys.2012.00195

Pound JM, George JE, Kammlah DM, Lohmeyer KH, Davey RB: Evidence for role of white-tailed deer (*Artiodactyla: Cervidae*) in epizootiology of cattle ticks and southern cattle ticks (*Acari: Ixodidae*) in reinfestations along the Texas/Mexico border in south Texas: a review and update. *J Econ Entomol.* 2010, 103 (2): 211-218. 10.1603/EC09359.

Ribeiro J. M. C. (1995). *How ticks make a living*. *Parasitol. Today* 11, 91–93 10.1016/0169-4758(95)80162-6

Roberts, J.A., 1968. Resistance of cattle to the tick *Boophilus microplus* (Canestrini). I. Development of ticks on *Bos taurus*. *J. Parasitol.* 54, 663–666.

Rodríguez-Vivas, R. I., Grisi, L., León, A. A., Villela, H. S., Torres-Acosta, J. F., Sánchez, H. F., . . . Carrasco, D. G. (2017). *Potential economic impact assessment for cattle parasites in Mexico. Review.* *Revista Mexicana De Ciencias Pecuarias*, 8(1), 61.
doi:10.22319/rmcp.v8i1.4305

Schoeler G. B., Wikel S. K. (2001). *Modulation of host immunity by haematophagous arthropods.* *Ann. Trop. Med. Parasitol.* 95, 755–771 10.1080/0003498012011118

Sousa, A. C., Szabó, M. P., Oliveira, C. J., & Silva, M. J. (2015). *Exploring the anti-tumoral effects of tick saliva and derived components.* *Toxicon*, 102, 69-73.
doi:10.1016/j.toxicon.2015.06.001

Sutherst, R., Wharton, R., & Utech, K. (1978). *Guide to studies on tick ecology.* Australia: Commonwealth Scientific and Industrial Research Organization.

Texas Department of Agriculture Website. (n.d.). Texas Ag Stats. Retrieved January 12, 2018, from <http://www.texasagriculture.gov/About/TexasAgStats.aspx>

Tirloni L, Reck J, Terra RMS, Martins JR, Mulenga A, et al. (2014). Proteomic Analysis of Cattle Tick *Rhipicephalus (Boophilus) microplus* Saliva: A Comparison between Partially and Fully Engorged Females. *PLoS ONE* 9(4): e94831. doi:10.1371/journal.pone.0094831

Tolleson, D.R., Teel, P.D., Stuth, J., Strey, O., Welsh, T., & Carstens, G. (2007). Fecal NIRS: Detection of tick infestations in cattle and horses. *Veterinary Parasitology*, 144(1-2)

Tolleson, D. R., Teel, P. D., Carstens, G. E., and Welsh, T. H. Jr. (2011). *The Physiology of Tick-Induced Stress in Grazing Animals*. Nova Science Publishers Inc.

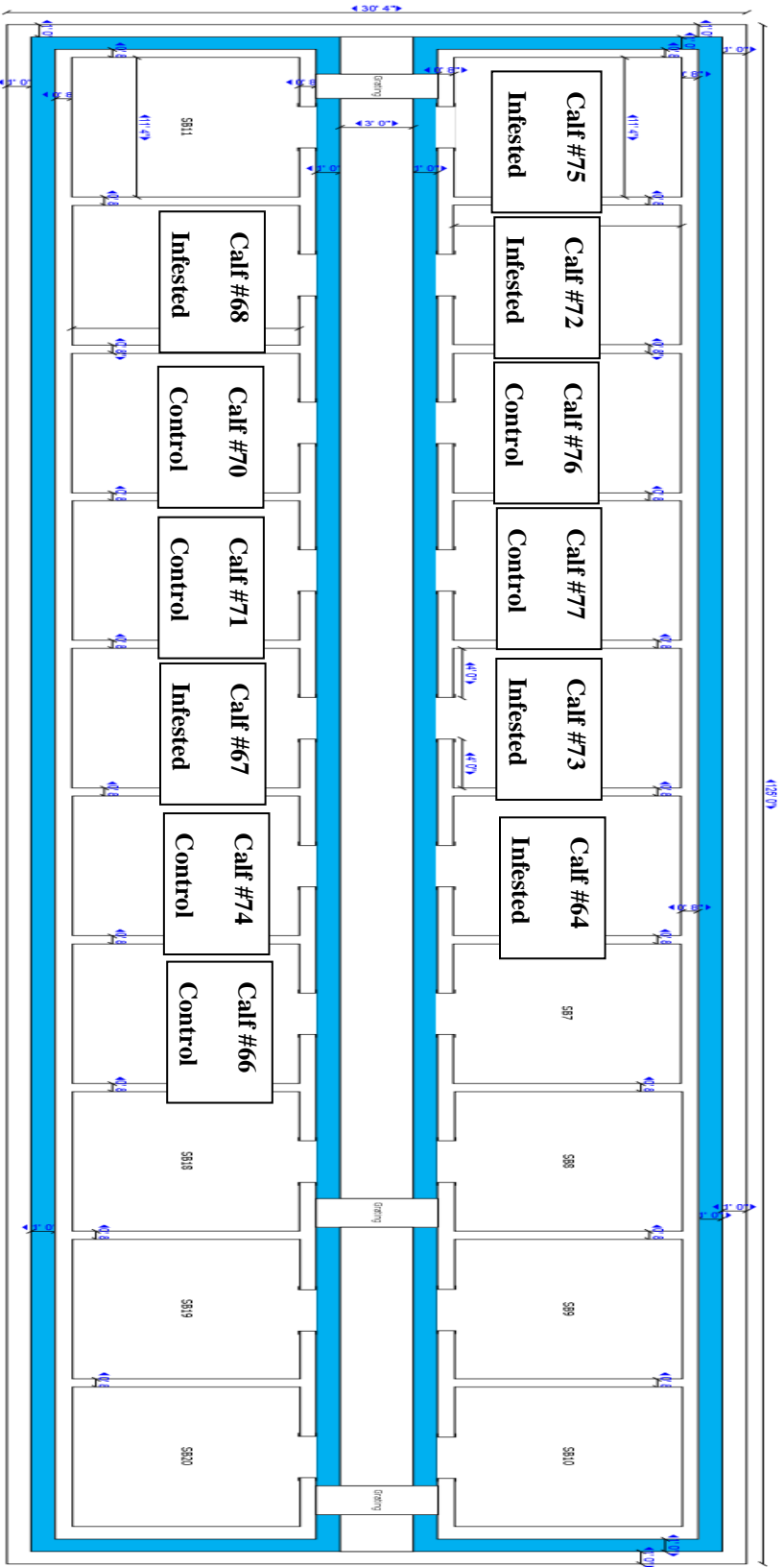
Ueti, M. W., Olafson, P. U., Freeman, J. M., Johnson, W. C., & Scoles, G. A. (2015). A Virulent *Babesia bovis* Strain Failed to Infect White-Tailed Deer (*Odocoileus virginianus*). *Plos One*, 10(6). doi:10.1371/journal.pone.0131018

Utech, K.B.W. Wharton, R.H. Kerr, J.D. (1978) Resistance to *Boophilus microplus* (Canestrini) in different breeds of cattle. *Aust. J. Agric. Res.*, 29 (1978), pp. 885-895

Webb SL, Demarais S, Zaiglin RE, Pollock MT, Whittaker DG (2010). *Size and fidelity of home ranges of male white-tailed deer (Odocoileus virginianus) in southern Texas*. *Southwest Nat.* 2010, 55 (2): 269-273. 10.1894/TAL-10.1.

Appendix A Figures

Figure 1. Blueprint with measurements illustrating the blind stalls where stanchions are positioned so that animals are facing East and are able to turn their heads to look out of the stall when the stall door is open. Blue areas are water filled troughs to prevent the escape of ticks hosting on animals housed in barn.



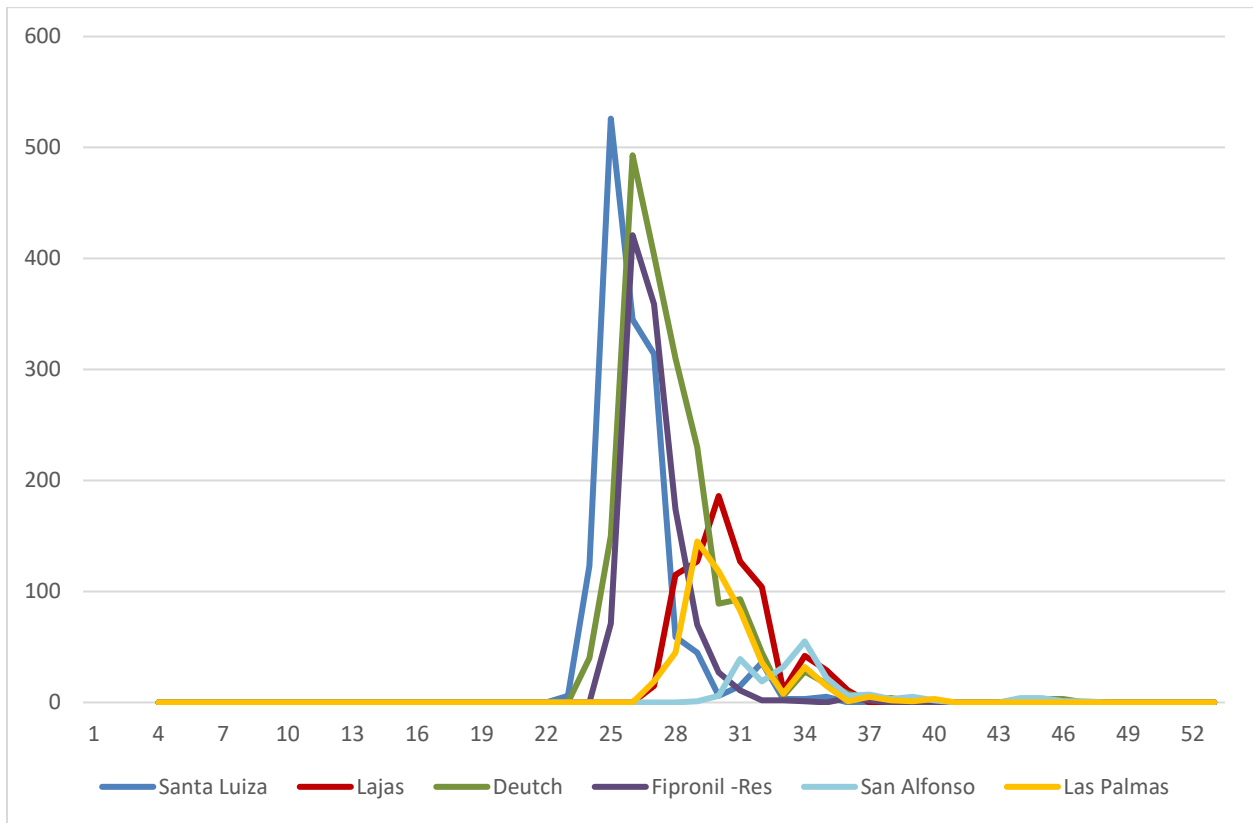


Figure 2. Number of engorged female *Rhipicephalus (Boophilus) microplus* collected per day from cattle infested with six geographic/acaricide resistant tick strains (color coded) on day zero. Days are shown at the bottom, with the infestation of animals occurring on day 12, and the number of females collected is shown on the left. Since we were able to look at six different strains of *R. microplus* we have labeled those strains by name and assigned a color to look at variation in female survivorship and length of drop.

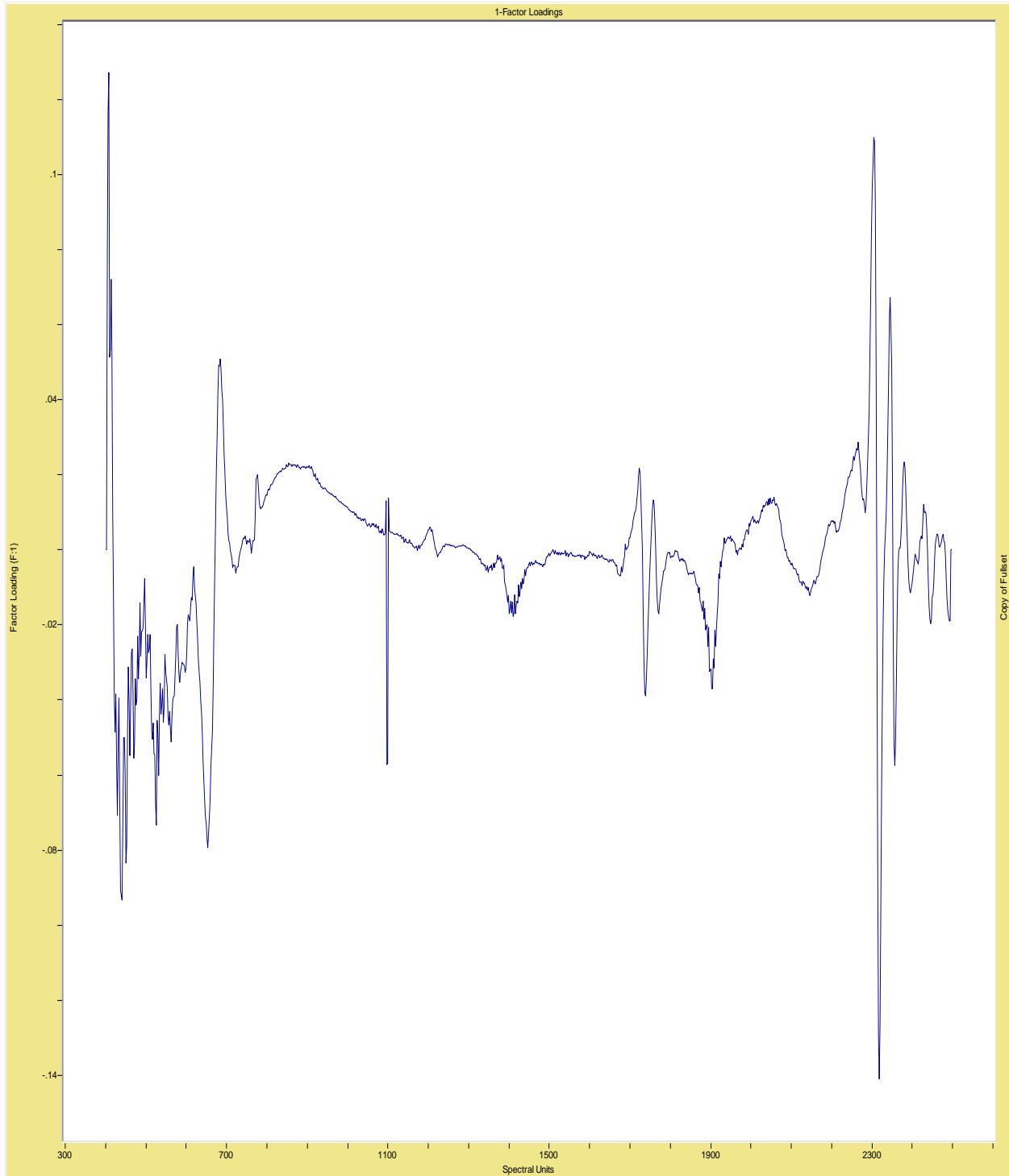


Figure 3. NIRS FCP illustrated by spectrograph. Each peak and valley represents a point of absorption or reflection with the factor loading as the “y” axis and the spectral units (in nanometers) as the “x” axis. This is the first most common spectral variation (factor) from the full objective-1 study spectra with all 12 animals included when using the full spectrum (400nm-2498nm). This first factor is representative of 21.78% of all variation within this group.

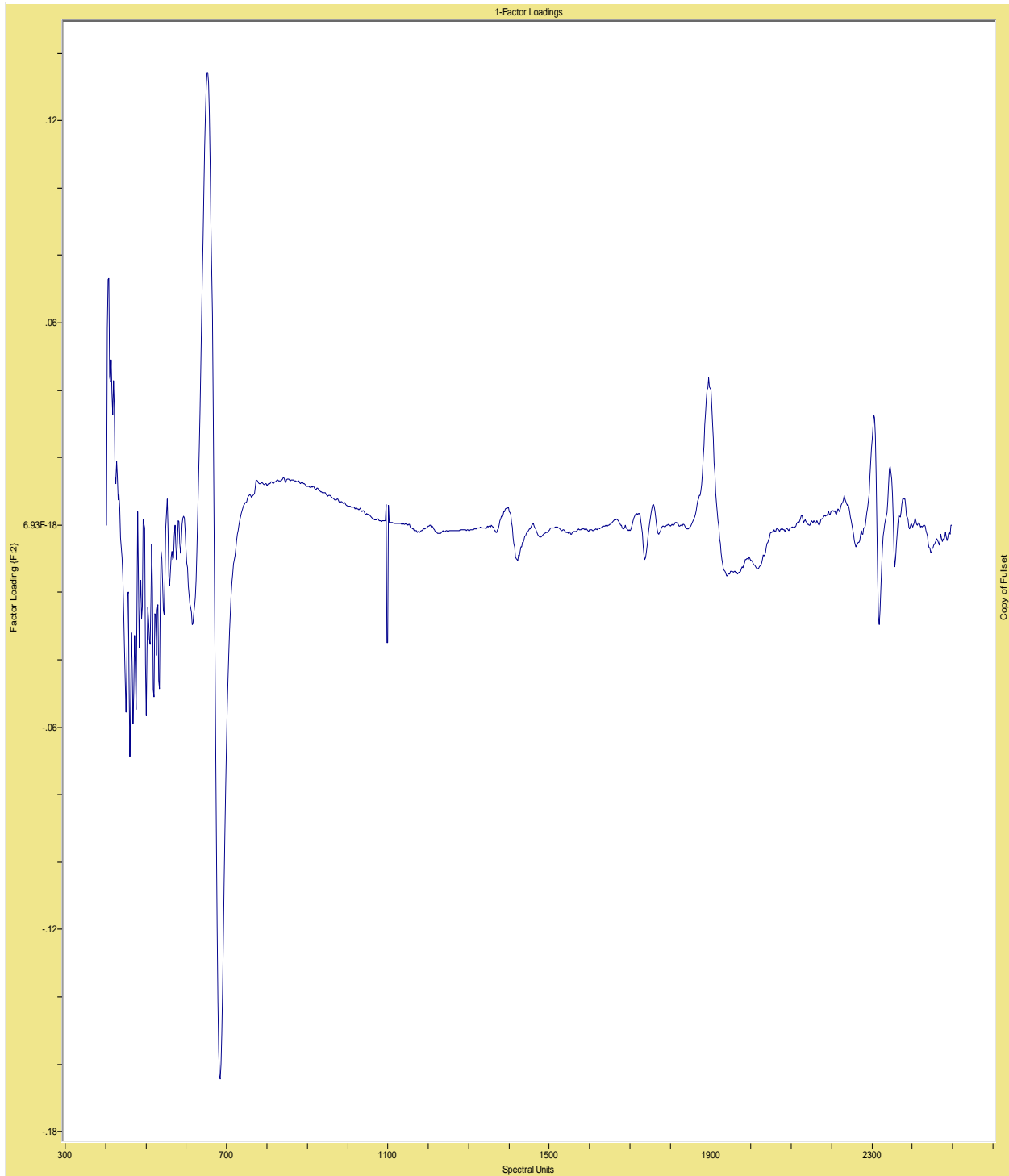


Figure 4. NIRS FCP illustrated by spectrograph. Each peak and valley represents a point of absorption or reflection with the factor loading as the “y” axis and the spectral units (in nanometers) as the “x” axis. This is the second most common spectral variation (factor) from the full objective-1 study spectra with all 12 animals included when using the entire allotted spectrum. This factor is representative of 21.09% of all variation within this group.

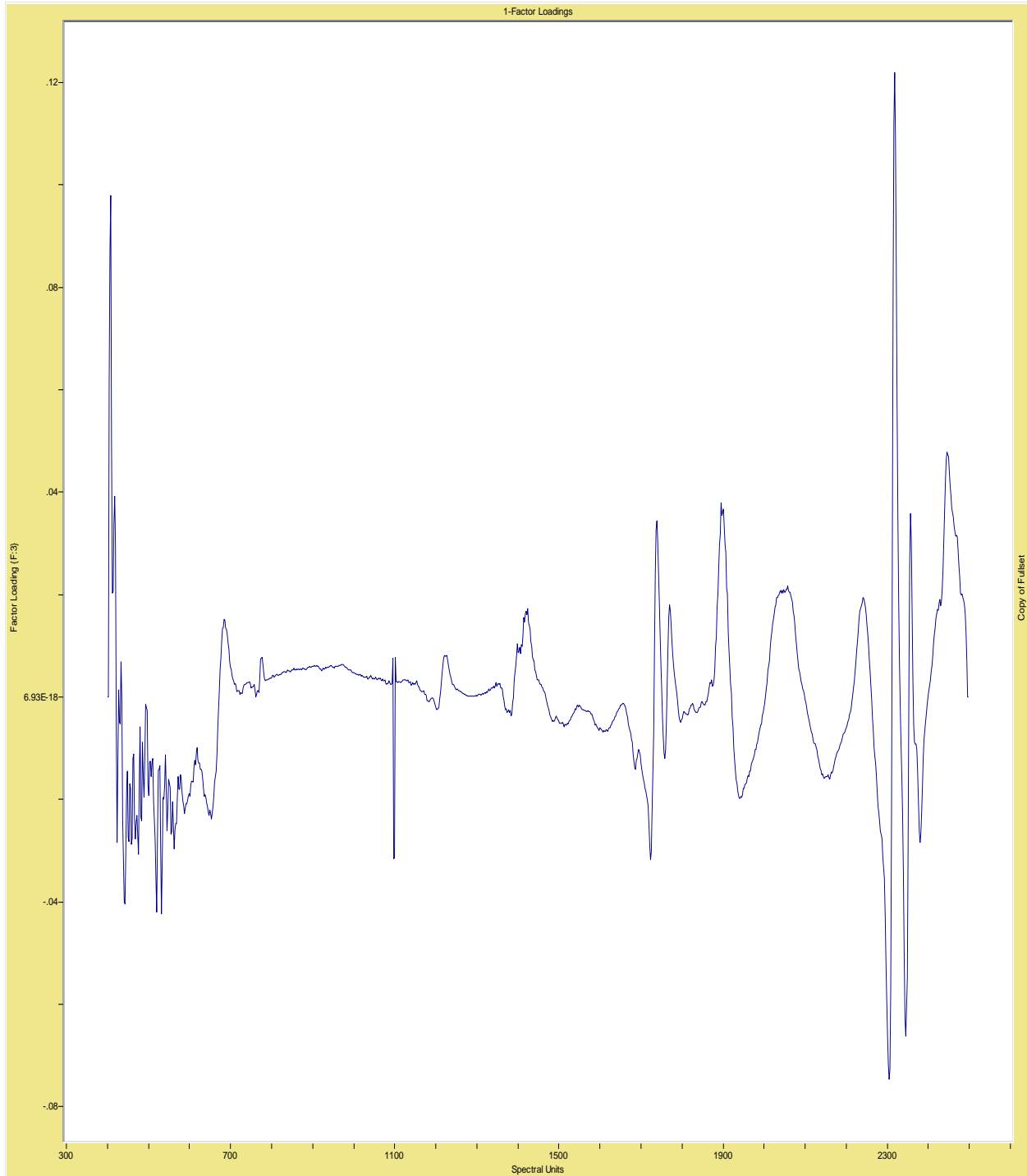
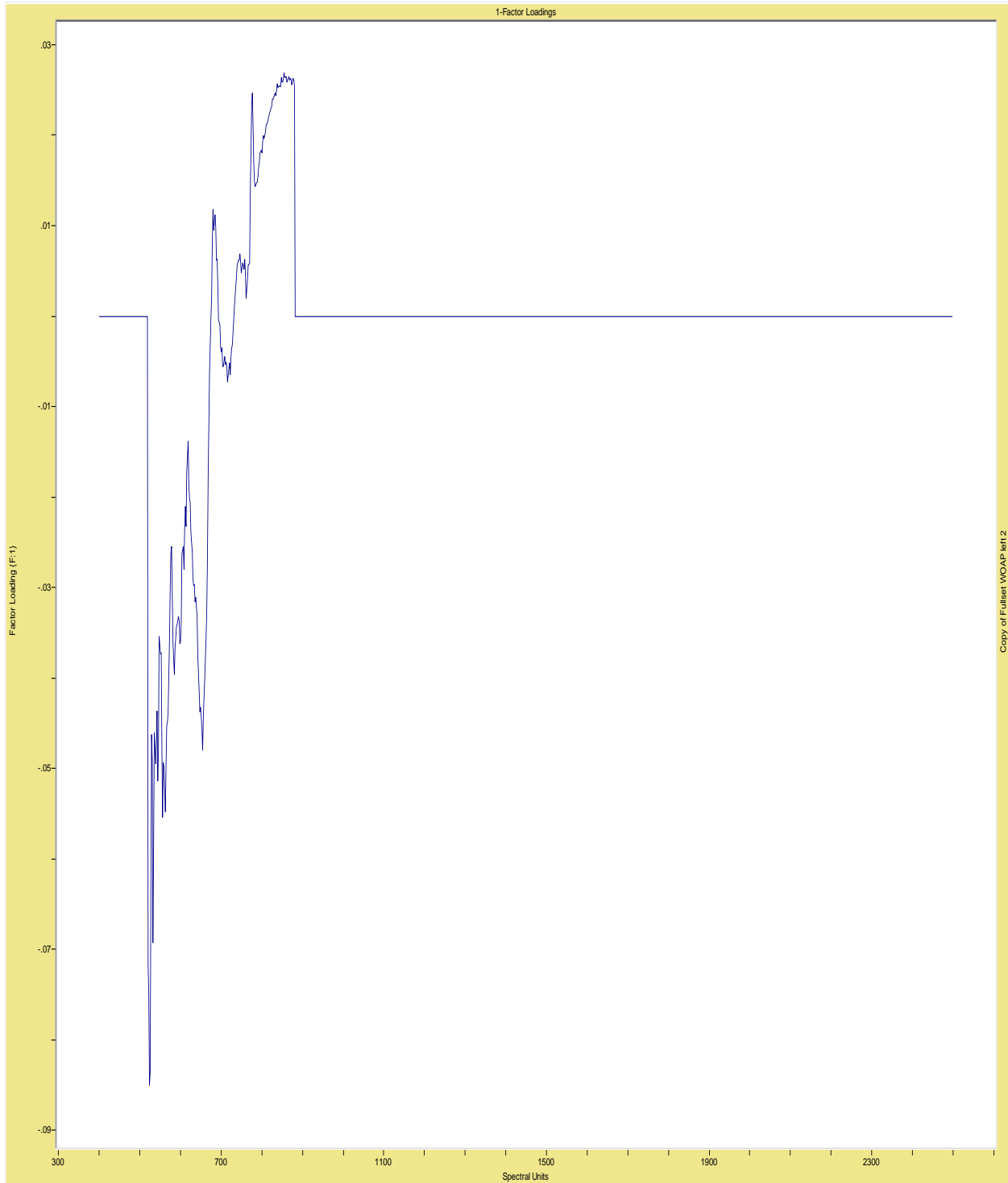


Figure 5. NIRS FCP illustrated by spectrograph. Each peak and valley represents a point of absorption or reflection with the factor loading as the “y” axis and the spectral units (in nanometers) as the “x” axis. This is the third most common spectral variation (factor) from the full objective-1 study spectra with all 12 animals included when using the entire allotted spectrum. This factor is representative of 11.3% of all variation within this group.



Copy of Fullset WOADP left 2

Figure 6. NIRS FCP illustrated by spectrograph. Each peak and valley represents a point of absorption or reflection with the factor loading as the “y” axis and the spectral units (in nanometers) as the “x” axis. This is the most common spectral variation (factor) from the full study with all 12 animals but using a narrowed spectrum (576nm-1126nm) to lessen the effect of noise and improve the contribution of each of the 25 factors. This spectral variation is representative of 72.38% of the total variation within this group.

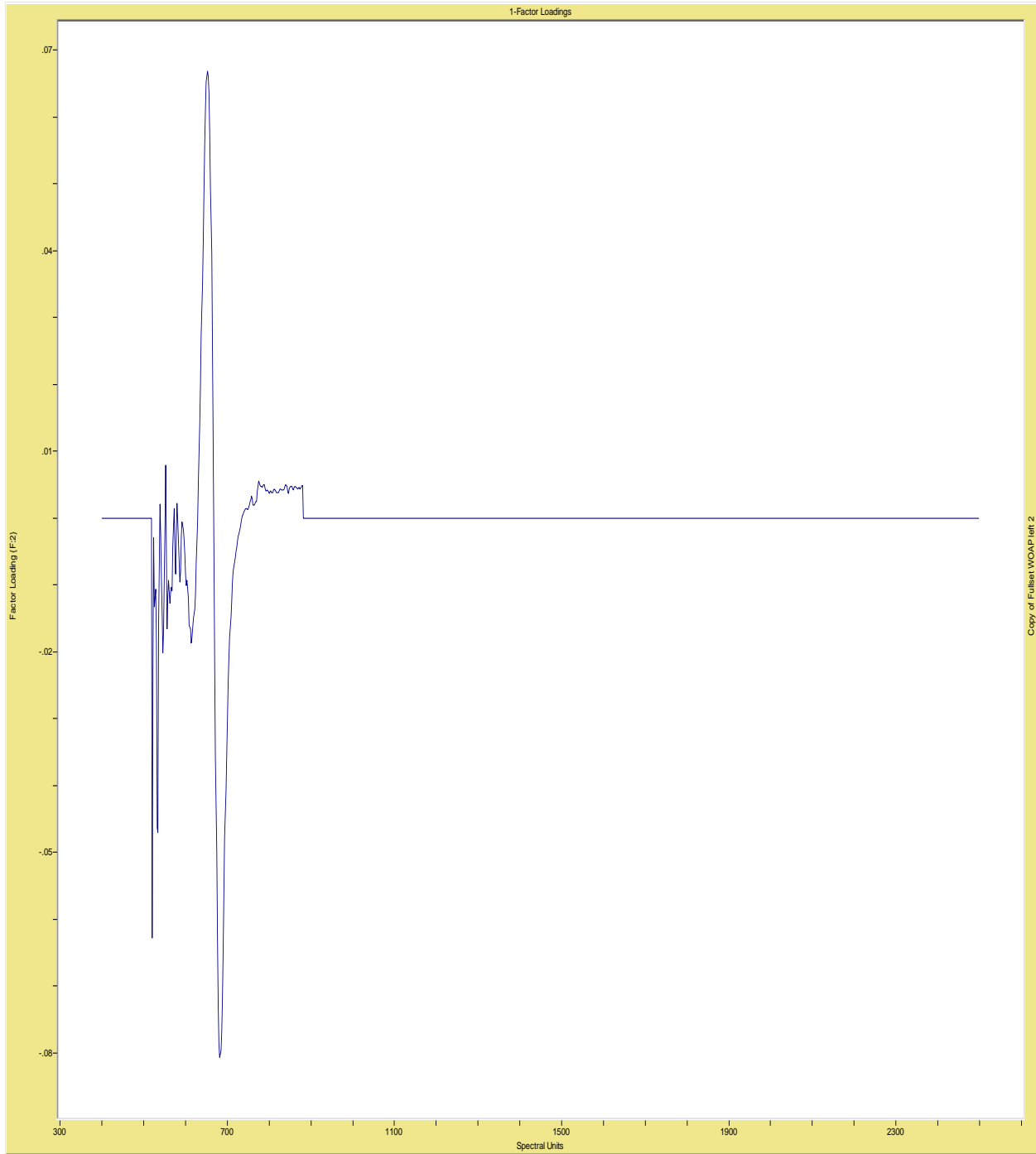


Figure 7. NIRS FCP illustrated by spectrograph. Each peak and valley represents a point of absorption or reflection with the factor loading as the “y” axis and the spectral units (in nanometers) as the “x” axis. This is the second most common spectral variation (factor) from the full study with all 12 animals but using a narrowed spectrum (576nm-1126nm) to lessen the effect of noise and improve the contribution of each of the 25 factors. This spectral variation is representative of 16.90% of the total variation within this group.

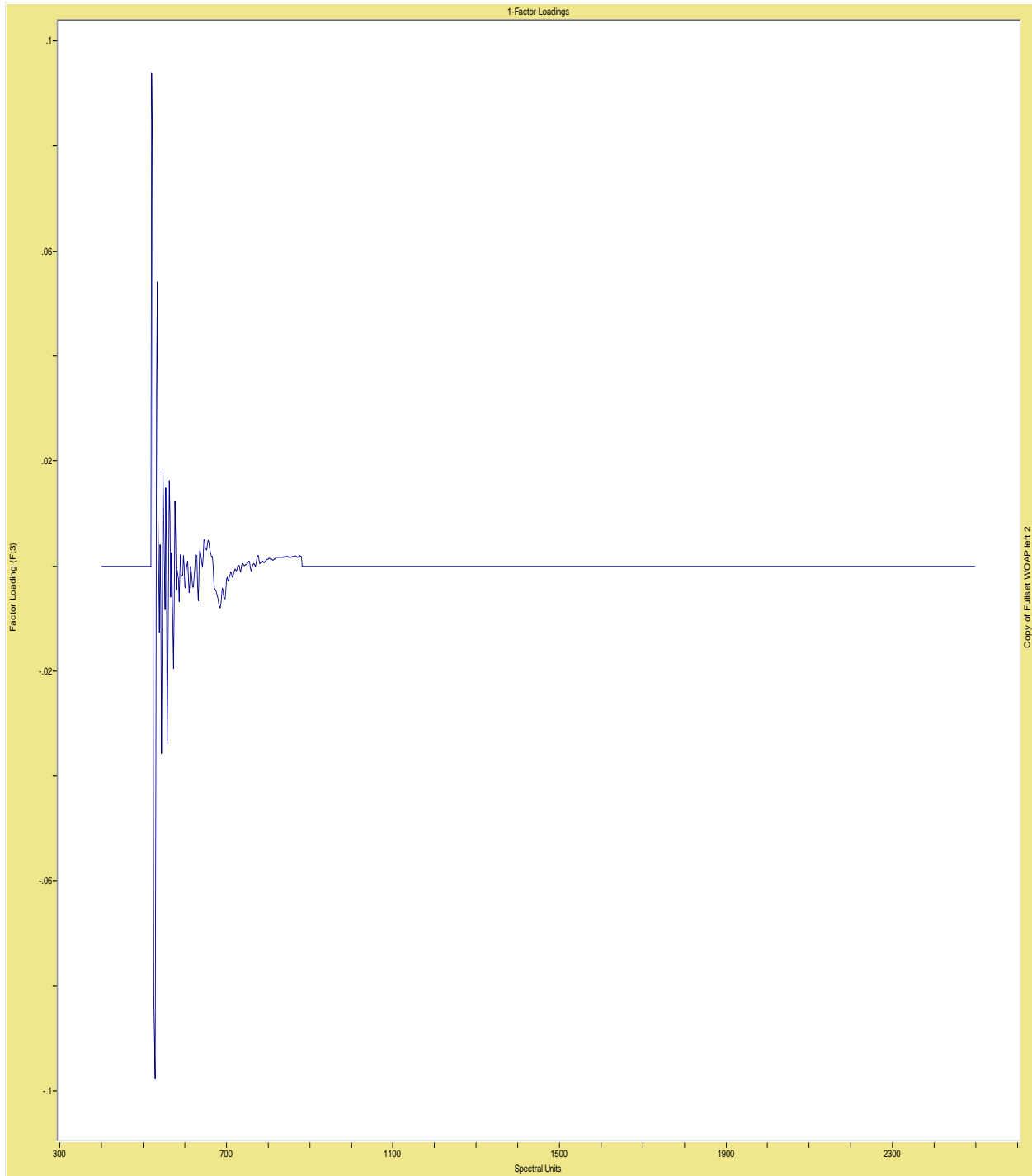


Figure 8. NIRS FCP illustrated by spectrograph. Each peak and valley represents a point of absorption or reflection with the factor loading as the “y” axis and the spectral units (in nanometers) as the “x” axis. This is the third most common spectral variation (factor) from the full study with all 12 animals but using a narrowed spectrum (576nm-1126nm) to lessen the effect of noise and improve the contribution of each of the 25 factors. This spectral variation is representative of 05.38% of the total variation within this group.

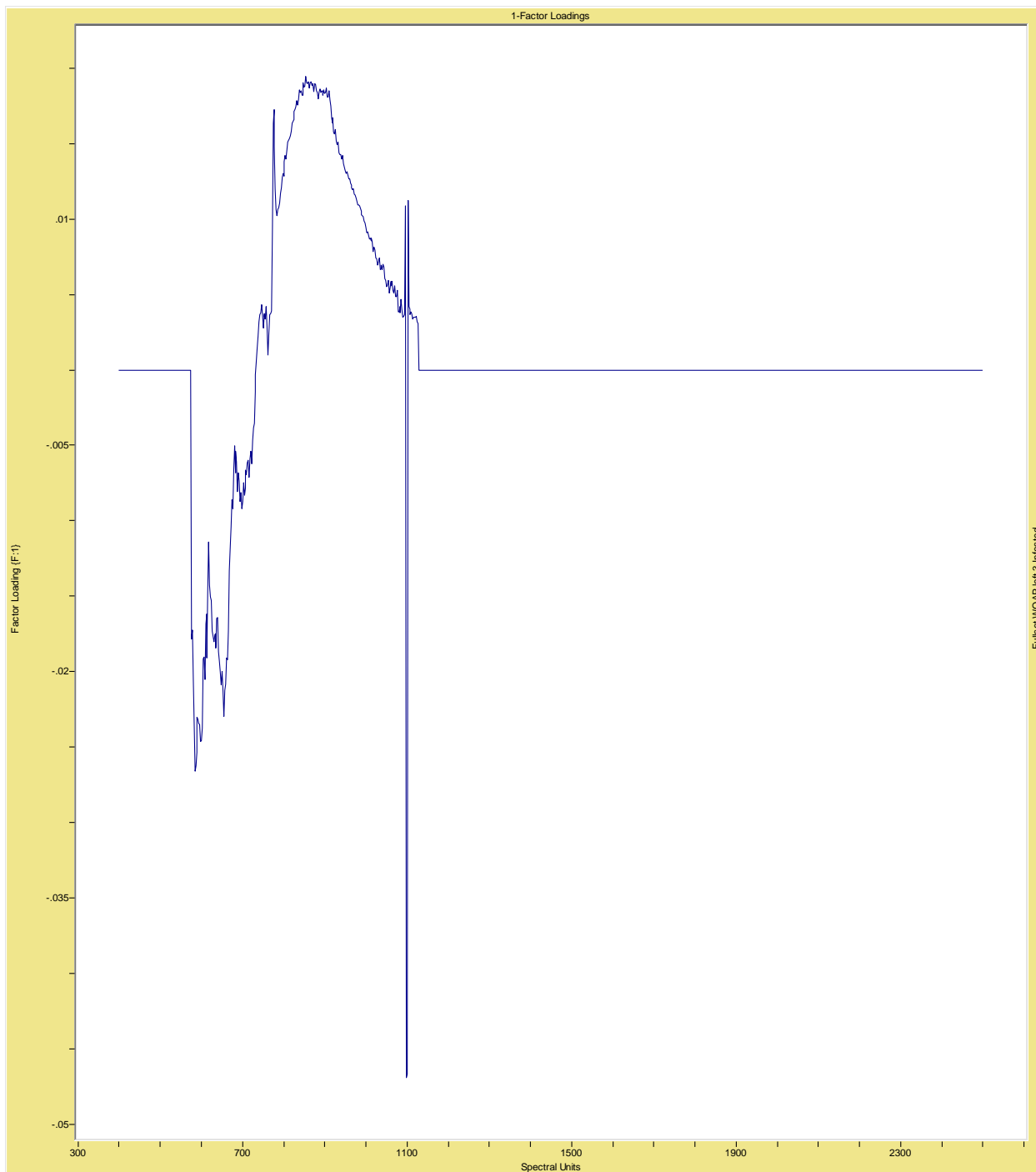


Figure 9. NIRS FCP illustrated by spectrograph. Each peak and valley represents a point of absorption or reflection with the factor loading as the “y” axis and the spectral units (in nanometers) as the “x” axis. This is the most common spectral variation (factor) from the full study using only the infested animals as well as using a narrowed spectrum (576nm-1126nm) to lessen the effect of noise and improve the contribution of each of the 25 factors. This spectral variation is representative of 53.48% of the total variation within this group.

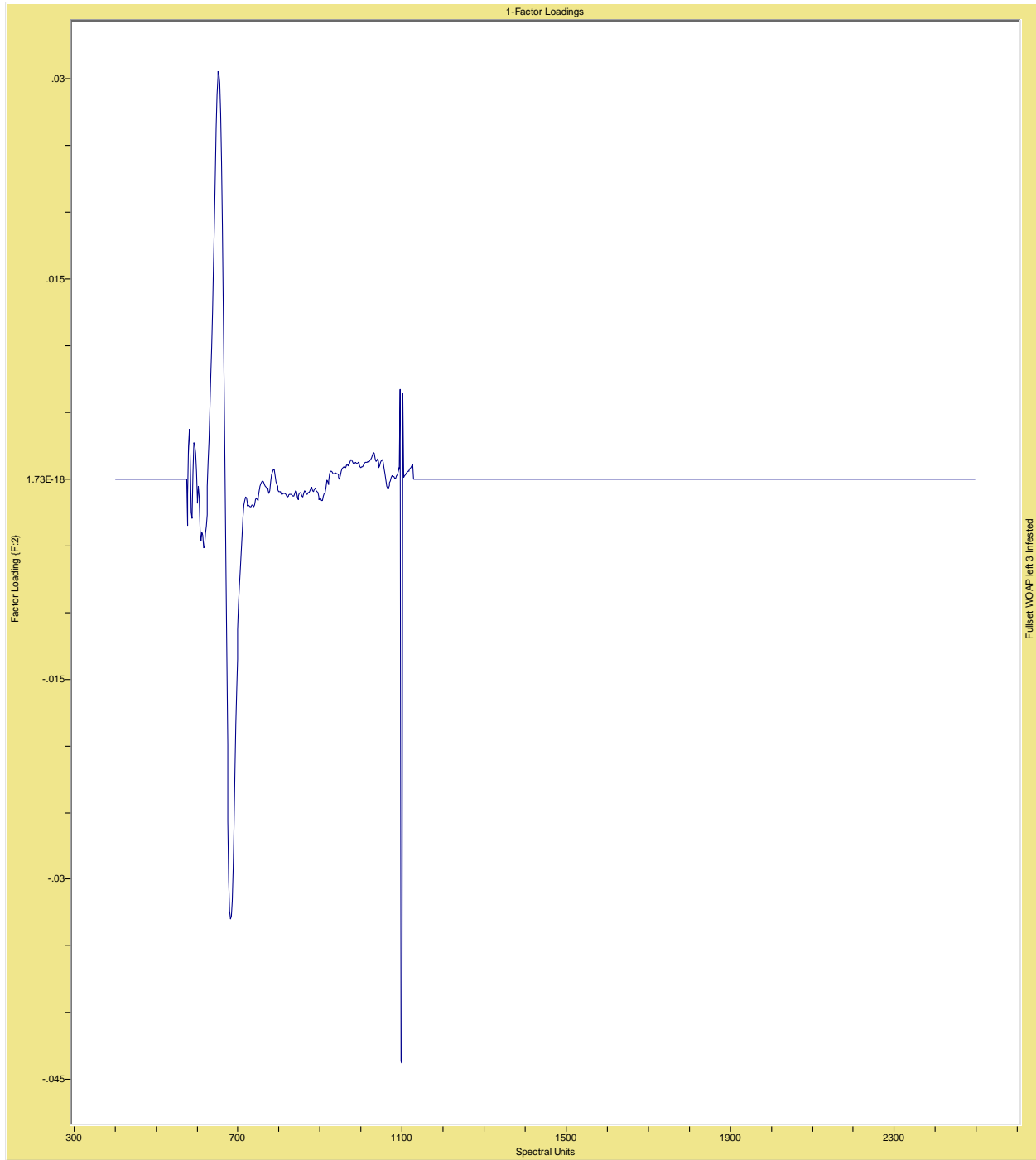


Figure 10. NIRS FCP illustrated by spectrograph. Each peak and valley represents a point of absorption or reflection with the factor loading as the “y” axis and the spectral units (in nanometers) as the “x” axis. This is the second most common spectral variation (factor) from the full study using only the infested animals as well as using a narrowed spectrum (576nm-1126nm) to lessen the effect of noise and improve the contribution of each of the 25 factors. This spectral variation is representative of 21.90% of the total variation within this group.

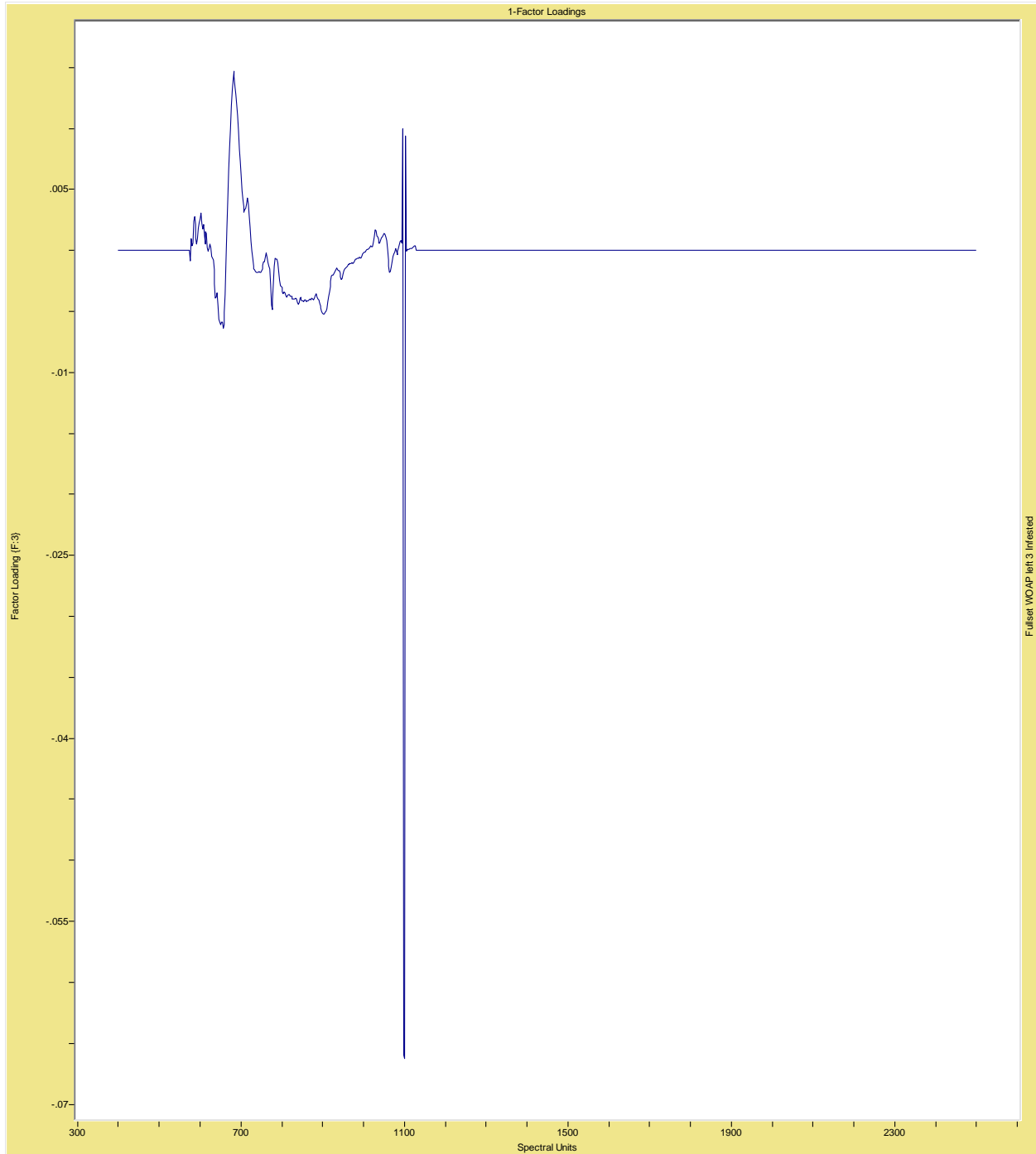


Figure 11. NIRS FCP illustrated by spectrograph. Each peak and valley represents a point of absorption or reflection with the factor loading as the “y” axis and the spectral units (in nanometers) as the “x” axis. This is the third most common spectral variation (factor) from the full study using only the infested animals as well as using a narrowed spectrum (576nm-1126nm) to lessen the effect of noise and improve the contribution of each of the 25 factors. This spectral variation is representative of 12.47% of the total variation within this group.

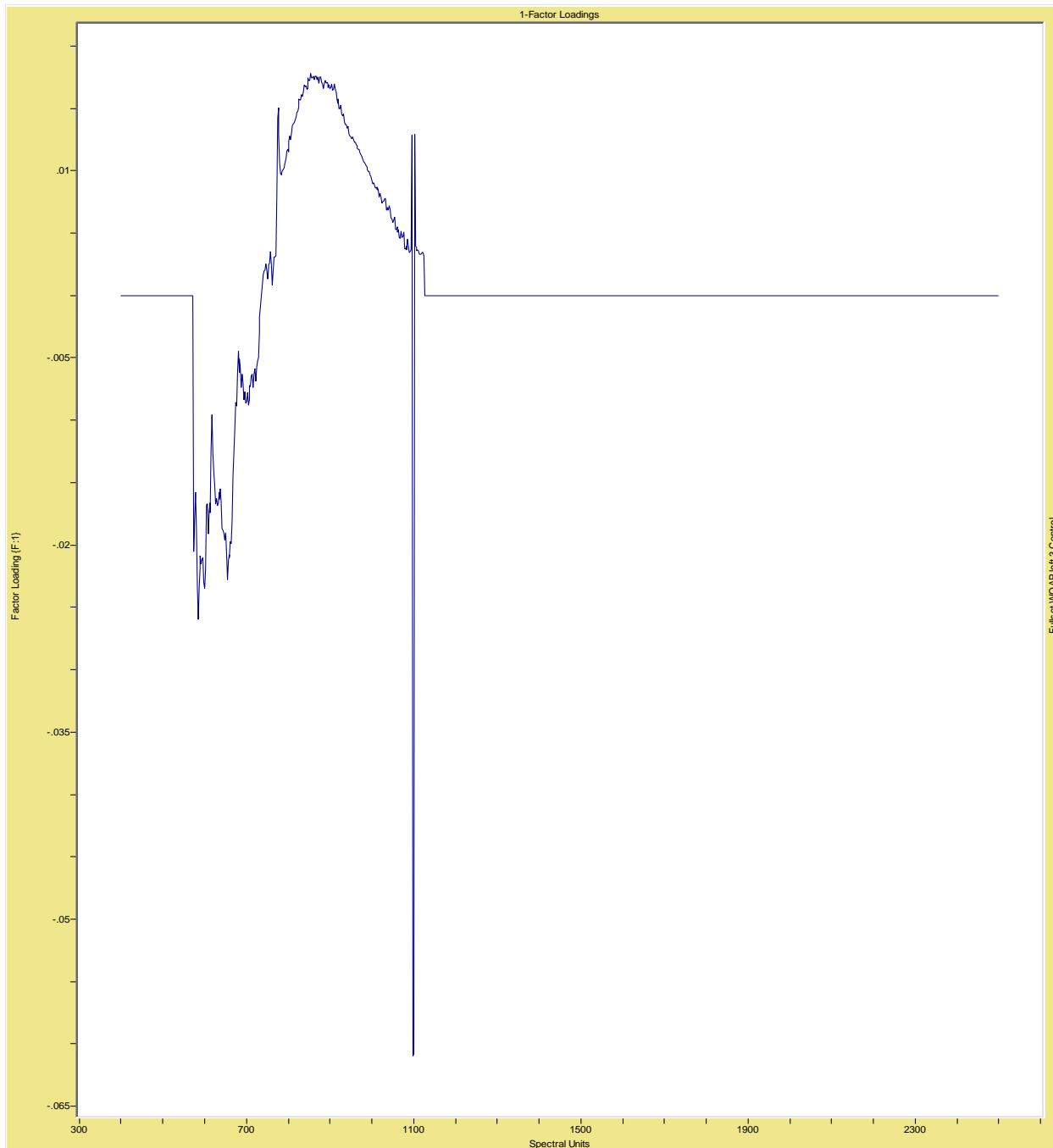


Figure 12. NIRS FCP illustrated by spectrograph. Each peak and valley represents a point of absorption or reflection with the factor loading as the “y” axis and the spectral units (in nanometers) as the “x” axis. This is the most common spectral variation (factor) from the full study using only the non-infested animals as well as using a narrowed spectrum (576nm-1126nm) to lessen the effect of noise and improve the contribution of each of the 25 factors. This spectral variation is representative of 49.87% of the total variation within this group.

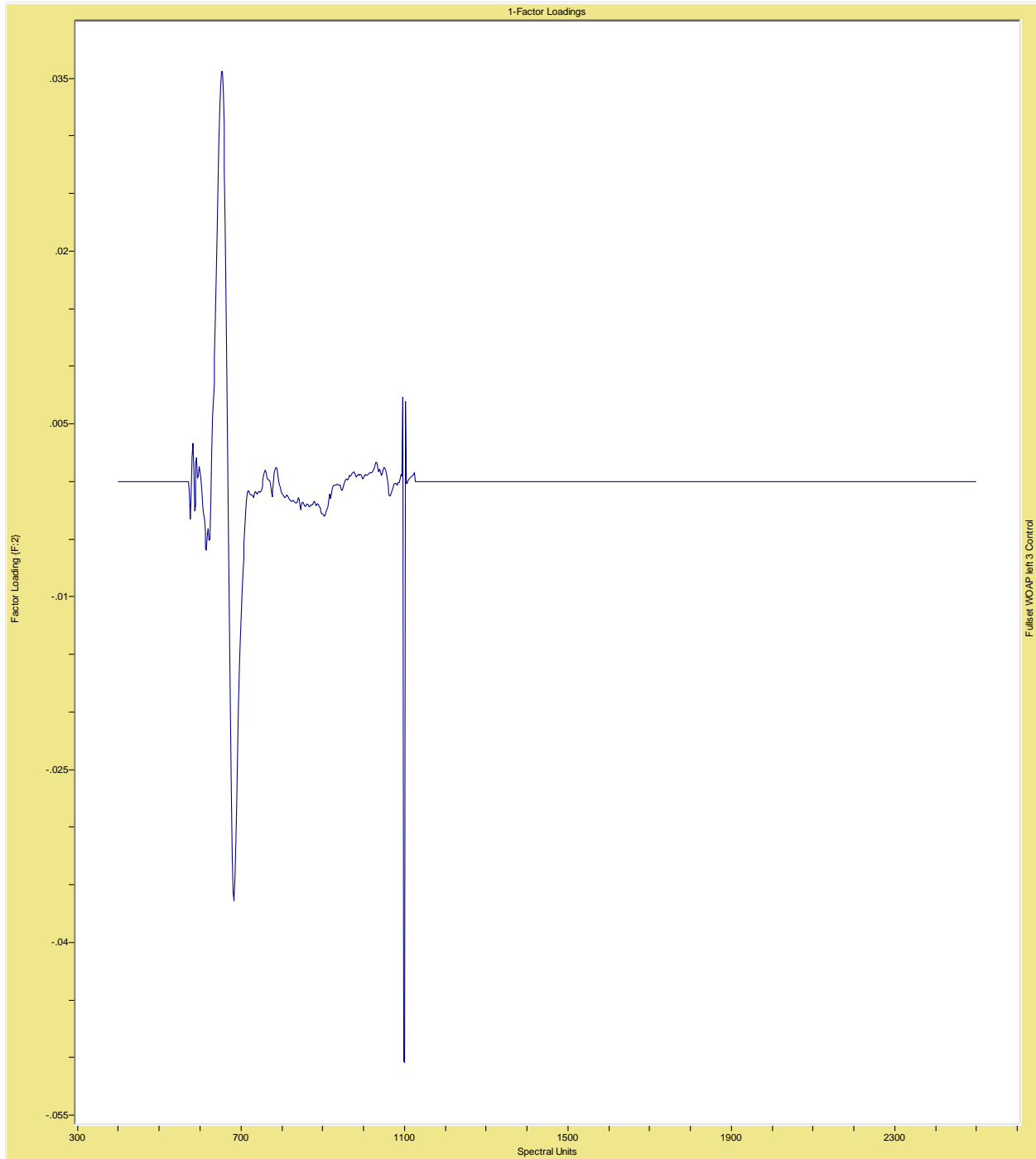


Figure 13. NIRS FCP illustrated by spectrograph. Each peak and valley represents a point of absorption or reflection with the factor loading as the “y” axis and the spectral units (in nanometers) as the “x” axis. This is the second most common spectral variation (factor) from the full study using only the non-infested animals as well as using a narrowed spectrum (576nm-1126nm) to lessen the effect of noise and improve the contribution of each of the 25 factors. This spectral variation is representative of 29.59% of the total variation within this group.

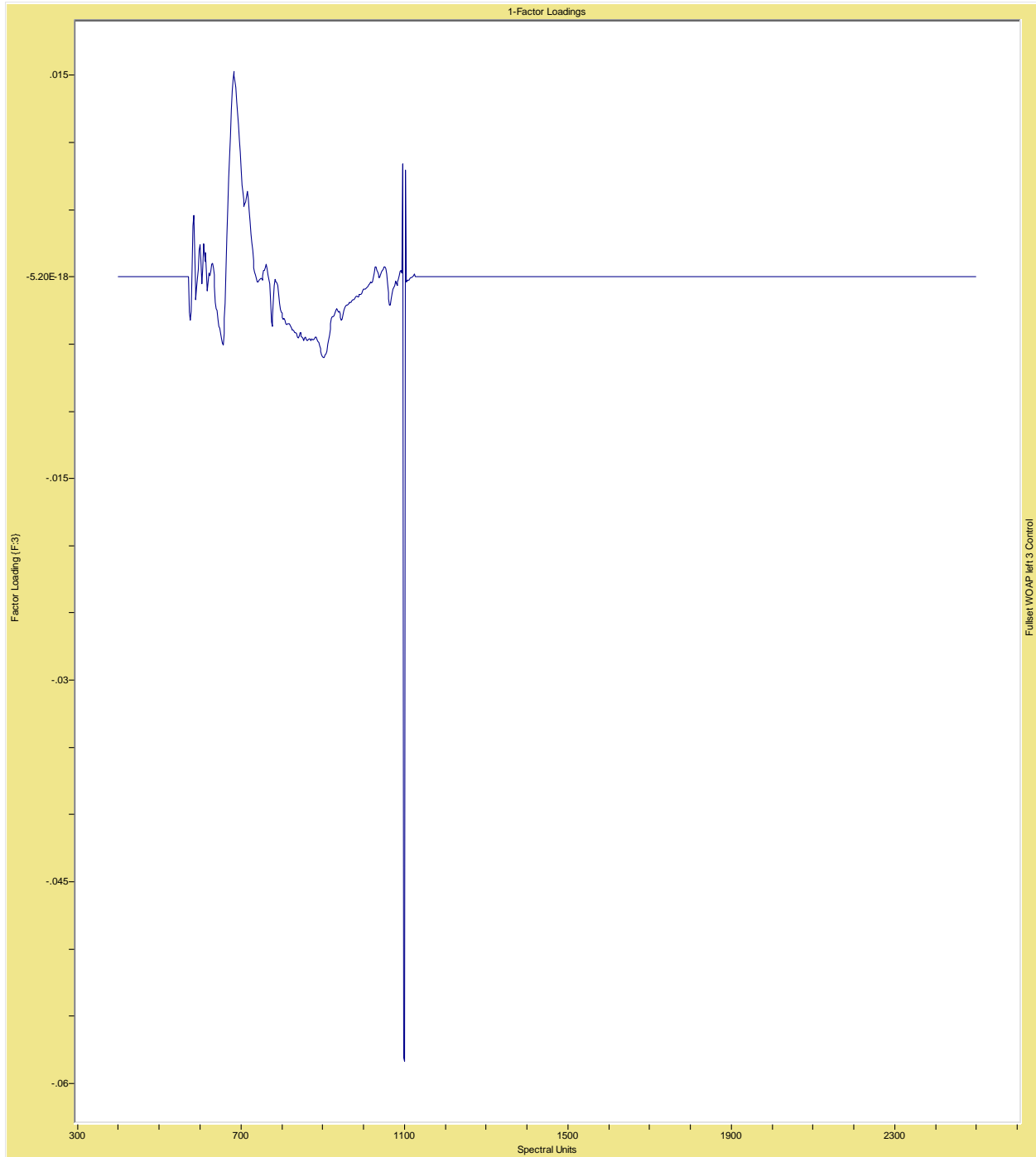


Figure 14. NIRS FCP illustrated by spectrograph. Each peak and valley represents a point of absorption or reflection with the factor loading as the “y” axis and the spectral units (in nanometers) as the “x” axis. This is the third most common spectral variation (factor) from the full study using only the non-infested animals as well as using a narrowed spectrum (576nm-1126nm) to lessen the effect of noise and improve the contribution of each of the 25 factors. This spectral variation is representative of 10.91% of the total variation within this group.

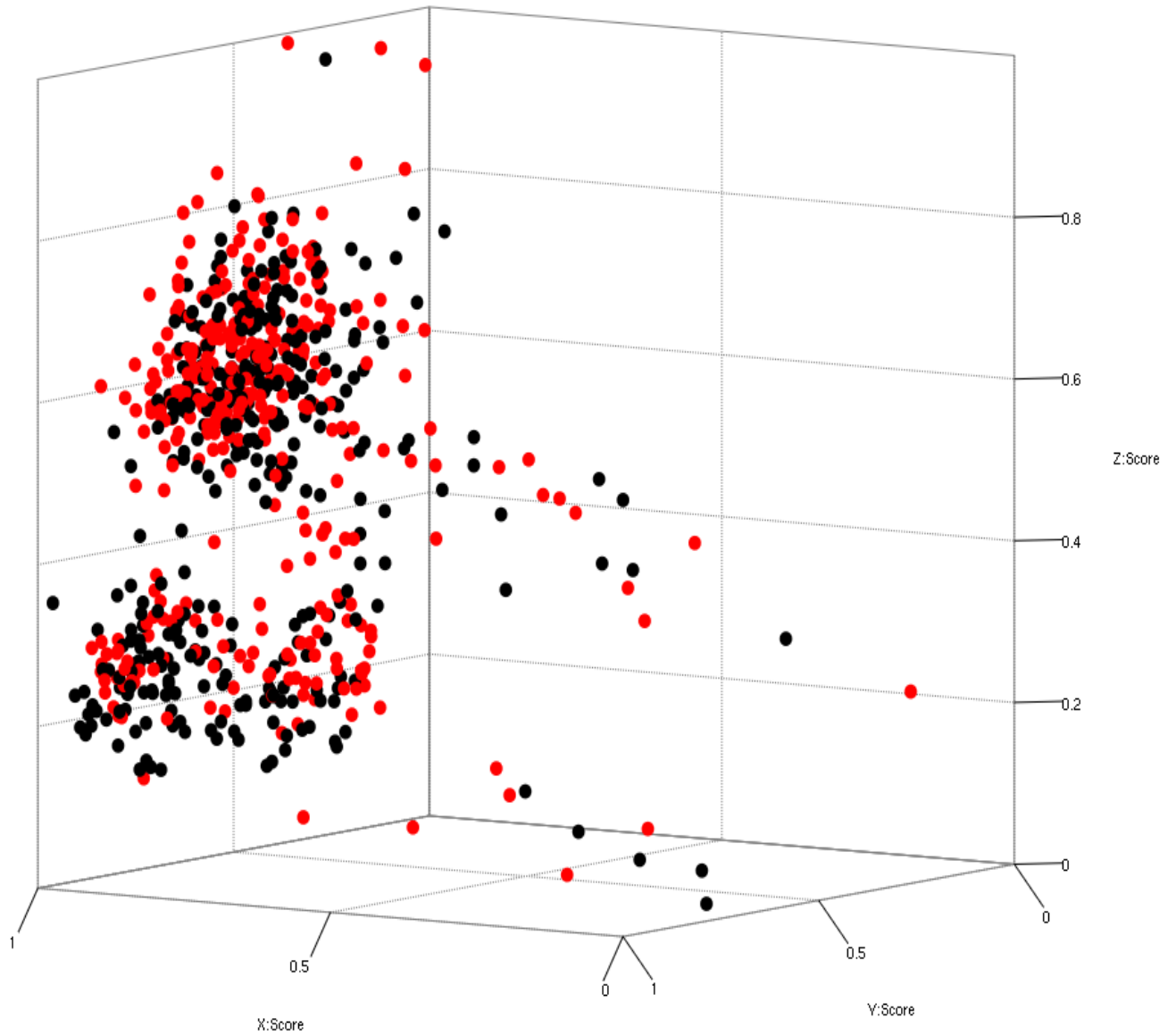


Figure 15. Three-dimensional Cluster analysis of daily fecal spectra (576nm – 1226nm) from 6 *Bos taurus* cattle infested with *R. microplus* and 6 non-infested *Bos taurus* cattle over the course of 59 days. Infested spectra are indicated in red, control spectra are indicated in black. Figure axes (“x”, “y” and “z”) correspond to the first three factor loadings, representative of 92% of total spectral variation within this group.

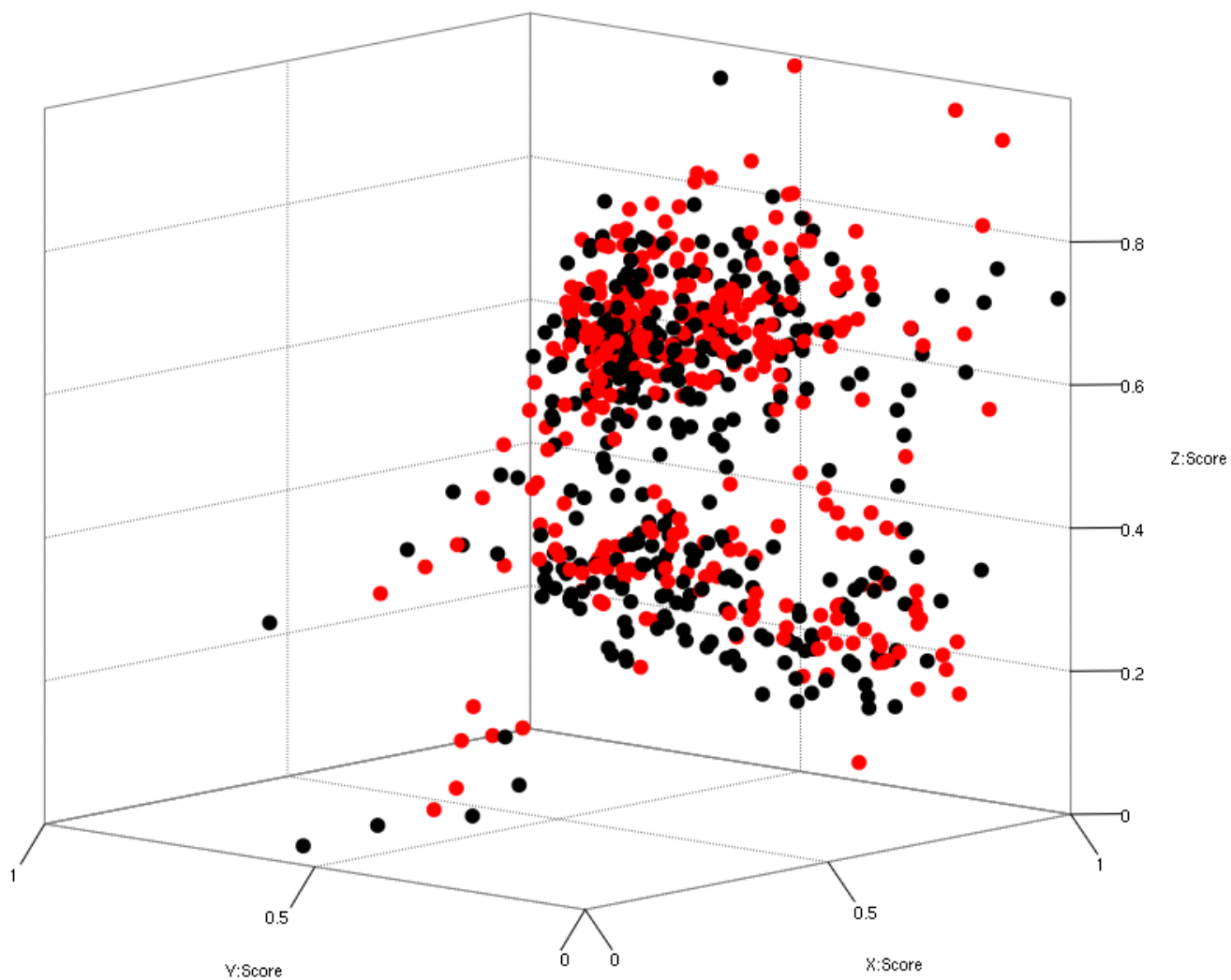


Figure 16. Three-dimensional Cluster analysis of daily fecal spectra (576nm – 1226nm) from 6 *Bos taurus* cattle infested with *R. microplus* and 6 non-infested *Bos taurus* cattle over the course of 59 days. Infested spectra are indicated in red, non-infested spectra are indicated in black. Figure axes correspond to the first three factor loadings, representative of 92% of total spectral variation.

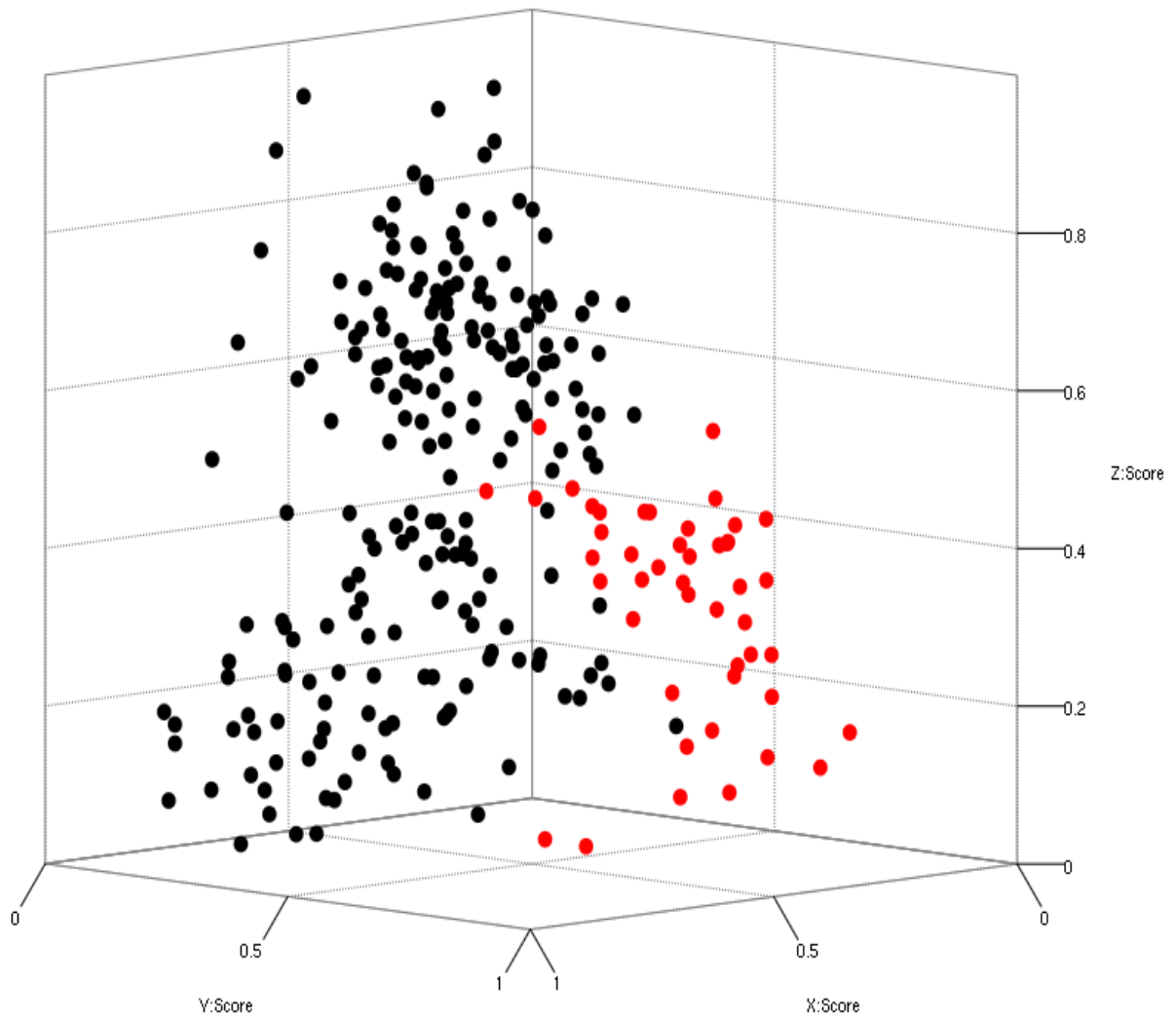


Figure 17. Three-dimensional Cluster analysis of daily fecal spectra (576nm – 1226nm) from 6 *Bos taurus* cattle infested with *R. microplus*. Spectra from the 1st day to the 22nd day are indicated in red, the spectra from all later days are indicated in black. Figure axes correspond to the first three most common spectral variations (factors), and are representative of 87.87% of total spectral variation.

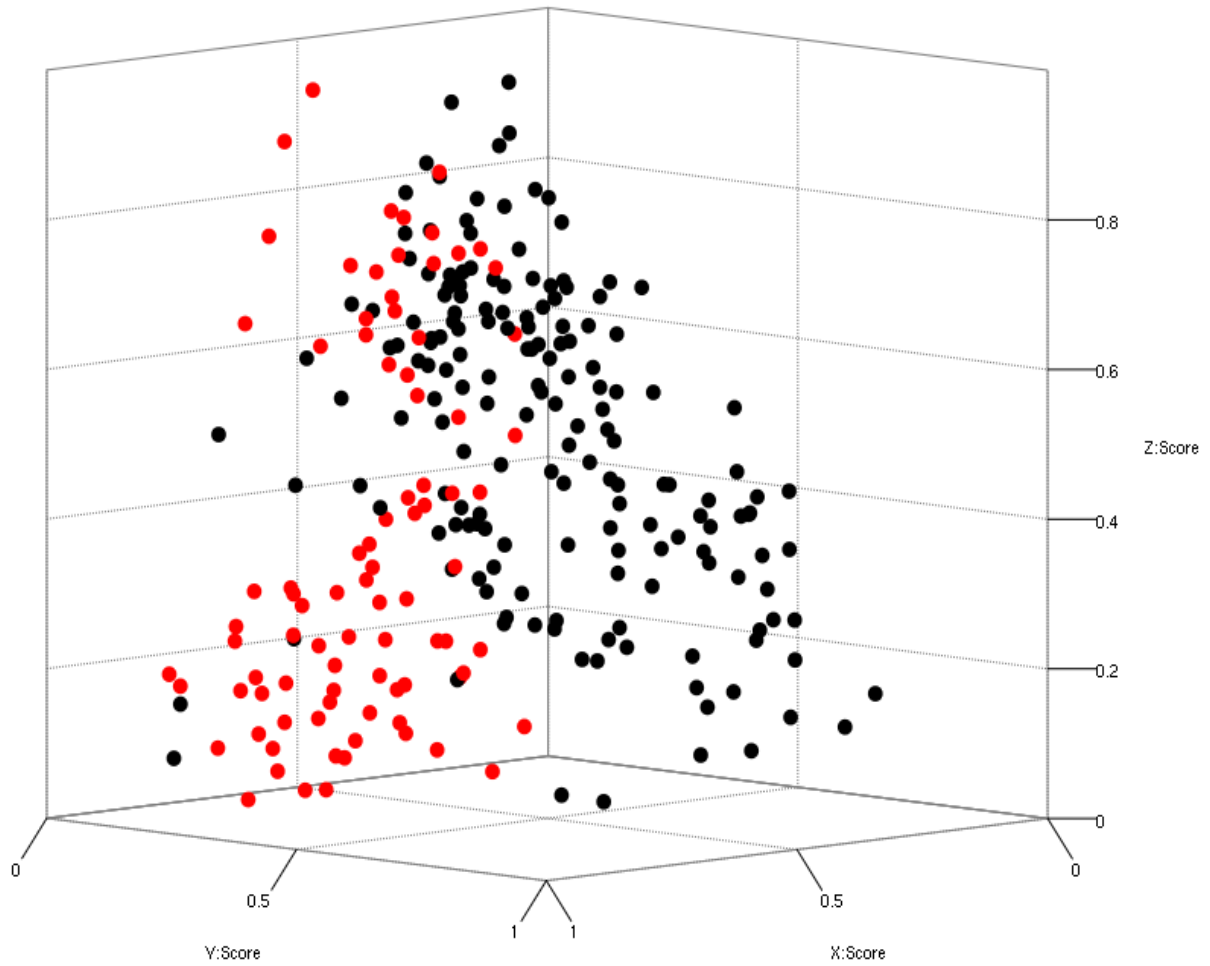


Figure 18. Three-dimensional Cluster analysis of daily fecal spectra (576nm – 1226nm) from 6 *Bos taurus* cattle infested with *R. microplus*. Spectra from the 24th day to the 36th day are indicated in red, the spectra from all prior and later days are indicated in black. Figure axes correspond to the first three most common spectral variations (factors), and are representative of 87.87% of total spectral variation.

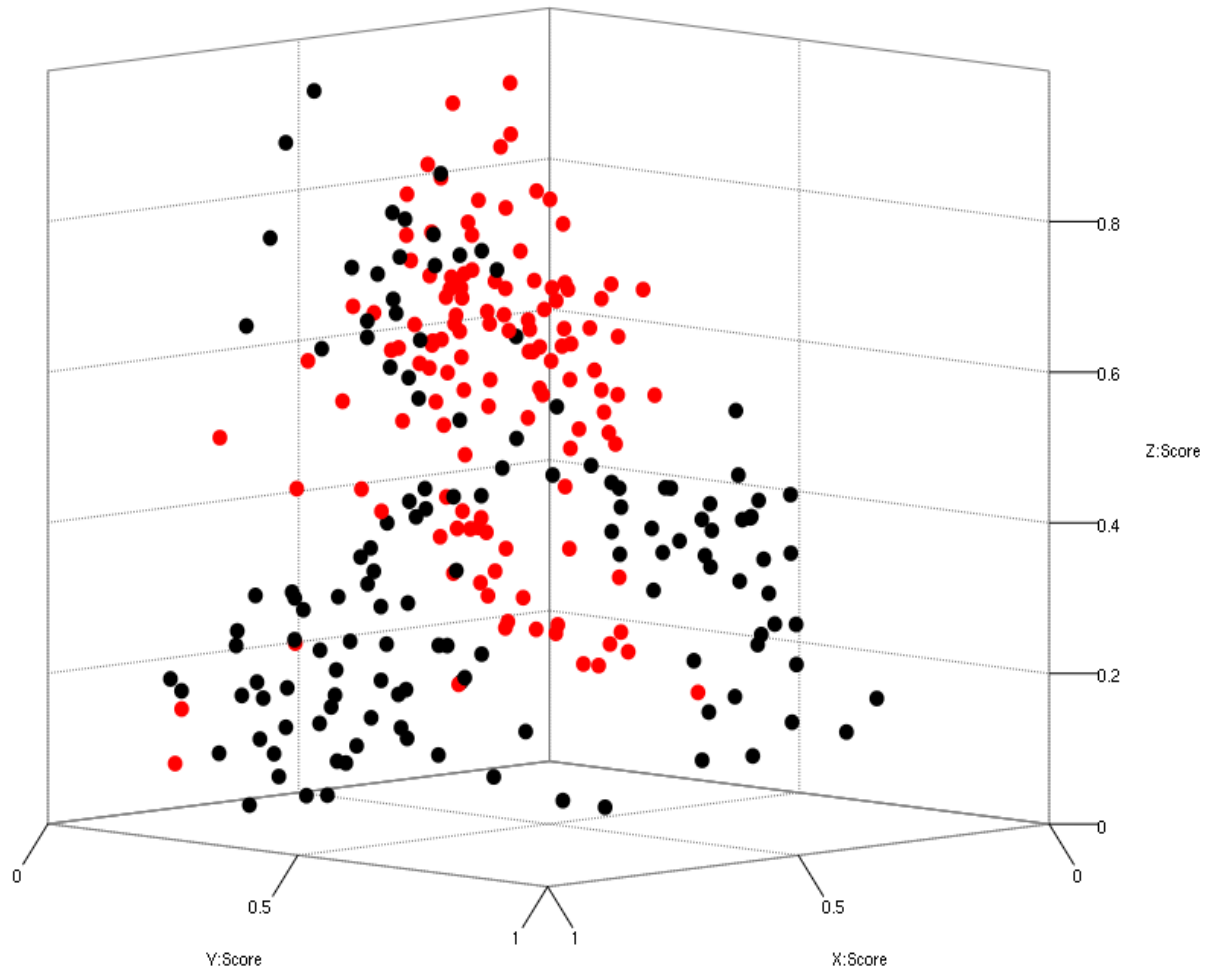


Figure 19. Three-dimensional Cluster analysis of daily fecal spectra (576nm – 1226nm) from 6 *Bos taurus* cattle infested with *R. microplus*. Spectra from the 37th day to the 59th day are indicated in red, the spectra from all prior and later days are indicated in black. Figure axes correspond to the first three most common spectral variations (factors), and are representative of 87.87% of total spectral variation.

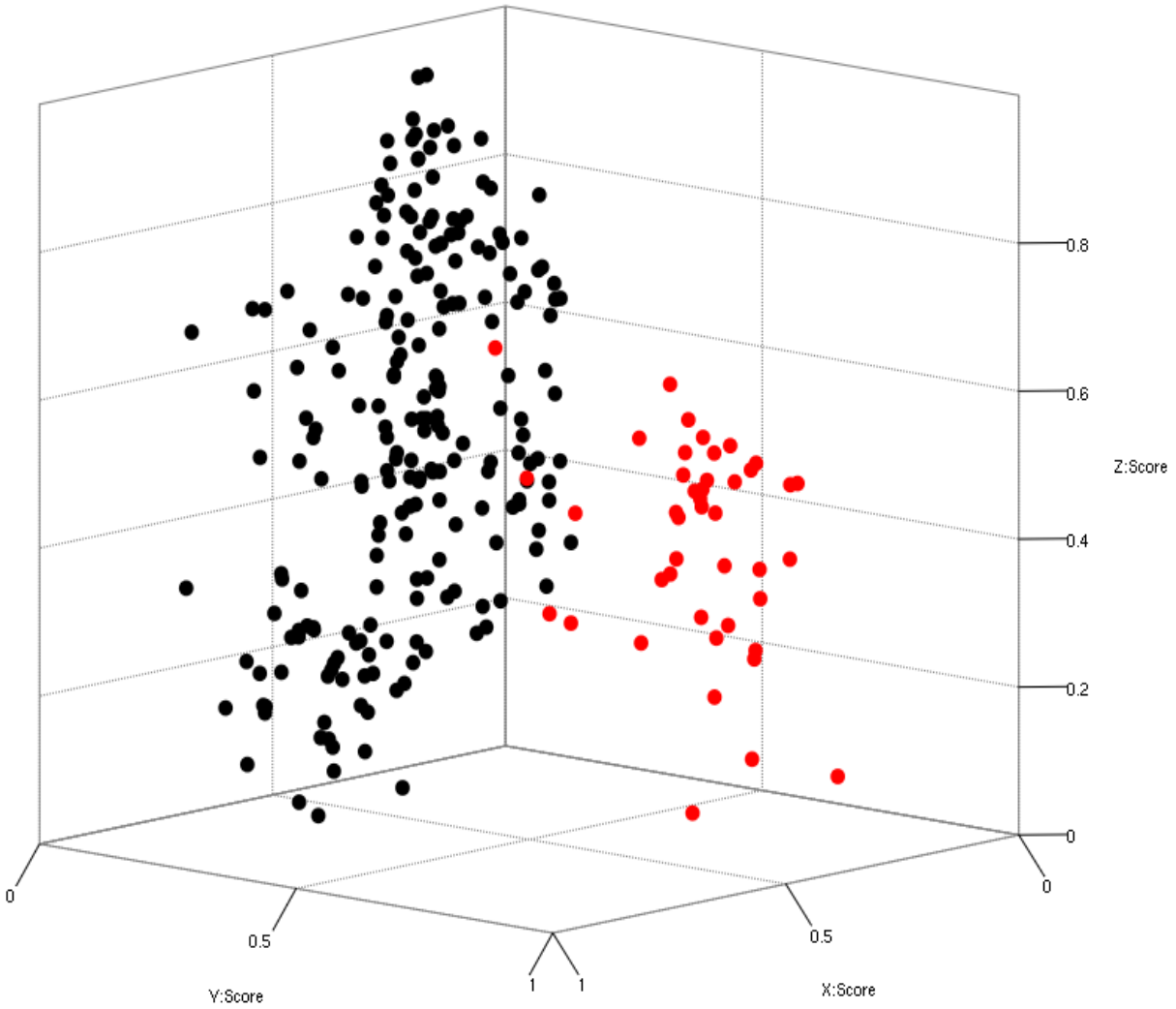


Figure 20. Three-dimensional Cluster analysis of daily fecal spectra (576nm – 1226nm) from 6 non-infested *Bos taurus* cattle. Spectra from the 1st day to the 22nd day are indicated in red, the spectra from all later days are indicated in black. Figure axes correspond to the first three most common spectral variations (factors), and are representative of 87.39% of total spectral variation.

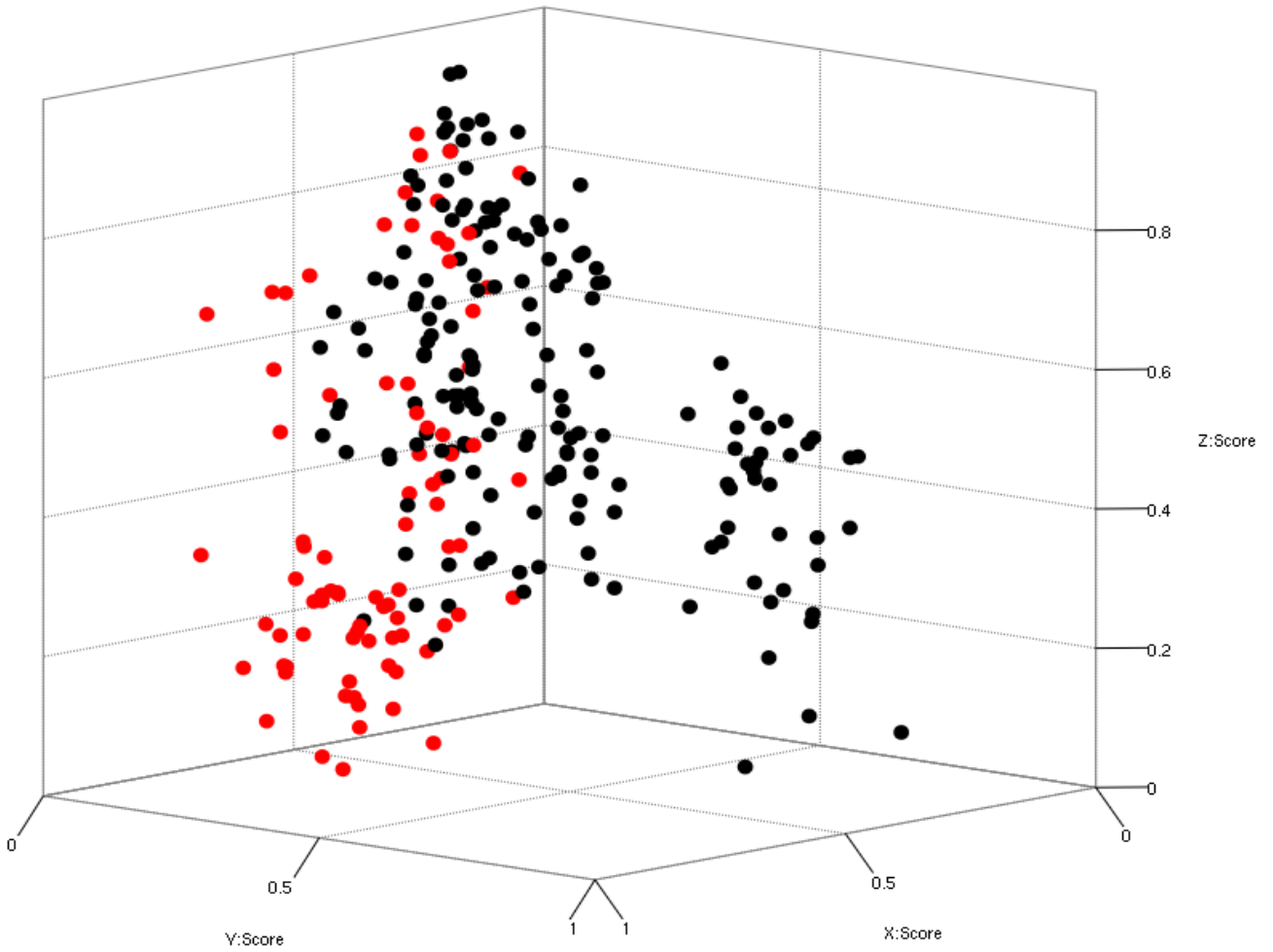


Figure 21. Three-dimensional Cluster analysis of daily fecal spectra (576nm – 1226nm) from 6 non-infested *Bos taurus* cattle. Spectra from the 24th day to the 36th day are indicated in red, the spectra from all prior and later days are indicated in black. Figure axes correspond to the first three most common spectral variations (factors), and are representative of 87.39% of total spectral variation.

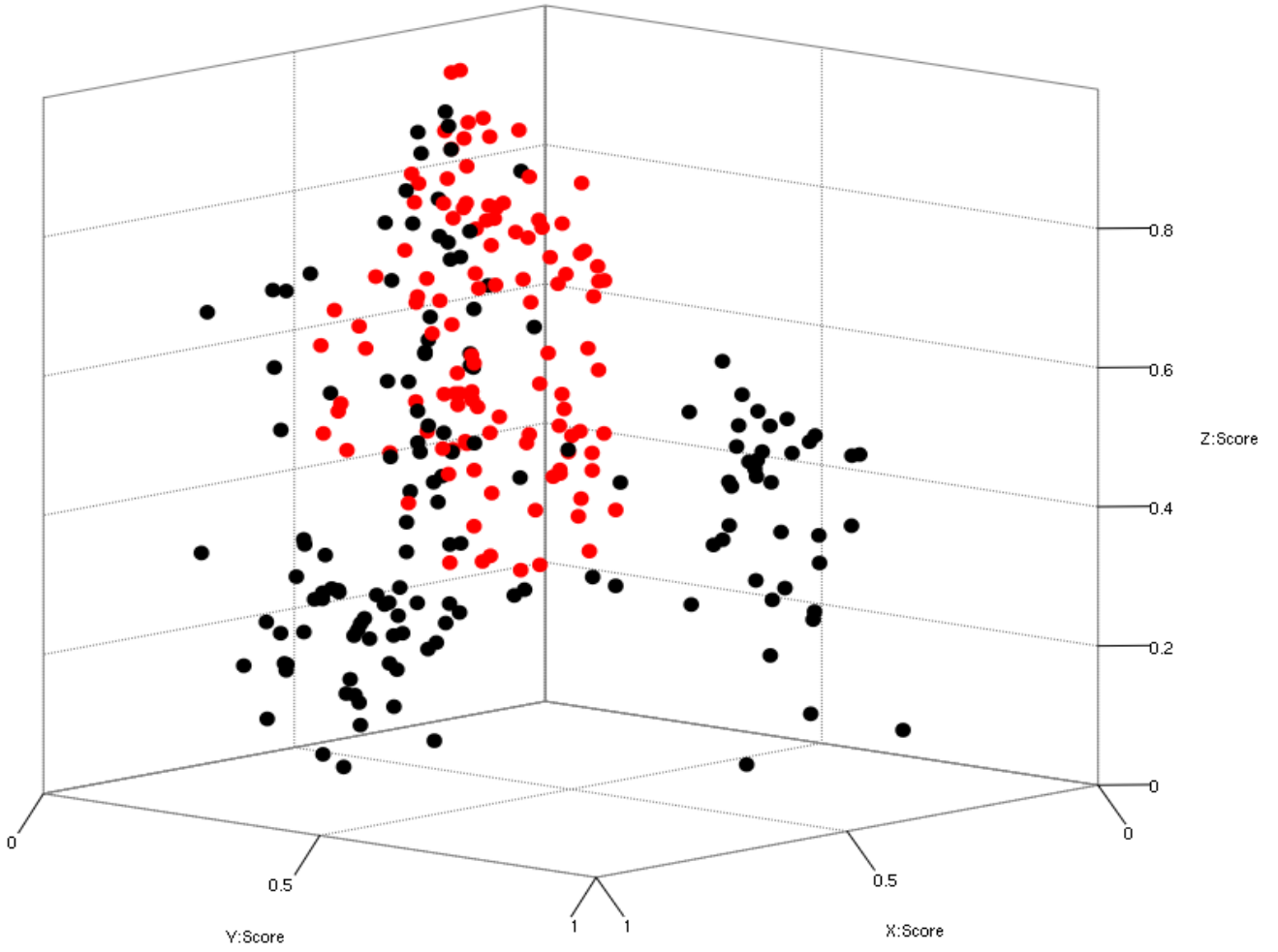


Figure 22. Three-dimensional Cluster analysis of daily fecal spectra (576nm – 1226nm) from 6 non-infested *Bos taurus* cattle. Spectra from the 37th day to the 59th day are indicated in red, the spectra from all prior and later days are indicated in black. Figure axes correspond to the first three most common spectral variations (factors), and are representative of 87.39% of total spectral variation.

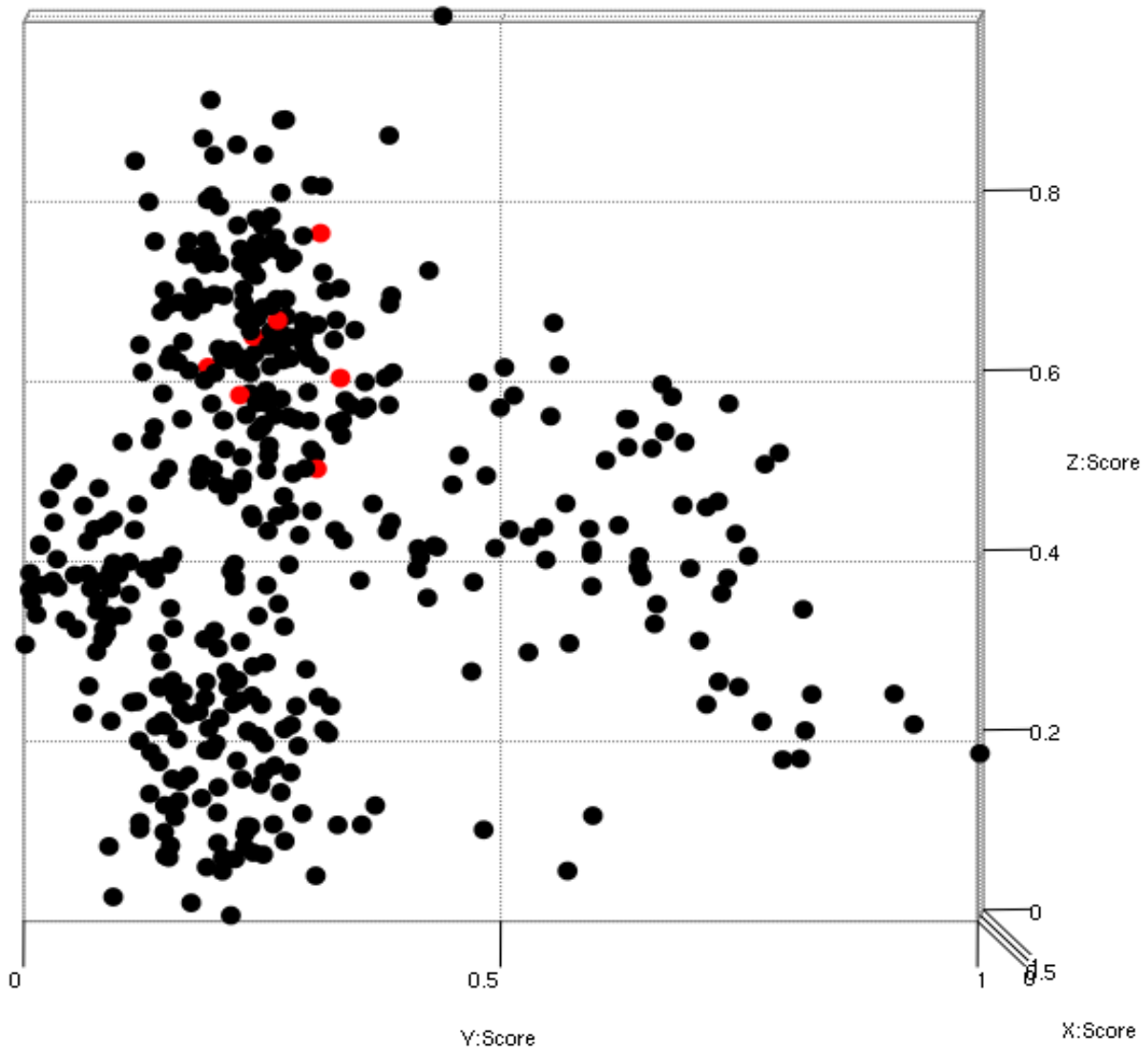


Figure 23. Three-dimensional Cluster analysis of daily fecal spectra (576nm – 1226nm) from 6 *Bos taurus* cattle infested with *R. microplus* from day-1 through day-59. Spectra from the ageing studies (each a 12-day elements exposure with cool and warm season studies, both shaded and exposed samples from the first 24-hour exposure) are indicated in black. Original samples from which the objective-2 samples were taken (day 34) are indicated in red, the spectra from all other days are indicated in black. Figure axes correspond to the first three most common spectral variations (factors), and are representative of 70.13% of total spectral variation.

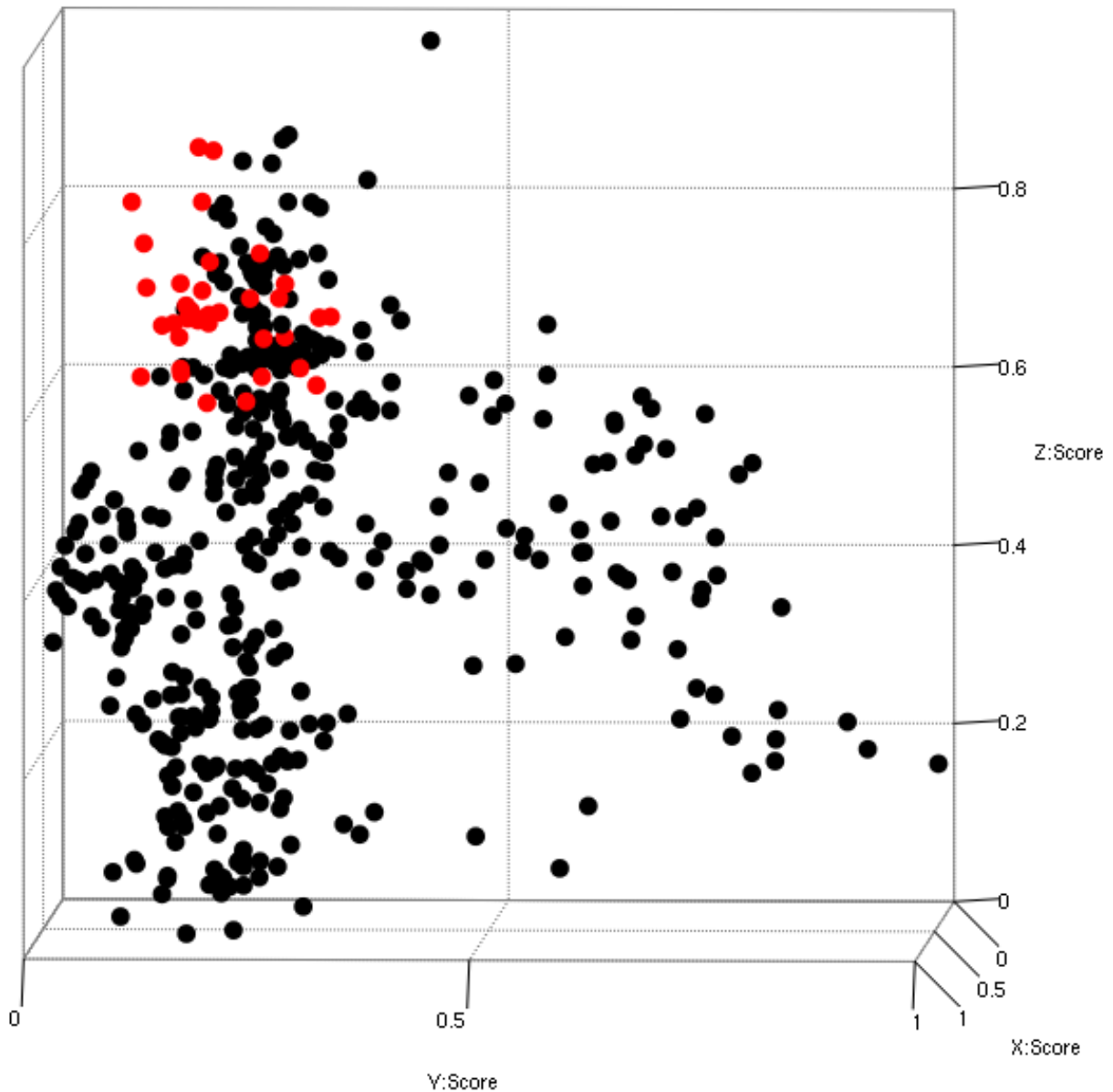


Figure 24. Three-dimensional Cluster analysis of daily fecal spectra (576nm – 1226nm) from 6 *Bos taurus* cattle infested with *R. microplus* from day-1 through day-59. Spectra from the ageing studies (each a 12-day elements exposure with cool and warm season studies, both shaded and exposed samples from the first 24-hour exposure) are indicated in red. Original samples from which the objective-2 samples were taken (day 34) and the spectra from all other days are indicated in black. Figure axes correspond to the first three most common spectral variations (factors), and are representative of 70.13% of total spectral variation.

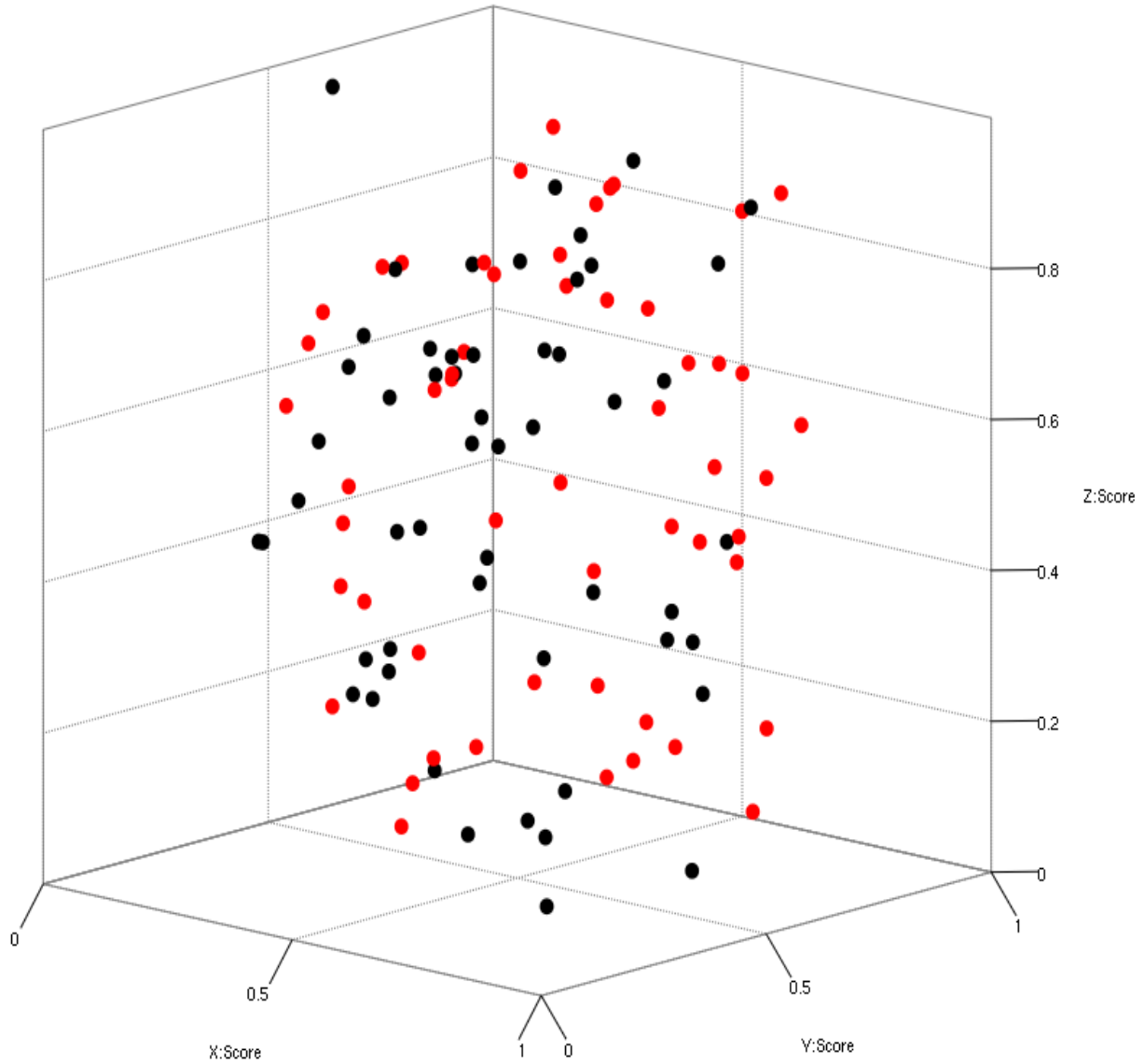


Figure 25. Three-dimensional Cluster analysis of daily fecal spectra (576nm – 1226nm) from 6 *Bos taurus* cattle infested with *R. microplus* collected on day-34 (exposed to elements for 12 days). Fecal samples from the cool-season study (exposed treatment) are indicated in red. Spectra from the cool-season (shaded treatment) are indicated in black. Figure axes correspond to the first three most common spectral variations (factors), and are representative of 75.2% of total spectral variation.

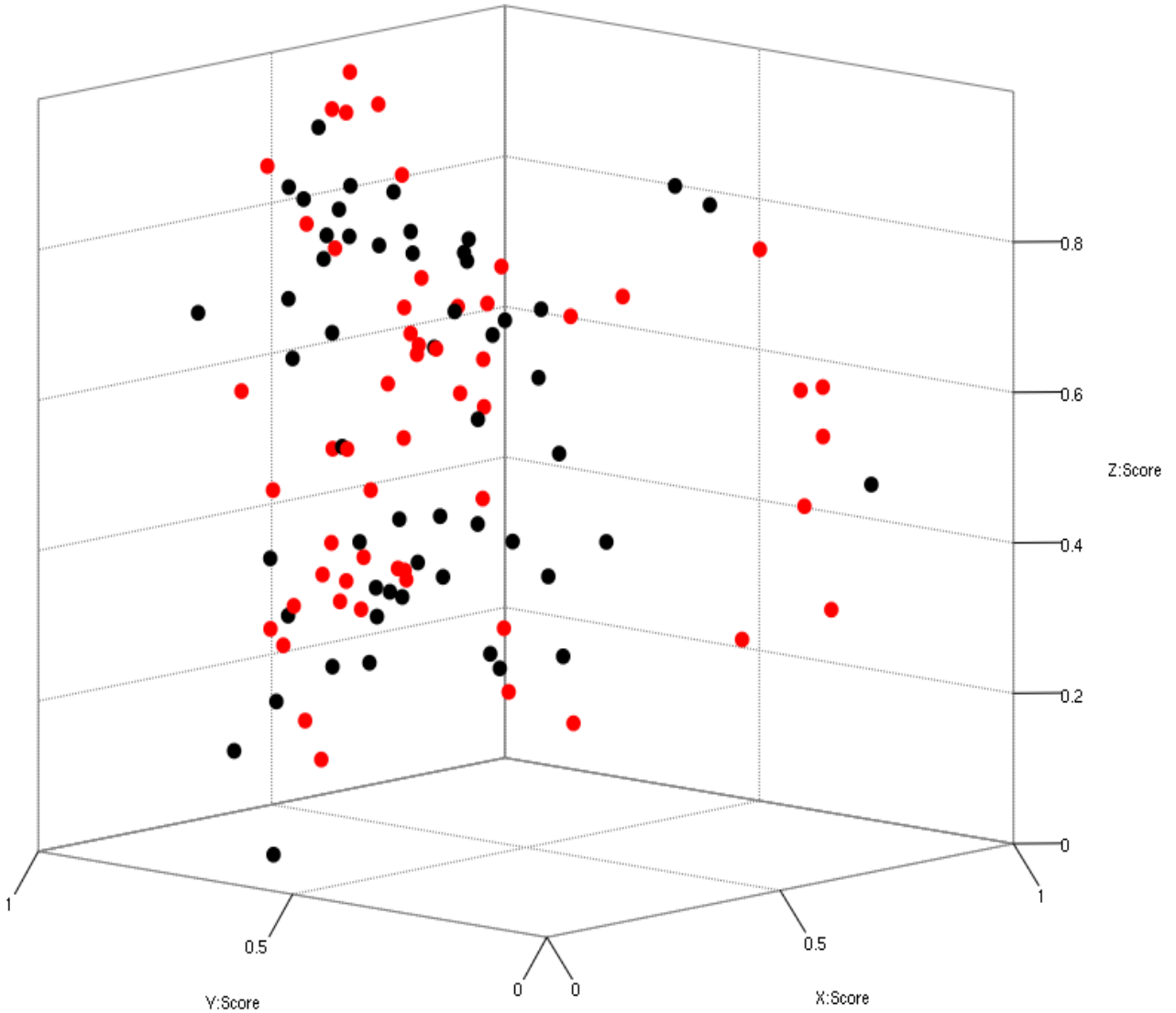


Figure 26. Three-dimensional Cluster analysis of daily fecal spectra (576nm – 1226nm) from 6 *Bos taurus* cattle infested with *R. microplus* collected on day-34 (exposed to elements for 12 days). Fecal samples from the warm-season study (exposed treatment) are indicated in red. Spectra from the warm-season (shaded treatment) are indicated in black. Figure axes correspond to the first three most common spectral variations (factors), and are representative of 83.01% of total spectral variation.

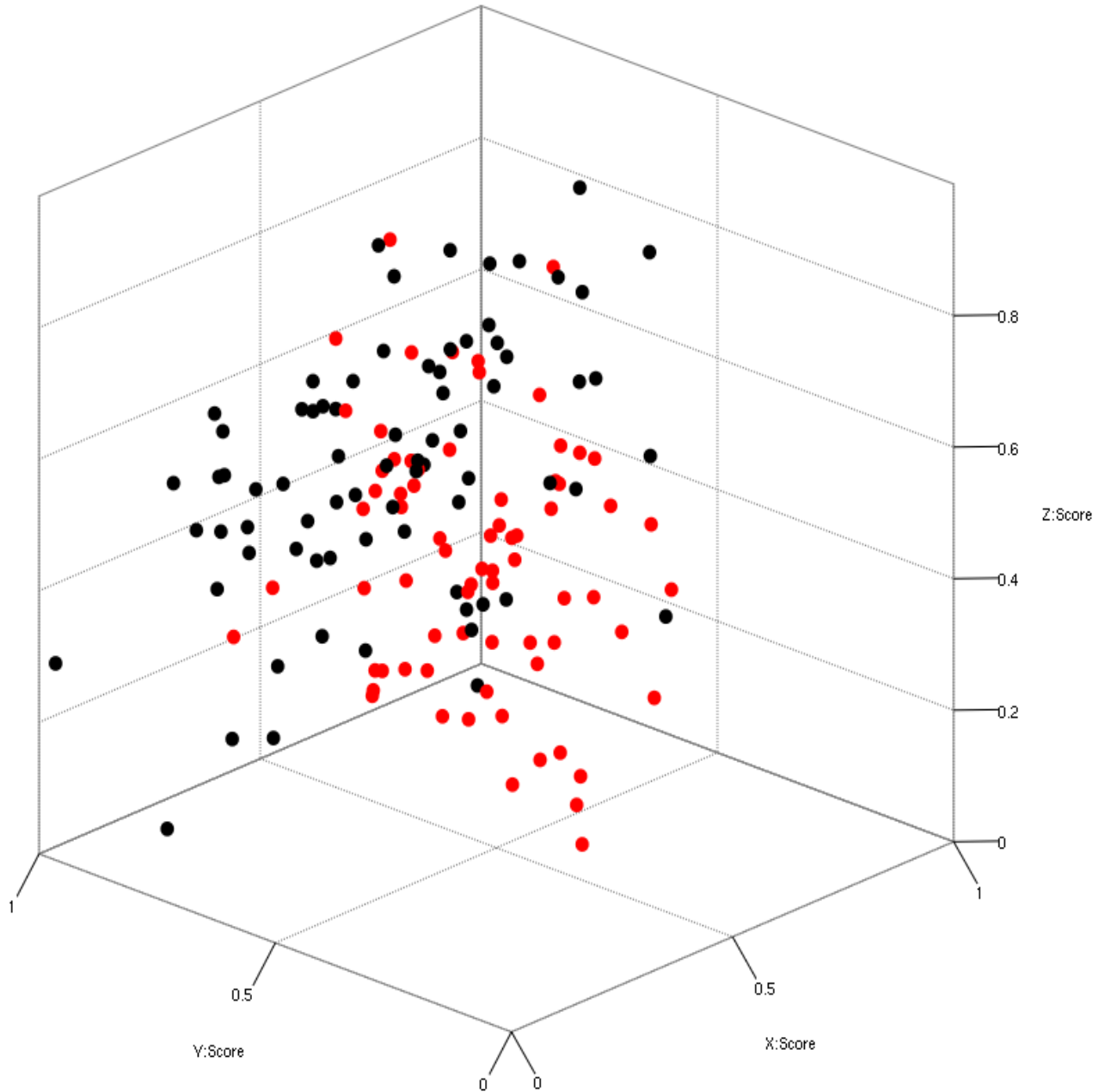


Figure 27. Three-dimensional Cluster analysis of daily fecal spectra (576nm – 1226nm) from 6 *Bos taurus* cattle infested with *R. microplus* collected on day-34 (exposed to elements for 12 days). Fecal samples from the cool-season study (exposed and shaded treatments) are indicated in red. Spectra from the warm-season (exposed and shaded treatments) are indicated in black. Figure axes correspond to the first three most common spectral variations (factors), and are representative of 91.1% of total spectral variation.

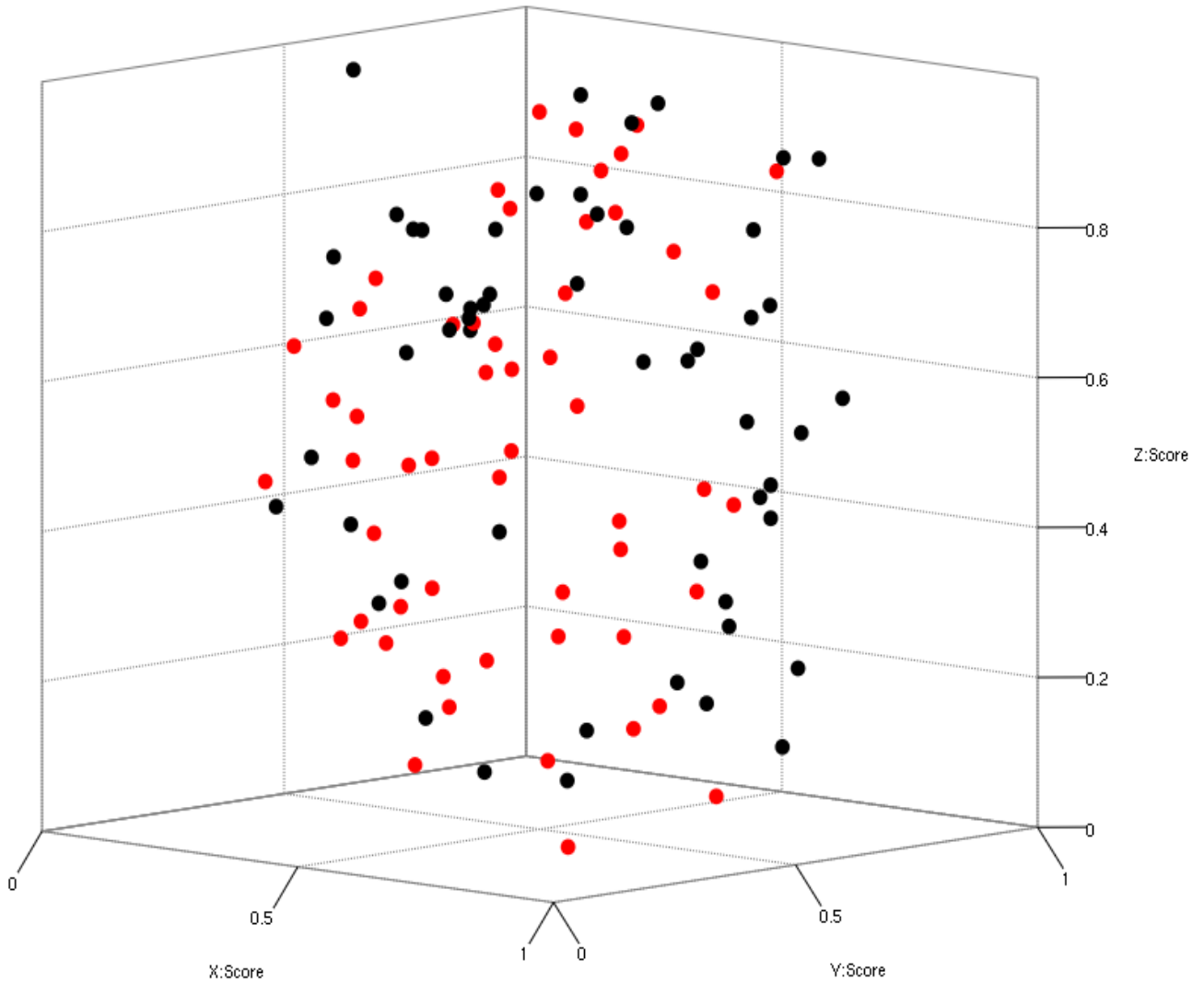


Figure 28. Three-dimensional Cluster analysis of daily fecal spectra (576nm – 1226nm) from 6 *Bos taurus* cattle infested with *R. microplus* collected on day-34 (exposed to elements for 12 days). Fecal samples from the cool-season study (exposed and shaded treatments) for the first six days of exposure are indicated in red. All other spectra (day-7 to day-12) are indicated in black. Figure axes correspond to the first three most common spectral variations (factors), and are representative of 75.2% of total spectral variation.

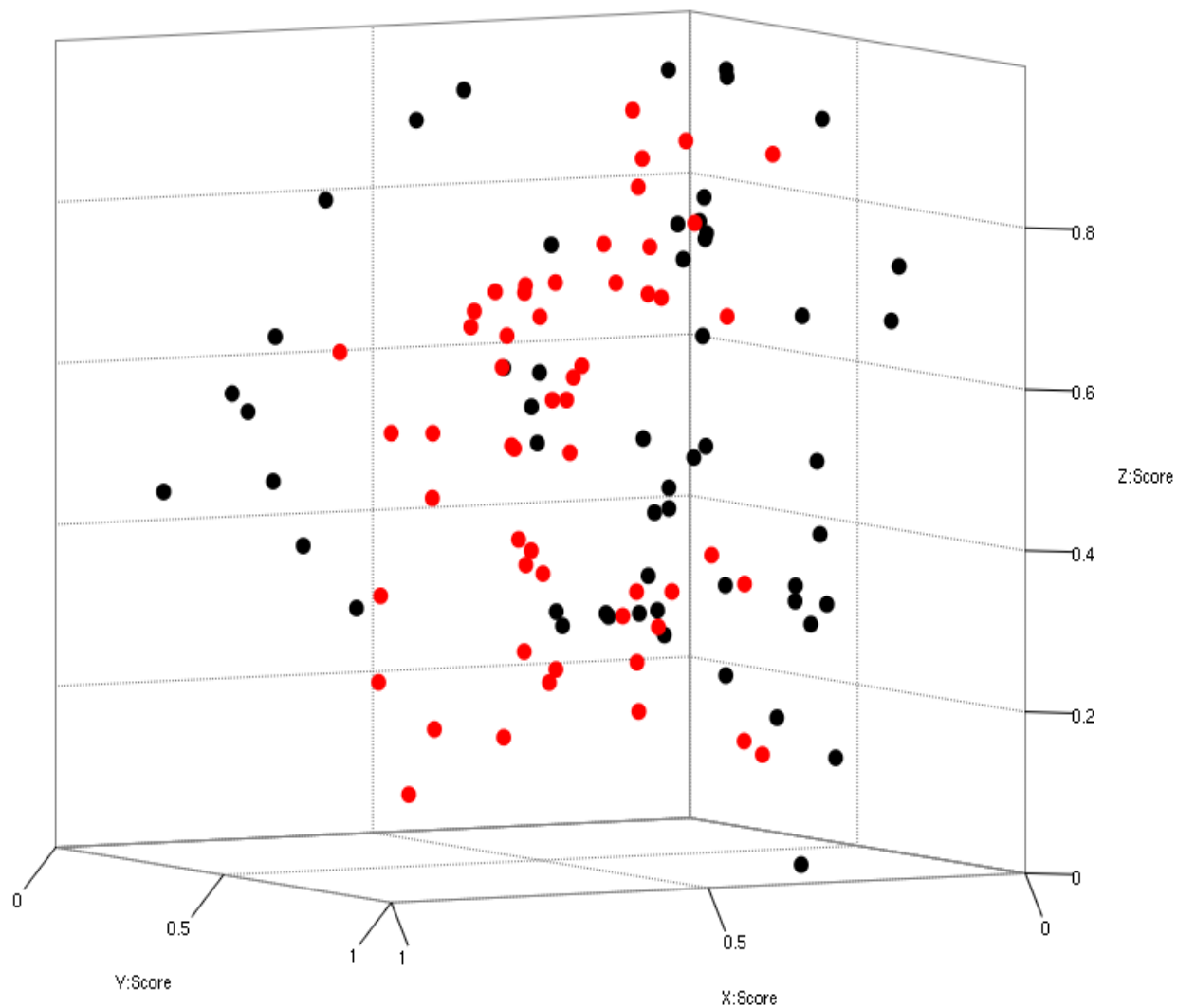


Figure 29. Three-dimensional Cluster analysis of daily fecal spectra (576nm – 1226nm) from 6 *Bos taurus* cattle infested with *R. microplus* collected on day-34 (exposed to elements for 12 days). Fecal samples from the warm-season study (exposed and shaded treatments) for the first six days of exposure are indicated in red. All other spectra (day-7 to day-12) are indicated in black. Figure axes correspond to the first three most common spectral variations (factors), and are representative of 83.01% of total spectral variation.

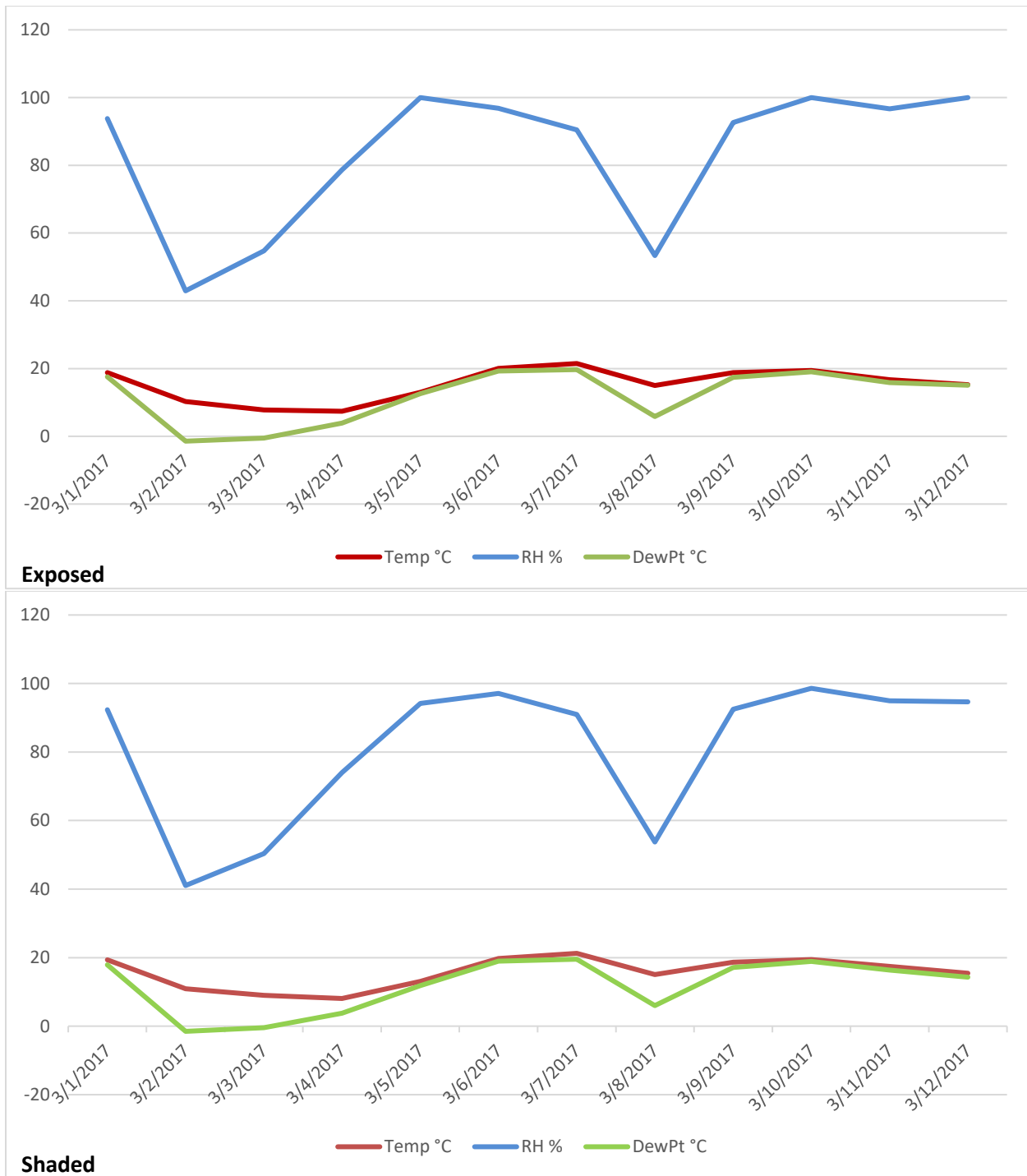


Figure 30. Twelve-day warm season comparison of temperature, relative humidity and dew point between non-shaded and shaded environments during exposure of fecal pies (days shown as “x” axis, percent/degrees Celsius shown as “y” axis) prepared from the feces of non-infested control cattle and cattle that were infested with *R. microplus*.

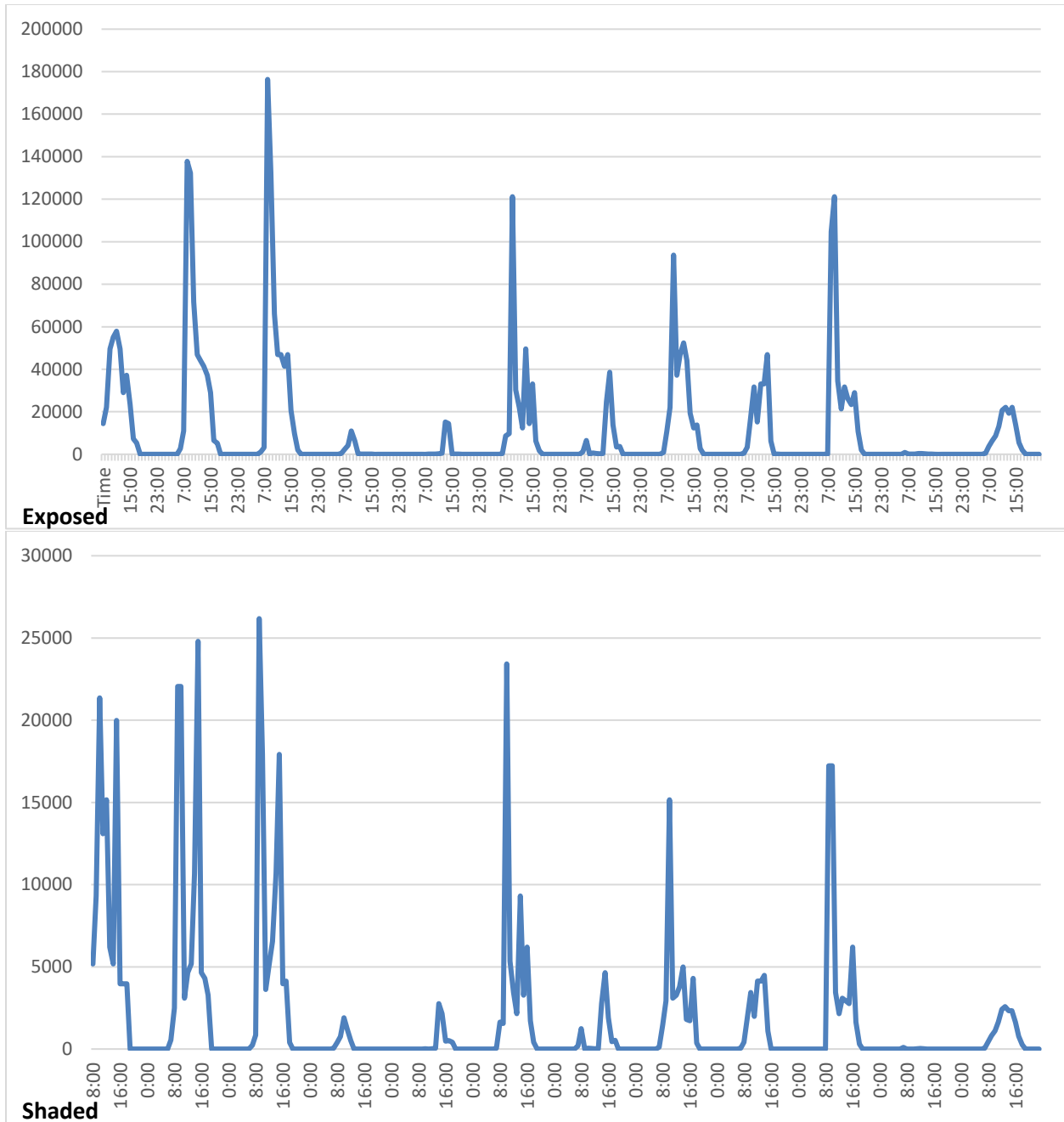


Figure 31. Twelve-day cool season comparison of light intensity measured in lux between shaded and non-shaded environments during exposure of fecal pies (hours of time shown as “x” axis, lux amount shown as “y” axis) prepared from the feces of non-infested control cattle and cattle that were infested with *R. microplus*.

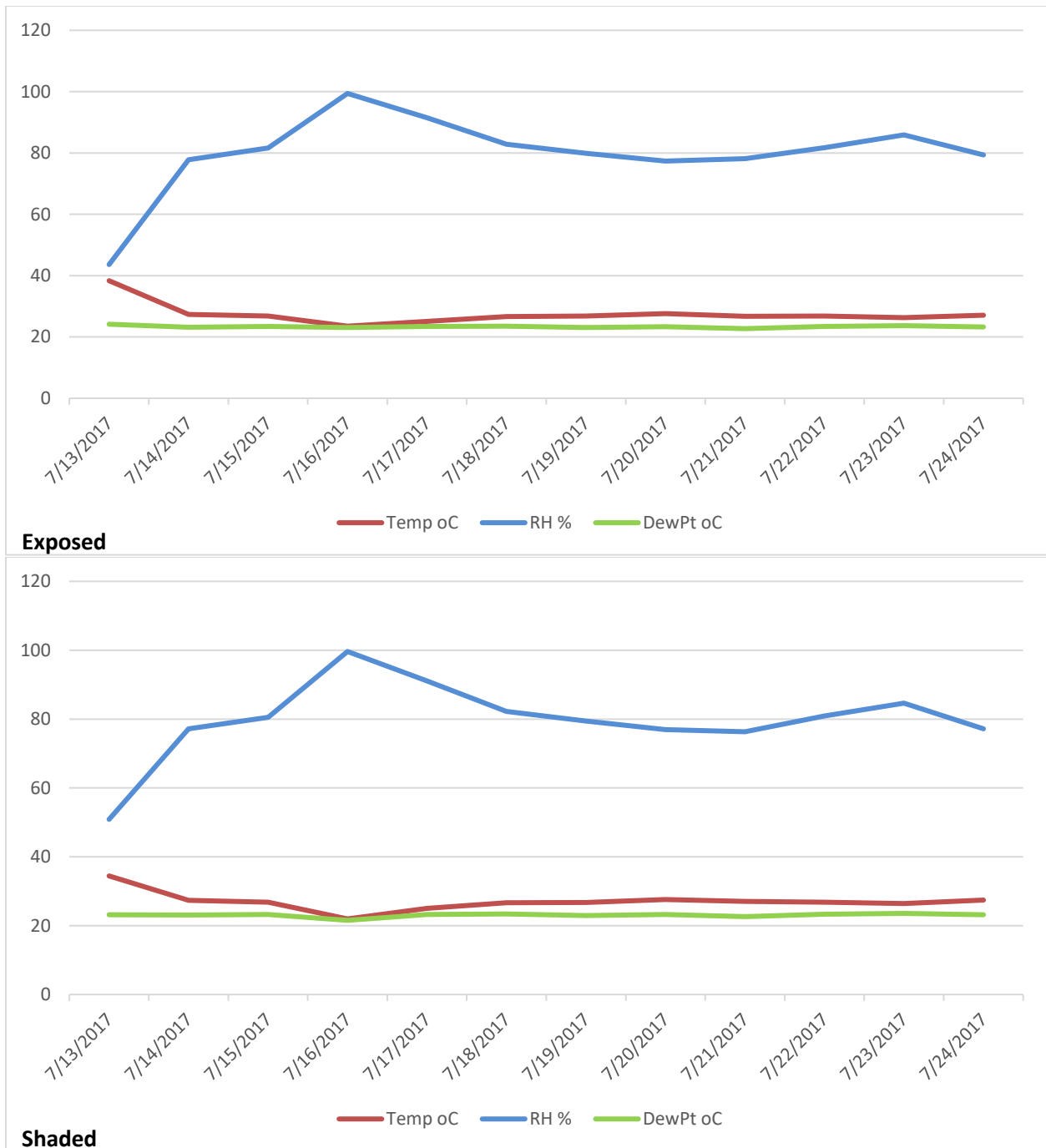


Figure 32. Twelve-day warm season comparison of temperature, relative humidity and dew point between non-shaded and shaded environments during exposure of fecal pies (days shown as “x” axis, percent/degrees Celsius shown as “y” axis) prepared from the feces of non-infested control cattle and cattle that were infested with *R. microplus*.

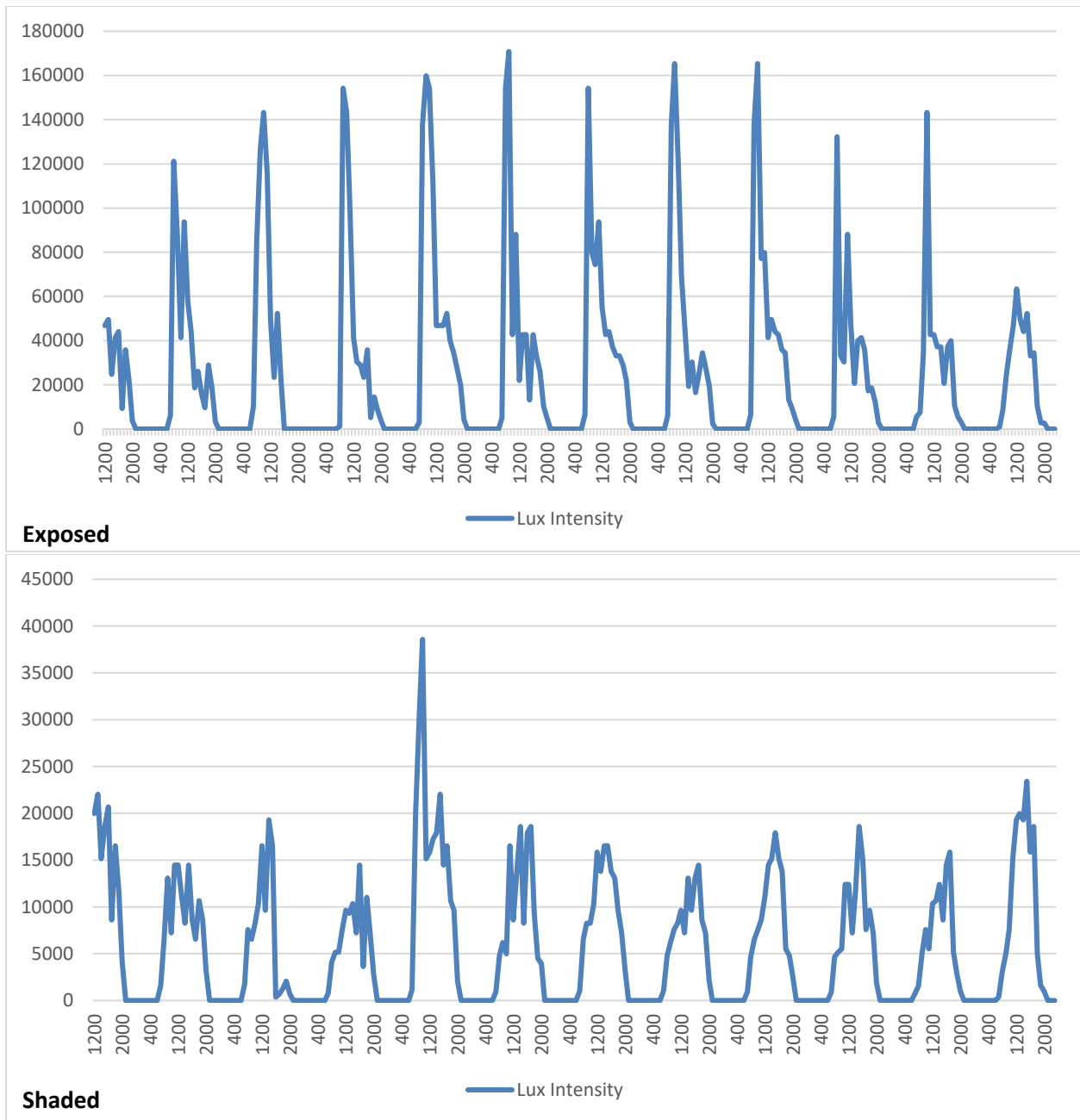


Figure 33. Twelve-day warm season comparison (July 13th to July 25th 2017) of light intensity measured in lux between shaded and non-shaded environments during exposure of fecal pies (hours of time shown as “x” axis, lux amount shown as “y” axis) prepared from the feces of non-infested control cattle and cattle that were infested with *R. microplus*.

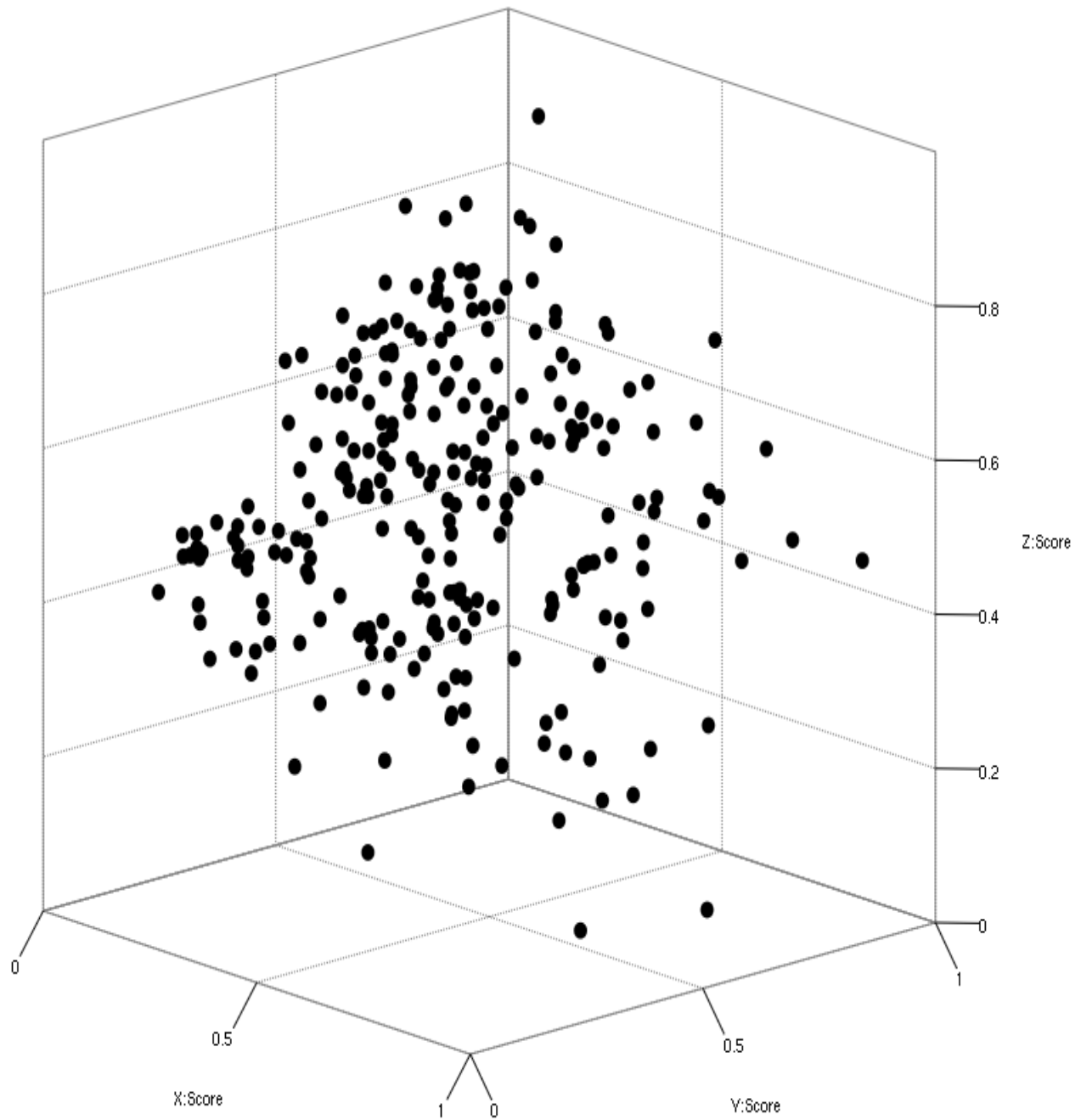


Figure 34. Three-dimensional Cluster analysis of daily fecal spectra (800nm – 1800nm) from 6 *Bos taurus* cattle infested with *R. microplus* from day-1 through day-59 demonstrating that this spectral range yields no separation of spectra. Figure axes correspond to the first three most common spectral variations (factors), and are representative of 86.36% of total spectral variation.

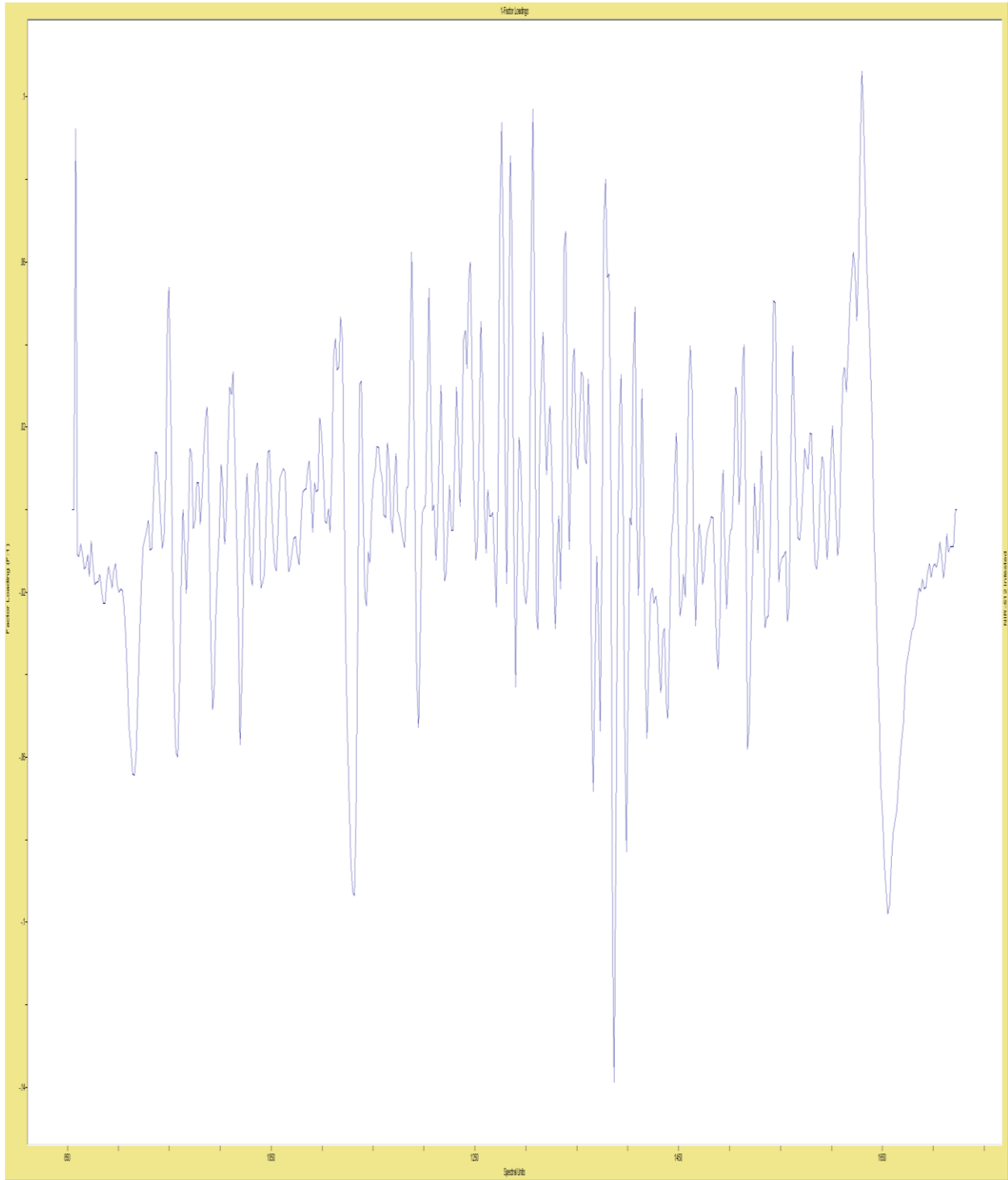


Figure 35. NIRS FCP illustrated by spectrograph produced by the Ocean Optics NIR-512 spectrometer. Each peak and valley represents a point of absorption or reflection with the factor loading as the “y” axis and the spectral units (in nanometers) as the “x” axis. This is the first most common spectral variation (factor) from the full study using only the infested animals as well as using a narrowed spectrum (800nm-1800nm fixed spectral range). This spectral variation is representative of 69.84% of the total variation within this group.

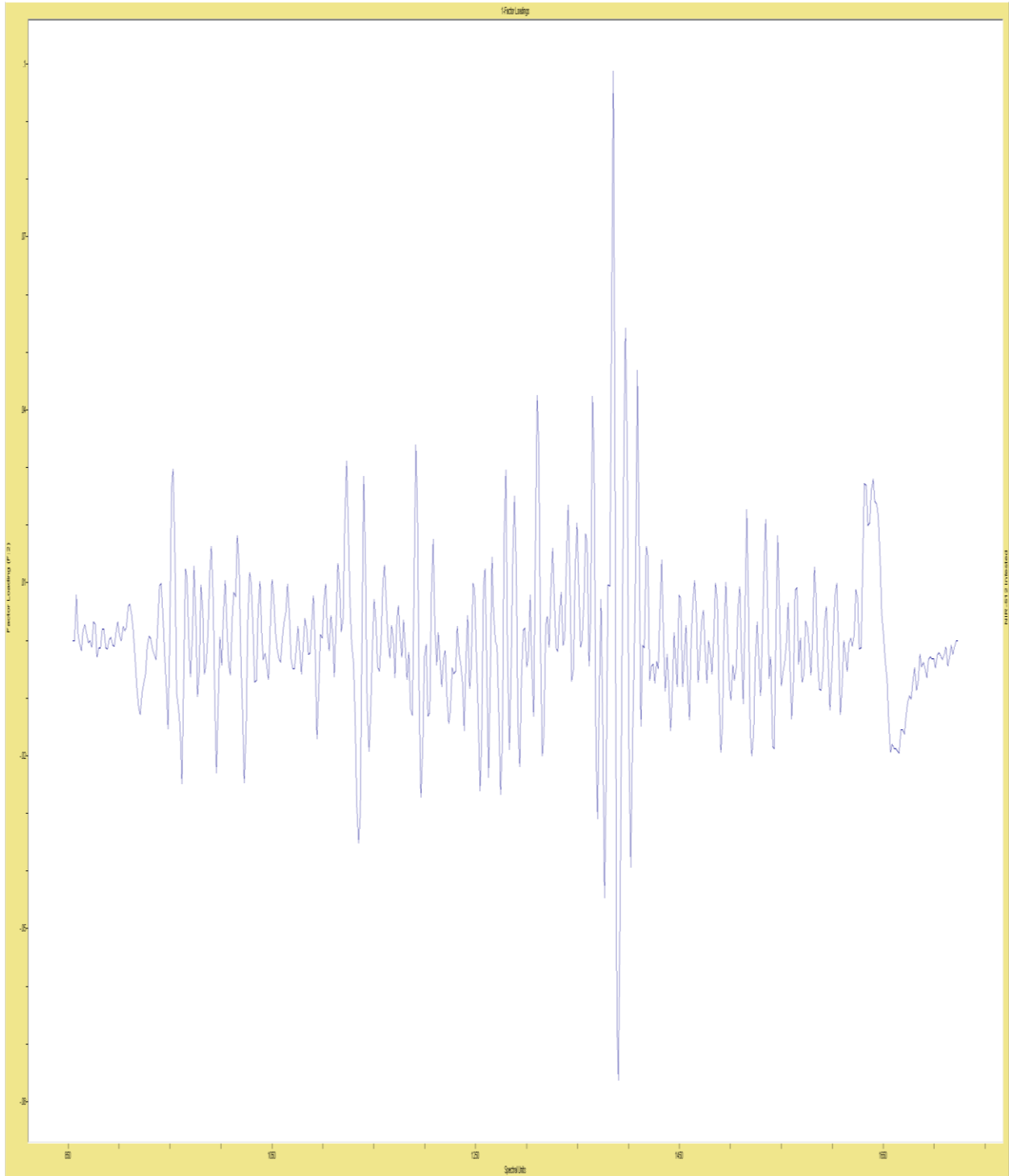


Figure 36. NIRS FCP illustrated by spectrograph produced by the Ocean Optics NIR-512 spectrometer. Each peak and valley represents a point of absorption or reflection with the factor loading as the “y” axis and the spectral units (in nanometers) as the “x” axis. This is the second most common spectral variation (factor) from the full study using only the infested animals as well as using a narrowed spectrum (800nm-1800nm fixed spectral range). This spectral variation is representative of 12.34% of the total variation within this group.

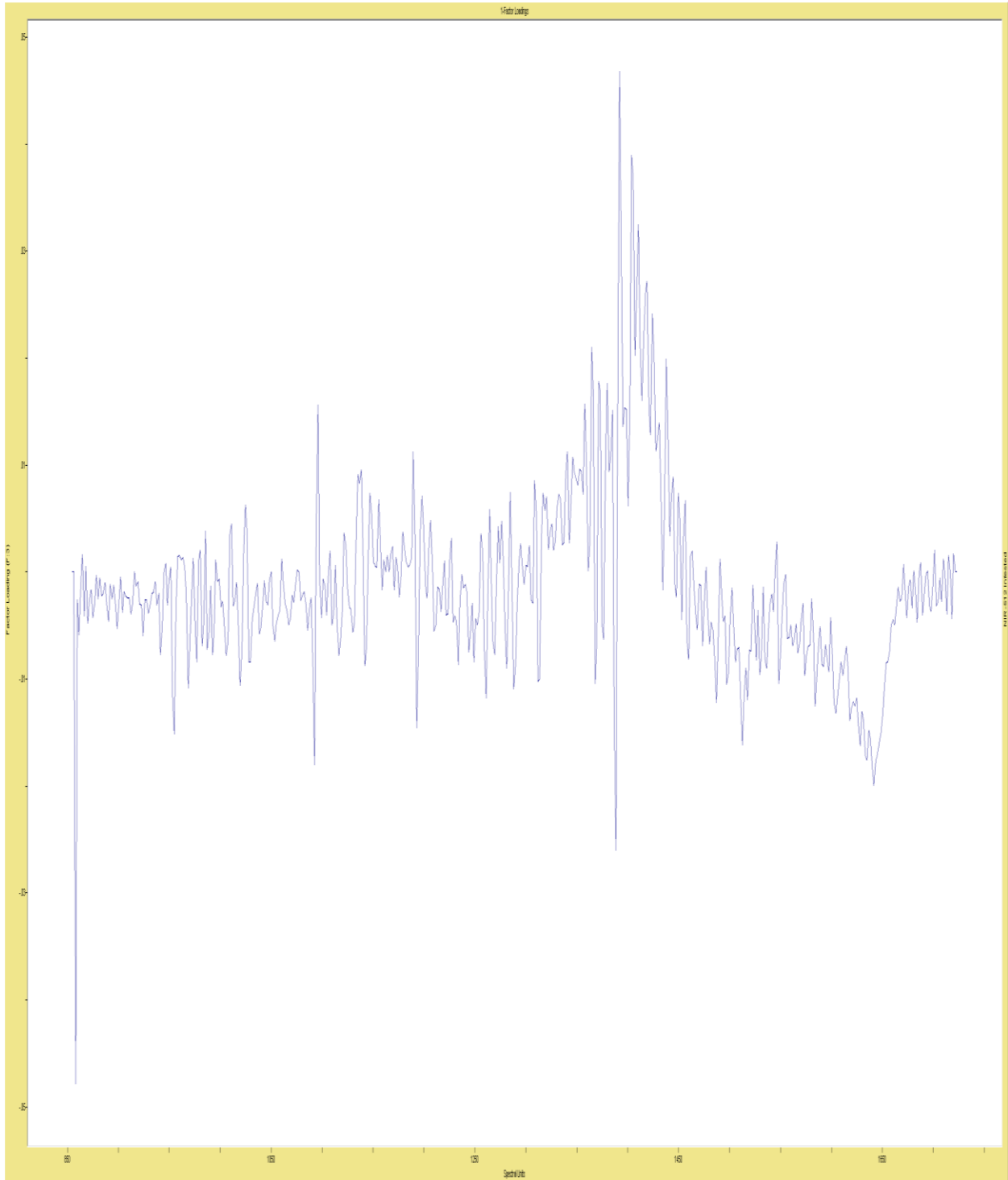


Figure 37. NIRS FCP illustrated by spectrograph produced by the Ocean Optics NIR-512 spectrometer. Each peak and valley represents a point of absorption or reflection with the factor loading as the “y” axis and the spectral units (in nanometers) as the “x” axis. This is the third most common spectral variation (factor) from the full study using only the infested animals as well as using a narrowed spectrum (800nm-1800nm fixed spectral range). This spectral variation is representative of 4.81% of the total variation within this group.

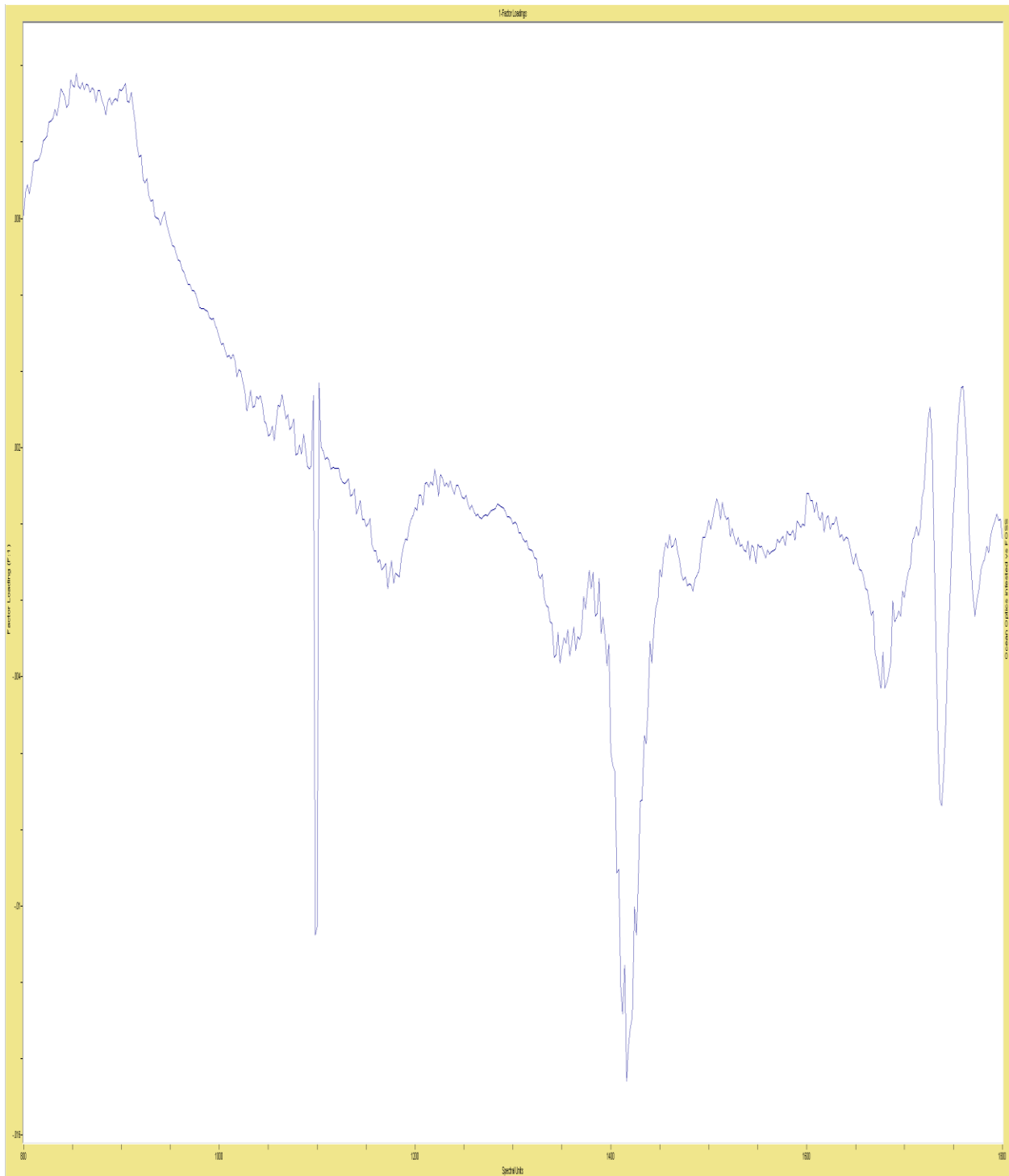


Figure 38. NIRS FCP illustrated by spectrograph produced by the FOSS 6500 spectrometer. Each peak and valley represents a point of absorption or reflection with the factor loading as the “y” axis and the spectral units (in nanometers) as the “x” axis. This is the first most common spectral variation (factor) from the full study using only the infested animals as well as using a narrowed spectrum (800nm-1800nm complementary spectral range to the NIR-512). This spectral variation is representative of 50.38% of the total variation within this group.

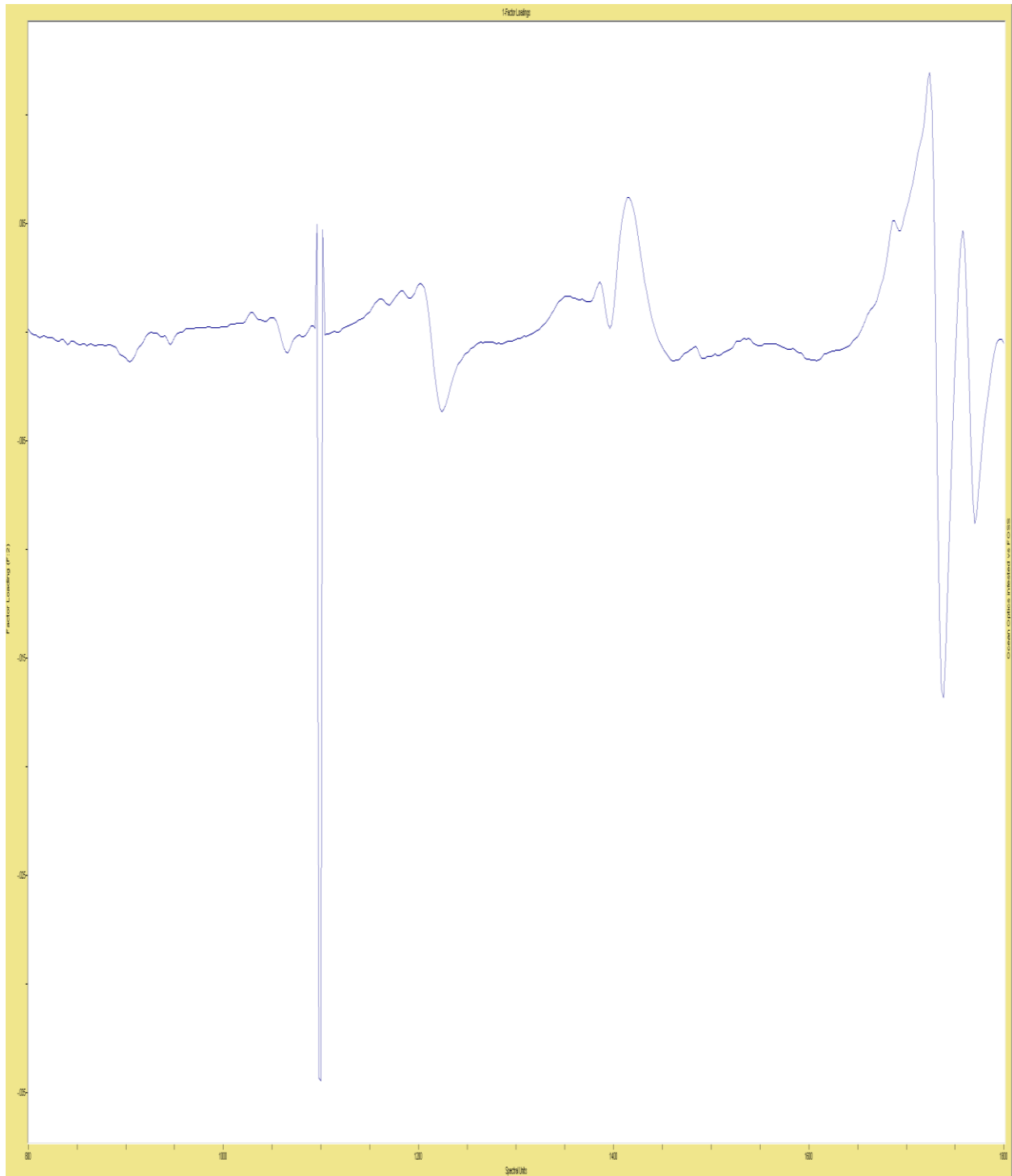


Figure 39. NIRS FCP illustrated by spectrograph produced by the FOSS 6500 spectrometer. Each peak and valley represents a point of absorption or reflection with the factor loading as the “y” axis and the spectral units (in nanometers) as the “x” axis. This is the second most common spectral variation (factor) from the full study using only the infested animals as well as using a narrowed spectrum (800nm-1800nm complementary spectral range to the NIR-512). This spectral variation is representative of 25.13% of the total variation within this group.

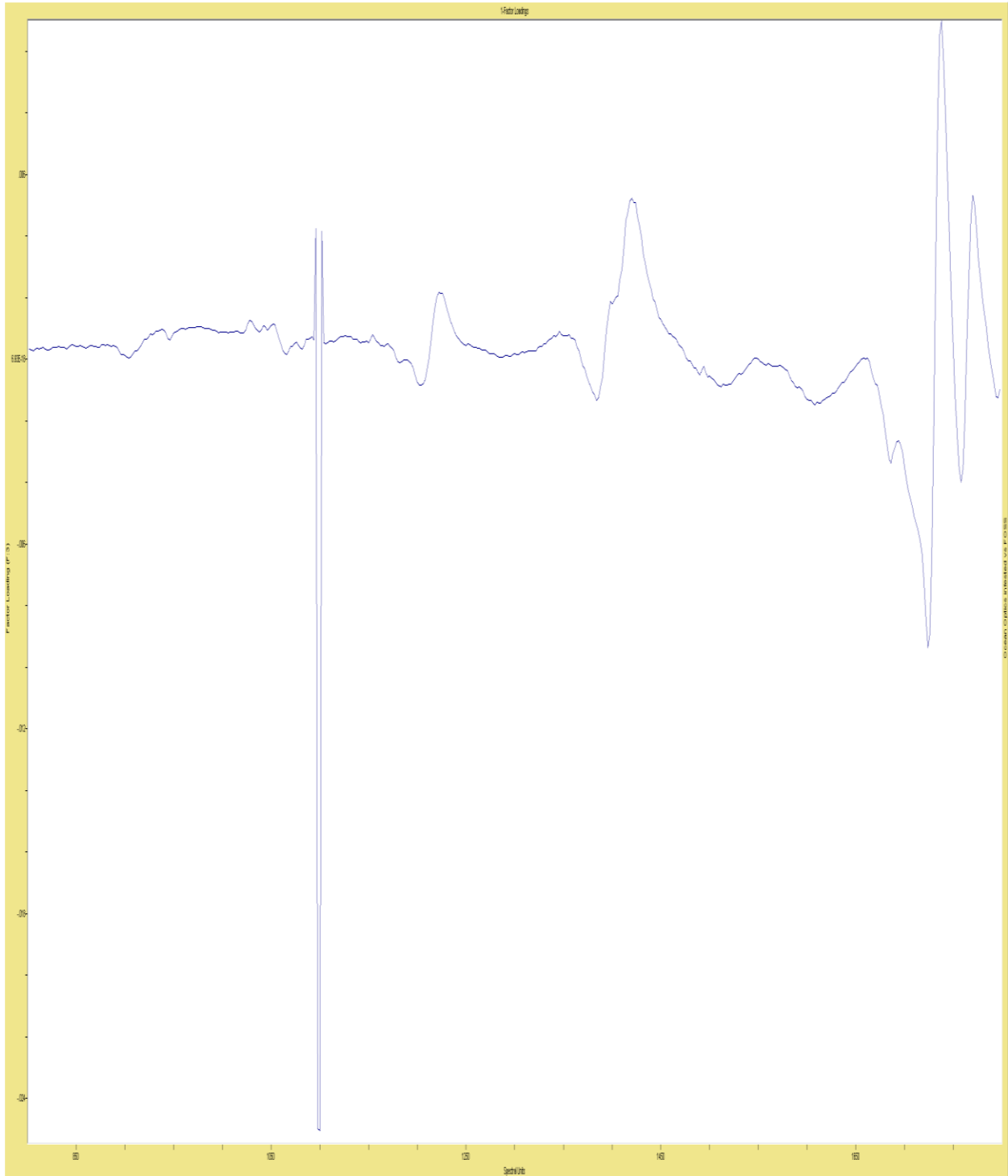
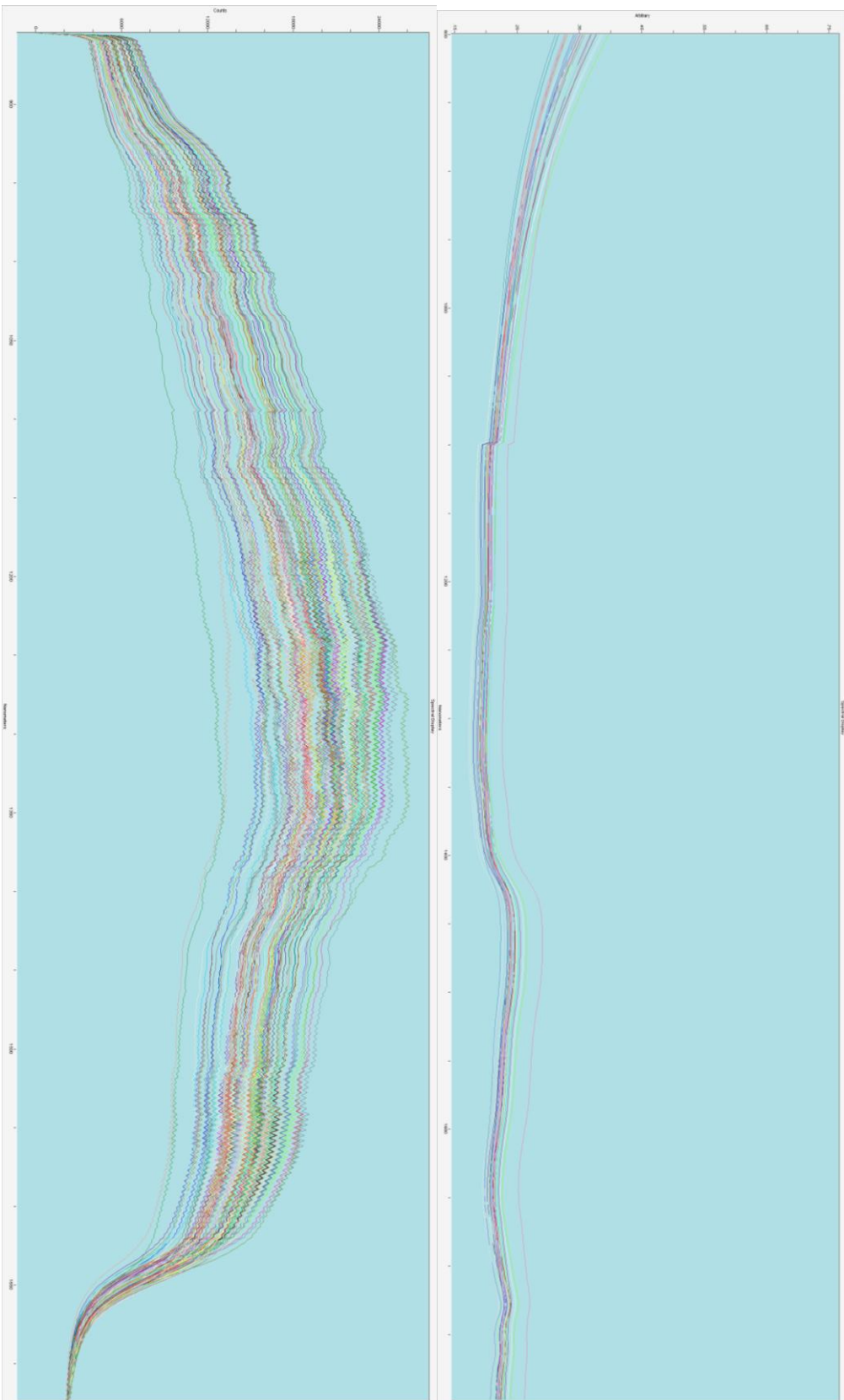


Figure 40. NIRS FCP illustrated by spectrograph produced by the FOSS 6500 spectrometer. Each peak and valley represents a point of absorption or reflection with the factor loading as the “y” axis and the spectral units (in nanometers) as the “x” axis. This is the third most common spectral variation (factor) from the full study using only the infested animals as well as using a narrowed spectrum (800nm-1800nm complementary spectral range to the NIR-512). This spectral variation is representative of 12.66% of the total variation within this group.

Figure 41. NIRS raw spectrograph produced by the FOSS 6500 (top) and the Ocean Optics NIR-512 (bottom) spectrometers using the same fecal samples from the infested animals in objective-1. Each peak and valley represents a point of absorption or reflection within the fecal samples exposed to near infrared light and using a narrowed spectrum (800nm-1800nm). The “x” axis is the spectral range in nanometers and the “y” axis are light intensity.



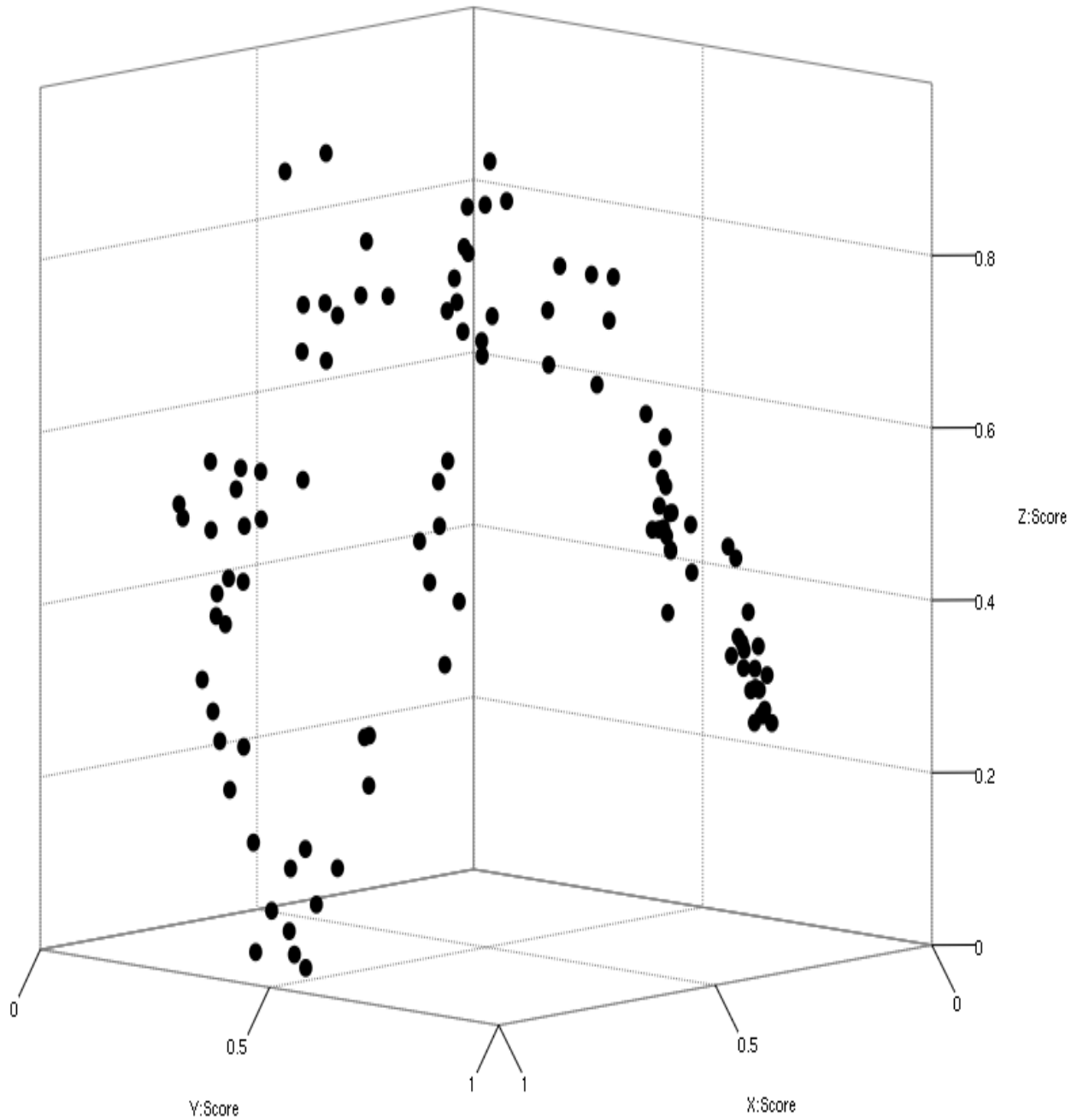


Figure 42. Three-dimensional Cluster analysis of daily fecal spectra generated by the Ocean Optics NIR-512 (800nm – 1800nm) from 6 *Bos taurus* cattle infested with *R. microplus* from day-1 through day-59 demonstrating that this spectral range yields no separation of spectra. Figure axes correspond to the first three most common spectral variations (factors), and are representative of 86.36% of total spectral variation.

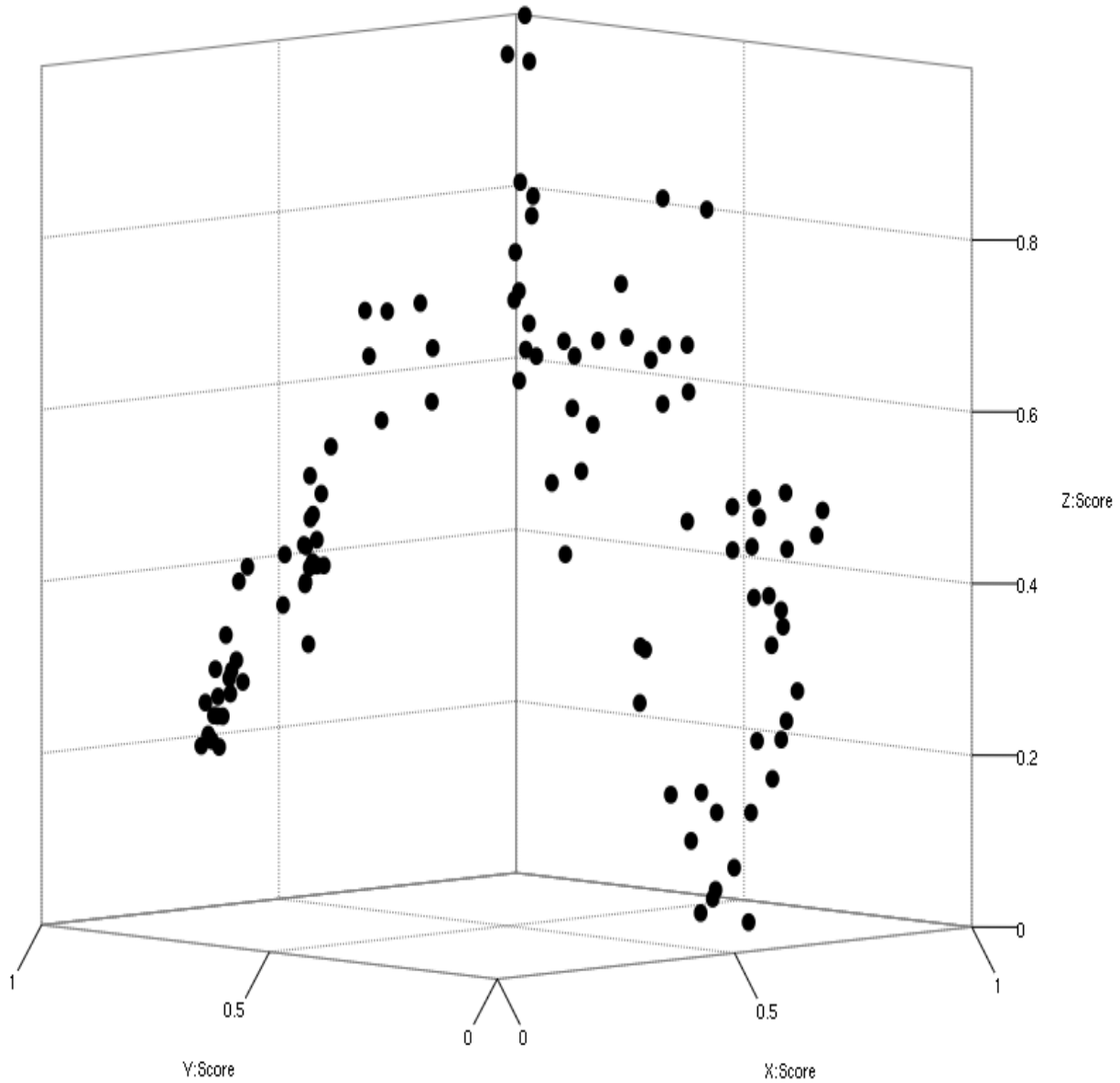


Figure 43. Three-dimensional Cluster analysis of daily fecal spectra generated by the Ocean Optics NIR-512 (800nm – 1800nm) from 6 *Bos taurus* cattle infested with *R. microplus* from day-1 through day-59 demonstrating that this spectral range yields no separation of spectra. Figure axes correspond to the first three most common spectral variations (factors), and are representative of 86.36% of total spectral variation.

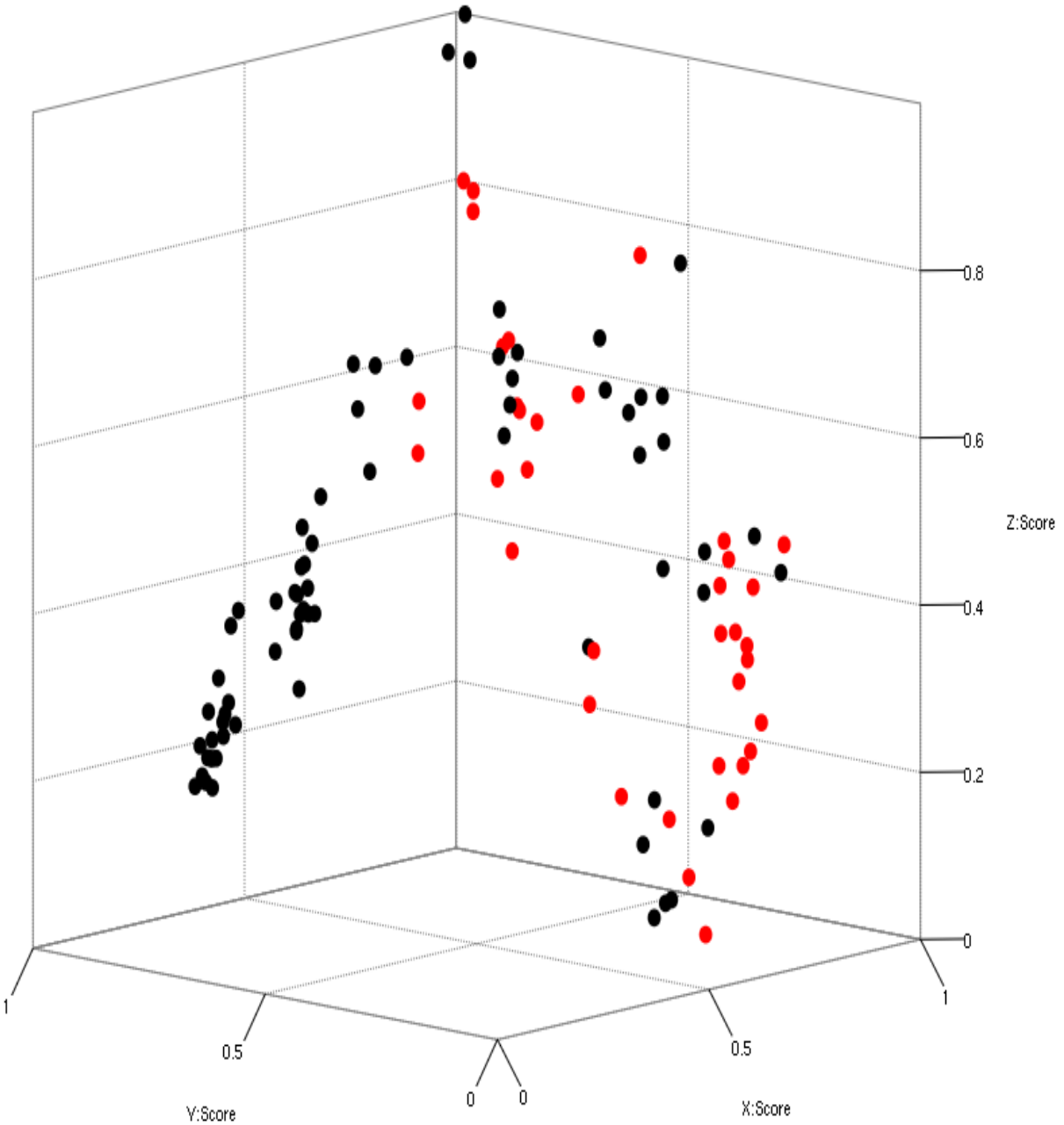


Figure 44. Three-dimensional Cluster analysis of daily fecal spectra generated by the Ocean Optics NIR-512 (800nm – 1800nm) from 6 *Bos taurus* cattle infested with *R. microplus* from day-1 through day-59 (Days 1-22 indicated in red, all other days in black) demonstrating that this spectral range yields no separation of spectra. Figure axes correspond to the first three most common spectral variations (factors), and are representative of 86.36% of total spectral variation.

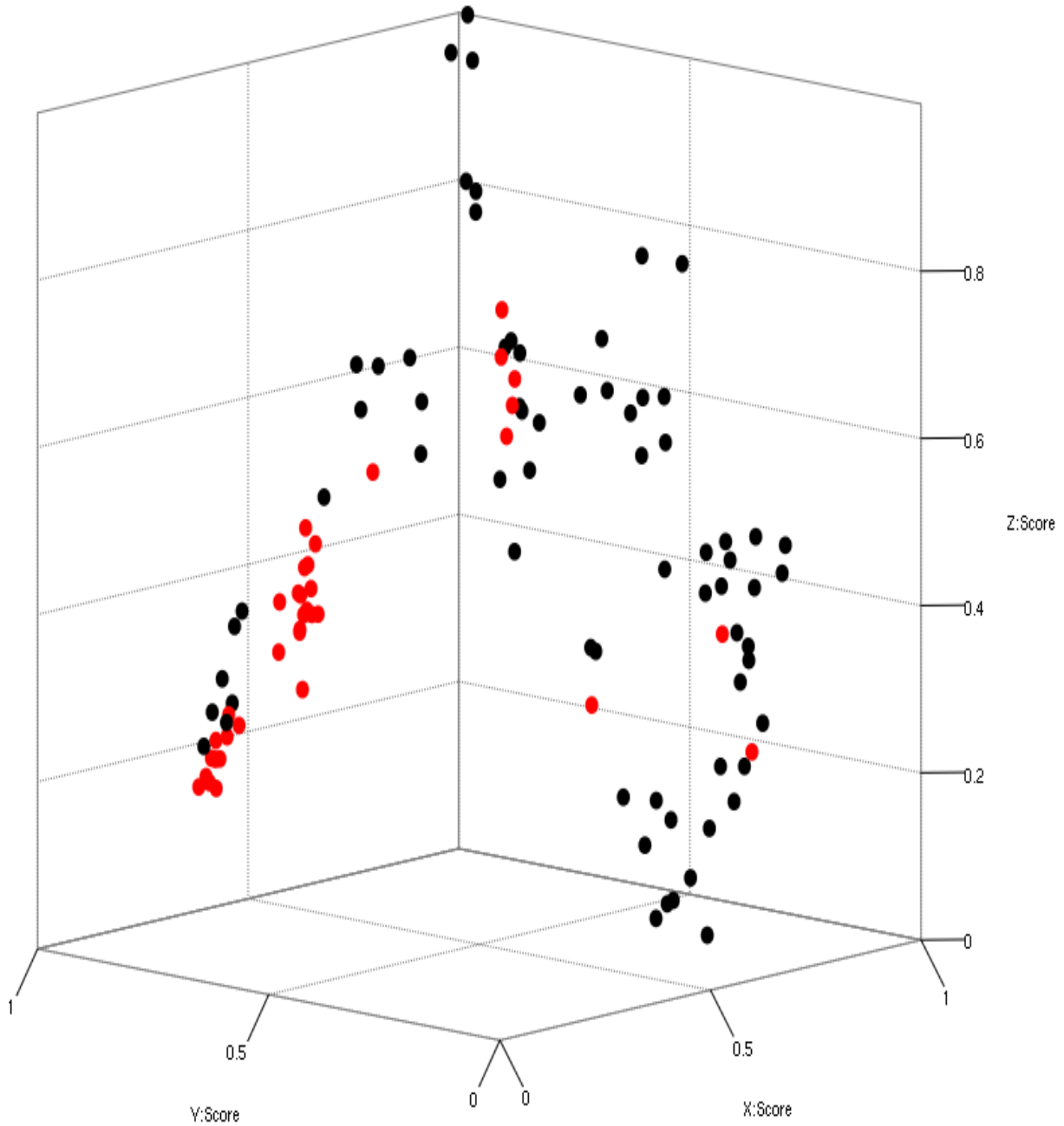


Figure 45. Three-dimensional Cluster analysis of daily fecal spectra generated by the Ocean Optics NIR-512 (800nm – 1800nm) from 6 *Bos taurus* cattle infested with *R. microplus* from day-1 through day-59 (Days 24-40 indicated in red, all other days in black) demonstrating that this spectral range yields no separation of spectra. Figure axes correspond to the first three most common spectral variations (factors), and are representative of 86.36% of total spectral variation.

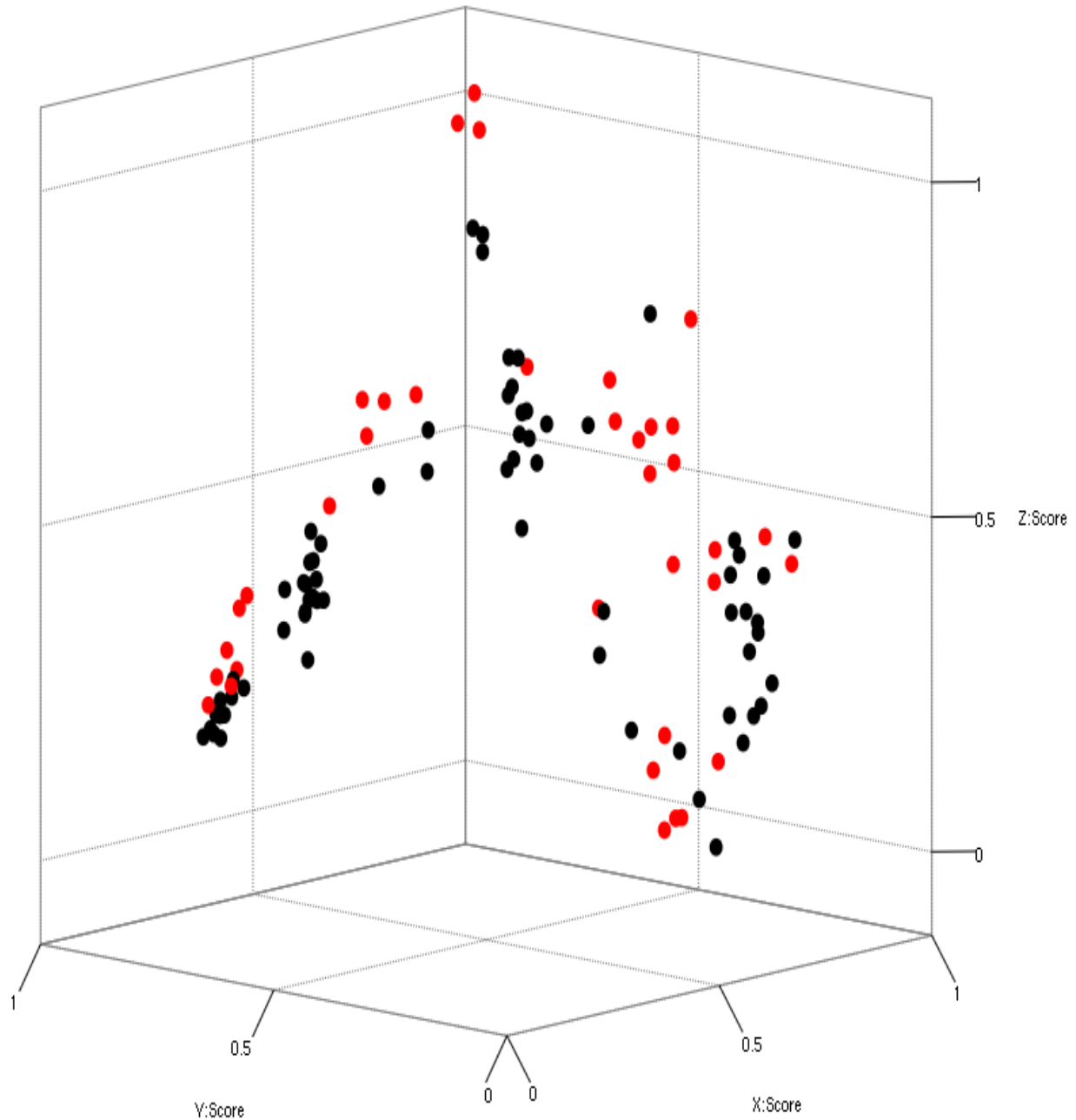


Figure 46. Three-dimensional Cluster analysis of daily fecal spectra generated by the Ocean Optics NIR-512 (800nm – 1800nm) from 6 *Bos taurus* cattle infested with *R. microplus* from day-1 through day-59 (Days 41-59 indicated in red, all other days in black) demonstrating that this spectral range yields no separation of spectra. Figure axes correspond to the first three most common spectral variations (factors), and are representative of 86.36% of total spectral variation.

Appendix B Tables

Table 1. Basic components of pelleted feed from three samples of the pelleted feed from the same lot with components listed on the right and the sample date shown on the top. Percentages are given where applicable, and parts per million (ppm) or mega calories per pound (Mcal/lb) used where appropriate.

Crude Protein	15.80%	13.30%	13.30%
Acid Detergent Fiber	20.30%	26.60%	19.80%
TDN-based on ADF	74.90%	69.00%	75.30%
Net Energy Lactation	0.78 Mcal/lb	0.71 Mcal/lb	0.78 Mcal/lb
Moisture	9.60%	8.00%	9.90%
Phosphorus	0.74%	0.66%	0.70%
Potassium	1.17%	1.07%	0.97%
Calcium	0.84%	0.85%	0.85%
Magnesium	0.33%	0.38%	0.32%
Sodium	4245.0 ppm	5246.0 ppm	1935.0 ppm
Zinc	65.0 ppm	153.0 ppm	70.0 ppm
Iron	51.0 ppm	31.0 ppm	31.0 ppm
Copper	11.0 ppm	65.0 ppm	18.0 ppm
Manganese	119.0 ppm	181.0 ppm	143.0 ppm
Sulfur	2080.0 ppm	2052.0 ppm	2311.0 ppm
Boron	4.39 ppm	4.22 ppm	6.78 ppm

Table 2. Factors 1-25 for each analysis illustrating the cumulative contribution to spectral variance. Full study represents combined spectra from all 12 animals with infested and control groups represented separately. Percentages represented graphically in blue. Factor number is listed on the left with the spectral range and animal group listed on the top.

Factor	400nm-2498nm	576nm-1126nm	576nm-1126nm	576nm-1126nm
	Full Study	Full Study	Infested Animals only	Control Animals only
1	21.78594	72.38922	53.48848	49.87894
2	42.88482	89.29528	75.39207	76.4734
3	54.19	94.67694	87.87038	87.39339
4	61.51916	96.67819	92.85979	92.89118
5	67.66376	97.44288	94.73086	94.76968
6	73.22971	98.00879	95.66361	95.68027
7	76.51666	98.3229	96.37738	96.3533
8	79.63357	98.59122	96.87218	96.8592
9	82.37924	98.77389	97.30032	97.28967
10	84.64315	98.94609	97.67673	97.68361
11	86.59132	99.07973	97.98611	97.98022
12	88.43527	99.19711	98.25663	98.26475
13	89.98115	99.30556	98.51714	98.51894
14	91.34967	99.40183	98.76183	98.75829
15	92.62869	99.49466	98.9731	98.9656
16	93.74588	99.57486	99.16496	99.14869
17	94.77711	99.64766	99.32245	99.2912
18	95.68108	99.71054	99.45084	99.42129
19	96.49361	99.76672	99.56568	99.5385
20	97.23692	99.81964	99.66464	99.64947
21	97.89057	99.86474	99.74911	99.7319
22	98.47958	99.90597	99.82127	99.81239
23	99.03899	99.9403	99.88664	99.88905
24	99.52657	99.97169	99.94962	99.9504
25	100	100	100	100

Table 3. Tick Strain Characterization showing the geographic origins of each strain of *Rhipicephalus (Boophilus) microplus* with the strain, acaricide resistance, geographic origin, generation as of April 2016, number of engorged females produced from a single initialized cohort of approximately 5000 larvae and the survivorship percentage for that cohort.

Strain	Acaricide Resistance	Geographic Origin	Generation	Number of Females Collected (total)	Survivorship Percentage
Santa Luiza	Amitraz Resistant	Brazil	F-56	1487	59%
Lajás	Susceptible	Puerto Rico	F-5	770	30%
Deutch	Susceptible	Webb Co., TX	F-59	1926	77%
Fipronil-Resistant	Fipronil Resistant	Tamaulipas, Mexico	F-30	1144	45%
San Alfonso	Amitraz Resistant	Tabasco, Mexico	F-56	207	8%
Las Palmas	Susceptible	Zapata Co., TX	F-35	513	20%

Table 4. Summary report of 25 factors derived from eigenvalues generated by GRAMS IQ software after analyzing NIR spectra (Objective-1 spectra, 400nm – 2498nm) from fecal samples of cattle infested with *Rhipicephalus (Boophilus) microplus* and non-infested cattle using the FOSS 6500 spectrometer.

Factors	Average Predicted Distance	Eigenvalue	Extracted Error	F-Ratio (REV)	F-Test (REV)	Imbedded Error	Malinowski's Indicator	Real Error (RE)	REV	Total % Variance
1	0.7294036	0.5935829	0	43.38203	0.999992	0	0	0	8.29338E-07	21.78594
2	0.8353058	0.5748633	0	42.11577	0.999999	0	0	0.001730157	8.051306E-07	42.88482
3	0.8702894	0.3080226	0.001728882	22.62122	0.9999665	0.0637581	3.774923E-09	0.001479583	4.324514E-07	54.19
4	0.9205438	0.1996914	0.001478493	14.7014	0.9996728	0.06677823	3.23777E-09	0.001326065	2.810402E-07	61.51916
5	0.9445682	0.1674169	0.001325088	12.35499	0.9992384	0.0691082	2.91043E-09	0.001216265	2.361914E-07	67.66376
6	0.9625723	0.1516504	0.001215369	11.21872	0.9988099	0.07086767	2.677371E-09	0.001115765	2.144693E-07	73.22971
7	0.9654568	0.0895569	0.001114943	6.641366	0.9902627	0.07121692	2.463443E-09	0.001015961	1.269635E-07	76.51666

Table 4 Continued

Factors	Average Predicted Distance	Eigenvalue	Extracted Error	F-Ratio (REV)	F-Test (REV)	Imbedded Error	Malinowski's Indicator	Real Error (RE)	REV	Total % Variance
8	0.9733502	0.08492368	0.001015212	6.313159	0.9884328	0.07004237	2.249771E-09	0.0009522548	1.206892E-07	79.63357
9	0.9785636	0.0748091	0.0009515533	5.574853	0.9827592	0.07018318	2.114989E-09	0.0008874709	1.065749E-07	82.37924
10	0.9815662	0.06168267	0.0008868171	4.607916	0.9701785	0.06937616	1.97699E-09	0.0008261003	8.808991E-08	84.64315
11	0.9829217	0.05308005	0.0008254917	3.974994	0.9566215	0.06807186	1.845783E-09	0.0007717843	7.599029E-08	86.59132
12	0.9857918	0.05024061	0.0007712153	3.771596	0.9509329	0.06670021	1.729589E-09	0.00072171	7.210191E-08	88.43527
13	0.9862722	0.04211924	0.0007211784	3.169693	0.9287474	0.06514607	1.622225E-09	0.0006707532	6.059528E-08	89.98115
14	0.9872578	0.03728695	0.0006702591	2.812946	0.9105507	0.06301868	1.512218E-09	0.0006247839	5.377533E-08	91.34967

Table 4 Continued

Factors	Average Predicted Distance	Eigenvalue	Extracted Error	F-Ratio (REV)	F-Test (REV)	Imbedded Error	Malinowski's Indicator	Real Error (RE)	REV	Total % Variance
15	0.98847	0.0348484	0.000624323 6	2.63546 1	0.89964 02	0.06091562	1.412819E-09	0.000580 983	5.0382 33E-08	92.628 69
16	0.9885409	0.03043903	0.000580555 1	2.30767 8	0.87540 27	0.05863325	1.317733E-09	0.000536 7181	4.4116 08E-08	93.745 88
17	0.9894071	0.02809702	0.000536322 7	2.13538 7	0.86009 14	0.0559424	1.22101E-09	0.000494 7484	4.0822 37E-08	94.777 11
18	0.9903626	0.02462994	0.000494383 9	1.87652	0.83292 25	0.05315495	1.128934E-09	0.000452 4645	3.5873 58E-08	95.681 08
19	0.9915245	0.02213833	0.000452131 2	1.69086 7	0.8097	0.05002138	1.035575E-09	0.000411 7603	3.2324 44E-08	96.493 61
20	0.9922042	0.02025234	0.000411457	1.55065 7	0.78965 17	0.0467688	9.452716E-10	0.000371 2921	2.9644 05E-08	97.236 92
21	0.992661	0.01780941	0.000371018 6	1.36699 7	0.75946 94	0.04326788	8.549582E-10	0.000329 8462	2.6133 E-08	97.890 57
22	0.9921357	0.01604809	0.000329603 2	1.23486 8	0.73448 15	0.03938728	7.618328E-10	0.000288 4211	2.3607 08E-08	98.479 58

Table 4 Continued

Factors	Average Predicted Distance	Eigenvalue	Extracted Error	F-Ratio (REV)	F-Test (REV)	Imbedded Error	Malinowski's Indicator	Real Error (RE)	REV	Total % Variance
23	0.9931293	0.01524171	0.000288208 7	1.17574	0.72226 84	0.03525115	6.681844E-10	0.000245 0514	2.2476 72E- 08	99.038 99
24	0.9922997	0.01328488	0.000244870 9	1.02734 6	0.68836 65	0.03062358	5.69442E-10	0.000194 9713	1.9639 86E- 08	99.526 57
25	0.9945627	0.01289904	0	1	0.68155 52	0	0	0	1.9117 08E- 08	100

Table 5. Summary report of 25 factors derived from eigenvalues generated by GRAMS IQ software after analyzing NIR spectra (Objective-1 spectra, 576nm – 1126nm) from fecal samples of cattle infested with *Rhipicephalus (Boophilus) microplus* and non-infested cattle using the FOSS 6500 spectrometer.

Factors	Eigenvalue	Extracted Error	F-Ratio (REV)	F-Test (REV)	Imbedded Error	Malinowski's Indicator	Real Error (RE)	REV	Total % Variance
1	0.5074067	0	2410.202	1	0	0	0	7.089348 E-07	72.38922
2	0.1185017	0	564.2525	1	0	0	0.0005213999	1.659687 E-07	89.29528
3	0.03772236	0.0005210158	180.0532	1	0.01921413	1.137611 E-09	0.0003248926	5.296069 E-08	94.67694
4	0.01402762	0.0003246533	67.11819	0.9999999	0.01466342	7.109621 E-10	0.0002292734	1.974209 E-08	96.67819
5	0.005360003	0.0002291045	25.70851	0.9999836	0.01194864	5.032064 E-10	0.0001812515	7.561879 E-09	97.44288
6	0.003966681	0.000181118	19.07199	0.9999151	0.01056091	3.989898 E-10	0.0001591446	5.60982 E-09	98.00879
7	0.002201728	0.0001590274	10.61184	0.9984726	0.01015787	3.513677 E-10	0.0001405393	3.121358 E-09	98.3229
8	0.001880776	0.0001404358	9.087072	0.9970334	0.00968906	3.112141 E-10	0.0001290749	2.672863 E-09	98.59122
9	0.001280383	0.0001289798	6.201373	0.9877251	0.009513089	2.866795 E-10	0.0001183878	1.824066 E-09	98.77389
10	0.001207068	0.0001183006	5.860596	0.9852555	0.009254717	2.637287 E-10	0.000105286	1.723831 E-09	98.94609

Table 5 Continued

Factors	Eigenvalue	Extracted Error	F-Ratio (REV)	F-Test (REV)	Imbedded Error	Malinowski's Indicator	Real Error (RE)	REV	Total % Variance
11	0.0009367342	0.000110447 2	4.559217	0.96932 03	0.009107719	2.469577 E-10	0.0001 025498	1.341044 E-09	99.07973
12	0.000822783	0.000102474 3	4.014434	0.95763 9	0.008862703	2.298169 E-10	9.5899 38E-05	1.180802 E-09	99.19711
13	0.0007602021	9.582873E- 05	3.718216	0.94930 84	0.008656479	2.15558E -10	8.9641 86E-05	1.093673 E-09	99.30556
14	0.0006747573	8.957582E- 05	3.308423	0.93469 29	0.008422042	2.020982 E-10	8.3430 44E-05	9.731366 E-10	99.40183
15	0.0006506604	8.336898E- 05	3.198136	0.93001 29	0.00813436	1.886606 E-10	7.7490 32E-05	9.406971 E-10	99.49466
16	0.0005621591	7.743324E- 05	2.769953	0.90803 32	0.007820383	1.757565 E-10	7.1277 95E-05	8.147516 E-10	99.57486
17	0.0005102975	7.122544E- 05	2.520627	0.89180 17	0.007429337	1.621542 E-10	6.5426 93E-05	7.414152 E-10	99.64766
18	0.0004407804	6.537874E- 05	2.182634	0.86449 05	0.007029362	1.492934 E-10	5.9607 16E-05	6.41998E -10	99.71054
19	0.0003937071	5.956325E- 05	1.954369	0.84167 78	0.00658976	1.364255 E-10	5.4067 59E-05	5.748564 E-10	99.76672
20	0.0003710203	5.402777E- 05	1.846321	0.82937 79	0.006141136	1.241221 E-10	4.8575 86E-05	5.430753 E-10	99.81964
21	0.0003160698	4.854007E- 05	1.576776	0.79356 78	0.005660703	1.118535 E-10	4.2743 41E-05	4.637915 E-10	99.86474

Table 5 Continued

Factors	Eigenvalue	Extracted Error	F-Ratio (REV)	F-Test (REV)	Imbedded Error	Malinowski's Indicator	Real Error (RE)	REV	Total % Variance
22	0.0002889952	4.271192E-05	1.445296	0.7729317	0.005104036	9.872278E-11	3.704457E-05	4.25118E-10	99.90597
23	0.0002406738	3.701728E-05	1.206633	0.7287344	0.004527629	8.582105E-11	3.091059E-05	3.54918E-10	99.9403
24	0.0002199861	3.088782E-05	1.105665	0.7068721	0.003862834	7.182896E-11	2.464773E-05	3.252193E-10	99.97169
25	0.0001984672	0	1	0.6815552	0	0	0	2.941392E-10	100

Table 6. Summary report of 25 factors derived from eigenvalues generated by GRAMS IQ software after analyzing NIR spectra (Objective-1 spectra, 576nm – 1126nm) from fecal samples of cattle infested with *Rhipicephalus (Boophilus) microplus* using the FOSS 6500 spectrometer.

Factors	Average Predicted Distance	Eigenvalue	Extracted Error	F-Ratio (REV)	F-Test (REV)	Imbedded Error	Malinowski's Indicator	Real Error (RE)	REV	Total % Variance
1	0.8316268	0.05487574	0	941.5937	1	0	0	0	2.008188E-07	53.48848
2	0.9117313	0.02247167	0	387.441	1	0	0	0.0004205126	8.263163E-08	75.39207
3	0.9321708	0.01280194	0.0004196969	221.7889	1	0.009552211	6.416514E-09	0.0003064664	4.730212E-08	87.87038
4	0.9697528	0.0051188	0.0003058719	89.11135	1	0.008526158	4.713055E-09	0.0002155851	1.900526E-08	92.85979
5	0.9794945	0.0019196	0.0002151669	33.5802	0.9999965	0.006925619	3.341576E-09	0.0001657312	7.161832E-09	94.73086
6	0.9823046	0.0009569459	0.0001654097	16.82189	0.9998354	0.005952495	2.589185E-09	0.0001426511	3.587695E-09	95.66361

Table 6 Continued

Factors	Average Predicted Distance	Eigenvalue	Extracted Error	F-Ratio (REV)	F-Test (REV)	Imbedded Error	Malinowski's Indicator	Real Error (RE)	REV	Total % Variance
7	0.9902371	0.000732277 7	0.00014237 44	12.93555	0.99938 77	0.005612554	2.246332E-09	0.000129 6669	2.758 836E- 09	96.377 38
8	0.9919767	0.000507629 4	0.00012941 54	9.011249	0.99692 92	0.005510462	2.058172E-09	0.000118 7518	1.921 878E- 09	96.872 18
9	0.9954247	0.000439250 9	0.00011852 14	7.835867	0.99465 99	0.005395043	1.900028E-09	0.000110 5647	1.671 198E- 09	97.300 32
10	0.9984202	0.000386167	0.00011035 03	6.922978	0.99157 91	0.005327798	1.783274E-09	0.000102 9252	1.476 501E- 09	97.676 73
11	1.000018	0.000317405	0.00010272 56	5.718502	0.98406 74	0.005227953	1.673472E-09	9.567309 E-05	1.219 616E- 09	97.986 11
12	1.00114	0.000277536	9.548749E- 05	5.025114	0.97654 1	0.005096781	1.56818E-09	8.925553 E-05	1.071 733E- 09	98.256 63
13	1.008151	0.000267270 8	8.908239E- 05	4.863439	0.97427 14	0.00496633	1.474908E-09	8.321336 E-05	1.037 252E- 09	98.517 14

Table 6 Continued

Factors	Average Predicted Distance	Eigenvalue	Extracted Error	F-Ratio (REV)	F-Test (REV)	Imbedded Error	Malinowski's Indicator	Real Error (RE)	REV	Total % Variance
14	1.01051	0.000251033 4	8.305193E- 05	4.590885	0.96988 09	0.004819196	1.386312E-09	7.690105 E-05	9.791 229E- 10	98.761 83
15	1.015387	0.000216750 5	7.675188E- 05	3.983872	0.95685 23	0.004621747	1.291673E-09	7.041431 E-05	8.496 62E- 10	98.973 1
16	1.0207	0.000196842	7.027772E- 05	3.636229	0.94669 72	0.004380427	1.192473E-09	6.42579E -05	7.755 182E- 10	99.164 96
17	1.027017	0.000161565 6	6.413324E- 05	2.9997	0.92064	0.004128539	1.097225E-09	5.806441 E-05	6.397 623E- 10	99.322 45
18	1.031784	0.000131726 1	5.795177E- 05	2.458127	0.88725 13	0.003845425	9.997144E-10	5.241176 E-05	5.242 579E- 10	99.450 84
19	1.036534	0.000117820 3	5.231009E- 05	2.209854	0.86695 34	0.003571699	9.099264E-10	4.728336 E-05	4.713 074E- 10	99.565 68
20	1.03985	0.000101522 2	4.719163E- 05	1.913918	0.83719 5	0.00331051	8.277753E-10	4.213755 E-05	4.081 917E- 10	99.664 64

Table 6 Continued

Factors	Average Predicted Distance	Eigenvalue	Extracted Error	F-Ratio (REV)	F-Test (REV)	Imbedded Error	Malinowski's Indicator	Real Error (RE)	REV	Total % Variance
21	1.043227	8.665894E-05	4.205581E-05	1.642112	0.8029931	0.003026873	7.439014E-10	3.710502E-05	3.50222E-10	99.74911
22	1.043636	7.402893E-05	3.703304E-05	1.410021	0.7669814	0.002731191	6.60596E-10	3.216137E-05	3.007228E-10	99.82127
23	1.051286	6.707269E-05	3.209899E-05	1.284141	0.7441546	0.002423013	5.774449E-10	2.72028E-05	2.738756E-10	99.88664
24	1.052857	6.460539E-05	2.715003E-05	1.24333	0.7361739	0.002095498	4.925812E-10	2.170983E-05	2.651718E-10	99.94962
25	1.058012	5.169198E-05	0	1	0.6815546	0	0	0	2.132754E-10	100

Table 7. Summary report of 25 factors derived from eigenvalues generated by GRAMS IQ software after analyzing NIR spectra (Objective-1 non-infested spectra, 576nm – 1126nm) from fecal samples of non-infested cattle using the FOSS 6500 spectrometer.

Factors	Average Predicted Distance	Eigenvalue	Extracted Error	F-Ratio (REV)	F-Test (REV)	Imbedded Error	Malinowski's Indicator	Real Error (RE)	REV	Total % Variance
1	0.826957	0.05252681	0	891.5736	1	0	0	0	1.92965E-07	49.87894
2	0.9206726	0.02800624	0	477.6661	1	0	0	0.0004431261	1.033822E-07	76.4734
3	0.9571526	0.01149969	0.0004422631	197.0862	1	0.01004636	6.814703E-09	0.0003041913	4.265575E-08	87.39339
4	0.9657993	0.00578964	0.0003035989	99.70777	1	0.008446445	4.714974E-09	0.0002231102	2.157994E-08	92.89118
5	0.9849818	0.001978215	0.0002226757	34.23461	0.9999968	0.007153457	3.485607E-09	0.000167871	7.409462E-09	94.76968
6	0.9918447	0.0009589308	0.0001675441	16.67633	0.9998278	0.006017655	2.643471E-09	0.0001442784	3.609291E-09	95.68027
7	0.9909898	0.0007087632	0.0001439974	12.38634	0.9992474	0.005665569	2.290097E-09	0.0001313799	2.6808E-09	96.3533

Table 7 Continued

Factors	Average Predicted Distance	Eigenvalue	Extracted Error	F-Ratio (REV)	F-Test (REV)	Imbedded Error	Malinowski's Indicator	Real Error (RE)	REV	Total % Variance
8	0.9920235	0.000532758 8	0.00013112 4	9.35638 8	0.99737 22	0.00557242 8	2.102078E- 09	0.0001209532 021E- 09	2.025 021E- 09	96.85 92
9	0.9955126	0.000453309 8	0.00012071 76	8.00047 6	0.99506 89	0.00548439 5	1.950826E- 09	0.0001124754 558E- 09	1.731 558E- 09	97.28 967
10	1.000612	0.000414862 4	0.00011225 63	7.35825 8	0.99324 26	0.00540935 2	1.828749E- 09	0.0001046943 562E- 09	1.592 562E- 09	97.68 361
11	0.9966987	0.000312363 6	0.00010449 04	5.56786 8	0.98269 22	0.00530749 6	1.716047E- 09	9.698275E-05 064E- 09	1.205 064E- 09	97.98 022
12	1.002244	0.000299620 4	9.679388E- 05	5.36741 3	0.98065 55	0.00515652 8	1.602597E- 09	9.07446E-05 68E- 09	1.161 68E- 09	98.26 475
13	1.006794	0.000267685 7	9.056788E- 05	4.81938 2	0.97361 19	0.00503939 0.00503939	1.51178E-09 1.51178E-09	8.428219E-05 068E- 09	1.043 068E- 09	98.51 894
14	1.011585	0.000252054 3	8.411806E- 05	4.56079 3	0.96934 8	0.00487162 7	1.415651E- 09	7.802416E-05 013E- 10	9.871 013E- 10	98.75 829

Table 7 Continued

Factors	Average Predicted Distance	Eigenvalue	Extracted Error	F-Ratio (REV)	F-Test (REV)	Imbedded Error	Malinowski's Indicator	Real Error (RE)	REV	Total % Variance
15	1.015946	0.000218320 1	7.787222E- 05	3.97034	0.95649 91	0.00468014 9	1.321346E- 09	7.158879E-05	8.593 082E- 10	98.96 56
16	1.021345	0.000192807 7	7.144938E- 05	3.52414 2	0.94288 79	0.00444485 1	1.222403E- 09	6.547475E-05	7.627 368E- 10	99.14 869
17	1.027624	0.000150078 1	6.534725E- 05	2.75708 1	0.90726 36	0.00419856	1.127301E- 09	5.952139E-05	5.967 203E- 10	99.29 12
18	1.029057	0.000136995 6	5.940548E- 05	2.52958 6	0.89243 61	0.00393426 9	1.033358E- 09	5.442434E-05	5.474 832E- 10	99.42 129
19	1.033238	0.000123429 7	5.431836E- 05	2.29076 6	0.87398 54	0.00370165 6	9.527905E- 10	4.927976E-05	4.957 95E- 10	99.53 85
20	1.035449	0.000116859 2	4.918379E- 05	2.17997 1	0.86424 6	0.00344359 4	8.699908E- 10	4.409968E-05	4.718 154E- 10	99.64 947
21	1.039373	8.681527E- 05	4.40138E- 05	1.62786 4	0.80098 15	0.00316167 4	7.85125E-10	3.851482E-05	3.523 218E- 10	99.73 19

Table 7 Continued

Factors	Average Predicted Distance	Eigenvalue	Extracted Error	F-Ratio (REV)	F-Test (REV)	Imbedded Error	Malinowski's Indicator	Real Error (RE)	REV	Total % Variance
22	1.044761	8.476033E-05	3.843981E-05	1.59756	0.79662 2	0.00282946 3	6.915185E-10	3.3754E-05	3.457 629E-10	99.81 239
23	1.046388	8.072335E-05	3.368827E-05	1.52937 6	0.78639 5	0.00253806 7	6.112086E-10	2.829618E-05	3.310 057E-10	99.88 905
24	1.053472	6.460813E-05	2.824107E-05	1.23044 1	0.73358 97	0.00217549 6	5.167686E-10	2.180713E-05	2.663 067E-10	99.95 04
25	1.058475	5.223476E-05	0	1	0.68155 46	0	0	0	2.164 319E-10	100

Table 8. Summary report of 25 factors derived from eigenvalues generated by GRAMS IQ software after analyzing NIR spectra (800-1800nm) from fecal samples of cattle infested with *Rhipicephalus (Boophilus) microplus* using the FOSS 6500 spectrometer.

Factors	Average Predicted Distance	Eigenvalue	Extracted Error	F-Ratio (REV)	F-Test (REV)	Imbedded Error	Malinowski's Indicator	Real Error (RE)	REV	Total % Variance
1	0.8744742	0.03931816	0	5363.479	1	0	0	0	3.012424E-07	44.15451
2	0.887414	0.02432318	0	3337.439	1	0	0	0.0006214665	1.874489E-07	71.46957
3	0.9222909	0.01326775	0.000620261	1831.21	1	0.01411701	9.482826E-09	0.000445066	1.028508E-07	86.36933
4	0.9591023	0.008716051	0.0004442026	1210.087	1	0.01238212	6.844536E-09	0.0003082327	6.796513E-08	96.1575
5	0.9693858	0.00116252	0.0003076348	162.3535	1	0.009901901	4.777617E-09	0.0001639759	9.118664E-09	97.46302
6	0.9716255	0.0007809549	0.0001636579	109.7134	1	0.005889453	2.561764E-09	0.0001335022	6.162109E-09	98.34003
7	0.9757776	0.0005521811	0.0001332433	78.03629	1	0.005252596	2.102265E-09	0.000108203	4.382946E-09	98.96014
8	0.9820504	0.0002357585	0.0001079931	33.51754	0.9999964	0.004598309	1.717481E-09	8.581065E-05	1.882529E-09	99.2249
9	0.982662	0.0001578926	8.564418E-05	22.58212	0.999961	0.003898486	1.37297E-09	7.423353E-05	1.268336E-09	99.40221
10	0.9846932	0.0001271978	7.408953E-05	18.30161	0.9998943	0.003577101	1.197296E-09	6.532278E-05	1.027919E-09	99.54505

Table 8 Continued

Factors	Average Predicted Distance	Eigenvalue	Extracted Error	F-Ratio (REV)	F-Test (REV)	Imbedded Error	Malinowski's Indicator	Real Error (RE)	REV	Total % Variance
11	0.9933847	9.423126E-05	6.519607E-05	13.64019	0.9995262	0.003317986	1.06209E-09	5.710106E-05	7.661078E-10	99.65088
12	1.006464	7.640995E-05	5.699029E-05	11.12755	0.9987648	0.003041938	9.359449E-10	5.012233E-05	6.249842E-10	99.73669
13	1.02362	5.501079E-05	5.00251E-05	8.059918	0.9952076	0.002788892	8.282493E-10	4.361745E-05	4.526892E-10	99.79846
14	1.035464	3.177807E-05	4.353283E-05	4.68438	0.9714721	0.002526049	7.266547E-10	3.82371E-05	2.631005E-10	99.83415
15	1.069884	2.87488E-05	3.816292E-05	4.263785	0.9634966	0.002298046	6.422516E-10	3.47579E-05	2.394775E-10	99.86643
16	1.077025	2.450094E-05	3.469047E-05	3.656101	0.947342	0.002162265	5.88628E-10	3.125604E-05	2.053467E-10	99.89395
17	1.097601	1.758901E-05	3.11954E-05	2.640862	0.899991	0.002008185	5.337074E-10	2.790867E-05	1.483253E-10	99.9137
18	1.110941	1.683833E-05	2.785453E-05	2.543792	0.8934337	0.001848304	4.805129E-10	2.522796E-05	1.428733E-10	99.93261
19	1.115784	1.333142E-05	2.517903E-05	2.026498	0.8493236	0.001719208	4.379855E-10	2.233971E-05	1.138192E-10	99.94759
20	1.107953	1.038934E-05	2.229638E-05	1.589111	0.7953854	0.001564099	3.910945E-10	1.97437E-05	8.92532E-11	99.95925
21	1.10875	8.107068E-06	1.97054E-05	1.247774	0.7370564	0.001418252	3.485576E-10	1.744478E-05	7.008185E-11	99.96835
22	1.111437	7.734599E-06	1.741094E-05	1.197913	0.7269266	0.001284059	3.105766E-10	1.540542E-05	6.728136E-11	99.97704

Table 8 Continued

Factors	Average Predicted Distance	Eigenvalue	Extracted Error	F-Ratio (REV)	F-Test (REV)	Imbedded Error	Malinowski's Indicator	Real Error (RE)	REV	Total % Variance
23	1.115773	7.400349E-06	1.537553E-05	1.153359	0.7174619	0.001160632	2.765982E-10	1.314975E-05	6.477897E-11	99.98535
24	1.127082	6.70861E-06	1.312424E-05	1.052154	0.6943833	0.001012957	2.381122E-10	1.052595E-05	5.909472E-11	99.99288
25	1.137732	6.335916E-06	0	1	0.6815536	0	0	0	5.616549E-11	100

Table 9. Summary report of 25 factors derived from eigenvalues generated by GRAMS IQ software after analyzing NIR spectra (800-1800nm) from fecal samples of cattle infested with *Rhipicephalus (Boophilus) microplus* using the Ocean Optics NIR-512 spectrometer.

Factors	Average Predicted Distance	Eigenvalue	Extracted Error	F-Ratio (REV)	F-Test (REV)	Imbedded Error	Malinowski's Indicator	Real Error (RE)	REV	Total % Variance
1	0.8895339	1.019891	0	516.7967	1	0	0	0	1.858029E-05	72.05866
2	0.9441024	0.1914281	0	98.10632	1	0	0	0.002725246	3.527198E-06	85.58369
3	0.9556834	0.055195	0.002712238	28.61256	0.9999911	0.03949257	2.568806E-07	0.001967013	1.028702E-06	89.4834
4	0.991977	0.04544827	0.001957624	23.83312	0.9999749	0.03491102	1.890632E-07	0.001688249	8.568678E-07	92.69447
5	1.031877	0.02852096	0.00168019	15.1313	0.9997168	0.03459881	1.654984E-07	0.001414048	5.440128E-07	94.70956
6	1.050514	0.01755497	0.001407298	9.423306	0.9974487	0.0323999	1.414048E-07	0.001209329	3.387944E-07	95.94988

Table 9 Continued

Factors	Average Predicted Distance	Eigenvalue	Extracted Error	F-Ratio (REV)	F-Test (REV)	Imbedded Error	Malinowski's Indicator	Real Error (RE)	REV	Total % Variance
7	1.103711	0.01054235	0.001203556	5.726315	0.9841329	0.03035391	1.233883E-07	0.001063445	2.058771E-07	96.69473
8	1.17778	0.007284694	0.001058369	4.004312	0.9573758	0.02883093	1.107294E-07	0.0009655814	1.439663E-07	97.20942
9	1.234668	0.00621888	0.0009609724	3.459814	0.9405637	0.02798521	1.026232E-07	0.0008917846	1.2439E-07	97.6488
10	1.239854	0.003457575	0.0008875278	1.947072	0.8408741	0.02741422	9.676482E-08	0.0008228247	7.000273E-08	97.8931
11	1.265894	0.003302319	0.0008188971	1.88255	0.8336144	0.02666257	9.117171E-08	0.0007829957	6.768296E-08	98.12642
12	1.289728	0.002735901	0.0007792582	1.579038	0.7938975	0.02661034	8.861426E-08	0.0007422863	5.677085E-08	98.31972
13	1.310501	0.002628952	0.0007387432	1.536344	0.7874631	0.02634855	8.582337E-08	0.000706722	5.523589E-08	98.50546
14	1.199375	0.002243822	0.0007033486	1.327876	0.7523771	0.02611049	8.34974E-08	0.0006701293	4.774089E-08	98.66399

Table 9 Continued

Factors	Average Predicted Distance	Eigenvalue	Extracted Error	F-Ratio (REV)	F-Test (REV)	Imbedded Error	Malinowski's Indicator	Real Error (RE)	REV	Total % Variance
15	1.21888	0.002095384	0.0006669305	1.255877	0.7386554	0.02569314	8.092371E-08	0.0006370629	4.515232E-08	98.81204
16	1.237216	0.002010235	0.000634022	1.220385	0.7315476	0.02528265	7.864974E-08	0.0006040578	4.387626E-08	98.95407
17	1.269313	0.001942857	0.0006011745	1.194841	0.7262839	0.024759	7.62603E-08	0.0005699742	4.295791E-08	99.09134
18	1.267541	0.001798363	0.0005672536	1.120522	0.7102195	0.02408099	7.360205E-08	0.0005342672	4.028591E-08	99.2184
19	1.301203	0.001737616	0.0005317169	1.097048	0.7049011	0.0232268	7.058622E-08	0.0004983469	3.944198E-08	99.34116
20	1.335263	0.001674475	0.0004959681	1.071362	0.6989389	0.02225887	6.738059E-08	0.00046019	3.851846E-08	99.45947
21	1.36532	0.001637981	0.0004579933	1.062209	0.6967776	0.02108855	6.369411E-08	0.0004192735	3.818939E-08	99.5752

Table 9 Continued

Factors	Average Predicted Distance	Eigenvalue	Extracted Error	F-Ratio (REV)	F-Test (REV)	Imbedded Error	Malinowski's Indicator	Real Error (RE)	REV	Total % Variance
22	1.416448	0.001560273	0.00041727 22	1.025662	0.68794 79	0.01968801	5.942085E-08	0.0003 738951	3.6875 42E- 08	99.68 544
23	1.463063	0.001509637	0.00037211 04	1.006096	0.68308 55	0.01797032	5.427422E-08	0.0003 236759	3.6171 96E- 08	99.79 21
24	1.488175	0.001479818	0.00032213 09	1	0.68155 09	0.01590629	4.81374E-08	0.0002 647381	3.5952 82E- 08	99.89 666
25	1.528286	0.001462684	0	1.002376	0.68215 02	0	0	0	3.6038 24E- 08	100